Effects of Diversity Combining, Coding and Equalization on Digital Microcellular Mobile Communication Systems

by

Abdullah Said M. Al-Ahmari

A Thesis Presented to the

FACULTY OF THE COLLEGE OF GRADUATE STUDIES

KING FAHD UNIVERSITY OF PETROLEUM & MINERALS

DHAHRAN, SAUDI ARABIA

In Partial Fulfillment of the
Requirements for the Degree of

MASTER OF SCIENCE

In

ELECTRICAL ENGINEERING

June, 1994

INFORMATION TO USERS

This manuscript has been reproduced from the microfilm master. UMI films the text directly from the original or copy submitted. Thus, some thesis and dissertation copies are in typewriter face, while others may be from any type of computer printer.

The quality of this reproduction is dependent upon the quality of the copy submitted. Broken or indistinct print, colored or poor quality illustrations and photographs, print bleedthrough, substandard margins, and improper alignment can adversely affect reproduction.

In the unlikely event that the author did not send UMI a complete manuscript and there are missing pages, these will be noted. Also, if unauthorized copyright material had to be removed, a note will indicate the deletion.

Oversize materials (e.g., maps, drawings, charts) are reproduced by sectioning the original, beginning at the upper left-hand corner and continuing from left to right in equal sections with small overlaps. Each original is also photographed in one exposure and is included in reduced form at the back of the book.

Photographs included in the original manuscript have been reproduced xerographically in this copy. Higher quality 6" x 9" black and white photographic prints are available for any photographs or illustrations appearing in this copy for an additional charge. Contact UMI directly to order.
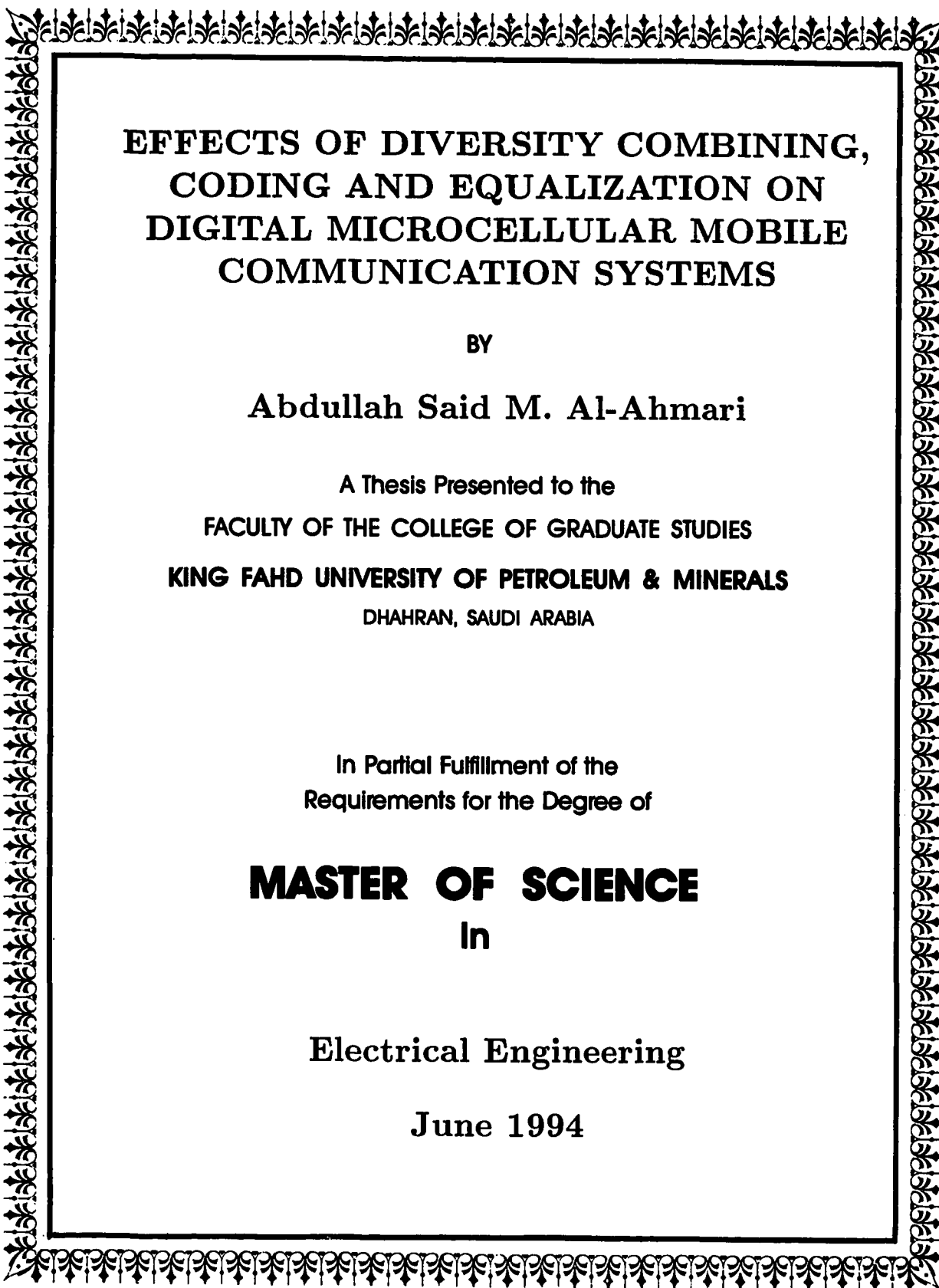
UMI

Effects of diversity combining, coding and equalization on digital microcellular mobile communications systems

Al-Ahmari, Abdullah Said M., M.S.

King Fahd University of Petroleum and Minerals (Saudi Arabia), 1994

EFFECTS OF DIVERSITY COMBINING, CODING AND EQUALIZATION ON DIGITAL MICROCELLULAR MOBILE COMMUNICATION SYSTEMS

BY

Abdullah Said M. Al-Ahmari

A Thesis Presented to the

FACULTY OF THE COLLEGE OF GRADUATE STUDIES

KING FAHD UNIVERSITY OF PETROLEUM & MINERALS

DHAHRAN, SAUDI ARABIA

In Partial Fulfillment of the
Requirements for the Degree of

MASTER OF SCIENCE
In

Electrical Engineering

June 1994

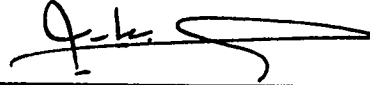# KING FAHD UNIVERSITY OF PETROLEUM & MINERALS
DHAHRAN, SAUDI ARABIA

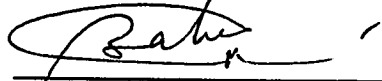This thesis, written by

ABDULLAH SAID M. AL-TALGI AL-AHMARI

under the direction of his Thesis Advisor, and approved by his Thesis Committee, has been presented to and accepted by the Dean of the College of Graduate Studies, in partial fulfillment of the requirements for the degree of

MASTER OF SCIENCE IN ELECTRICAL ENGINEERING

<u>Thesis Committee</u>
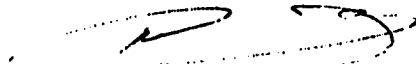
_____
Chairman (Dr. Khaled H. Biyary)
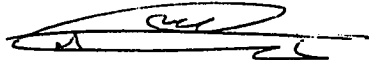
_____
Member (Dr. Hussein Baher)

_____
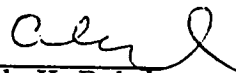Member (Dr. Jamil Bakhashwain)

_____
Member (Dr. Ahmed Yamani)

_____
Member (Dr. Mohammad A. Chaudhry)

_____
Dr. Abdallah M. Al-Shehri
Department Chairman

_____
Dr Ala H. Rabeh
Dean, College of Graduate Studies

Date: _____Sep 24, 1994_____

To those who shared their care and concern

Acknowledgement

First of all, praise be to "Allah" whose help made it possible to complete this research.

I wish to express my sincere gratitude to my thesis advisor, Dr. Khaled H. Biyari, for his patient guidance and his generous support during the course of this work. I would like to express my deep appreciation to my committee members, Dr. Hussein Baher, Dr. Jamil Bakhashwain, Dr. Ahmed Yamani and Dr. Mohammad A. Chaudhry, for their valuable suggestions, helpful remarks, and kind cooperation.

Thanks to all my friends and colleagues for their support and help to complete this work.

Finally, special thanks to my parents and family for their encouragement and support during my studies.

خلاصة الرسالة

اسم الطالب : عبد الله سعيد محمد آل طلقي الأحمري

عنوان الرسالة : تأثير التنويع والترميز والتعديل على أداء أنظمة الاتصالات النقالة الخلوية الصغرى الرقمية

التخصص : هندسة كهربائية

تاريخ الدرجة : محرم ١٤١٥هـ

حظيت أنظمة الاتصالات النقالة الخلوية الصغرى الرقمية باهتمام شديد لما تتميز به مثل هذه الانظمة من زيادة هائلة في فاعلية الطيف المخصص للاتصالات النقالة . في هذه الرسالة دراسة لتأثير التنويع والترميز والتعديل على أداء هذا النوع من الأنظمة العاملة على قنوات الخبو انتقائيه التردد ، نظراً لأن هذا النوع من القنوات هو السائد في حالة الاتصالات النقالة . هذا وقد تم استخدام برامج المحاكاة على الحاسب الآلي في اغلب اجزاء الرسالة .

أثناء الدراسة تم افتراض وجود اشارات غير مرغوب فيها نتيجة الضجيج والتداخل من الاشارات المنبعثة من خلايا قريبة تعمل على نفس قناة الاشارات المرغوب فيها وهو ما يسمى بتداخل نفس القناة . تتعرض الاشارات المرغوب فيها واشارات تداخل نفس القناة لظاهرتي الخبو إنتقائي التردد والحجب كما تخضع قدرة الاشارات لمنحني المسار مزدوج الميل . طرق التضمين المستخدمة هي التضمين بواسطة ازاحة الطور في الخانة الثنائية والتضمين بواسطة ازاحة الطور التفاضلي في الخانة الثنائية . بالاضافة إلى ذلك ، فإن مقياسي الأداء المستخدمين أثناء الرسالة هما معدل الخطأ في الخانة الثنائية وفاعلية الطيف .

من خلال نتائج الدراسة وجد أن معدل الخطأ في الخانة الثنائية الغير قابلة للاختزال نتيجة تداخل نفس القناة وتداخل الرموز الداخلي ، قد تم تقليله من ٠,٠٠٣ إلى ٠,٠٠٠١٢٥ في حالة استخدام التنويع الثنائي . أما في حالة استخدام التعديل التكيفي الخطي فقد تم اختزاله من ٠,٠٠٣ إلى ٠,٠٠٠٨ . بالاضافة إلى ذلك ، تم تحقيق كسب مقداره ٢٣,٨ ديسبل عند معدل خطأ في الخانة يساوي ٠,٠٠٣ ، باستخدام ترميز قولاي .

درجة الماجستير في العلوم الهندسية

جامعة الملك فهد للبترول والمعادن

الظهران – المملكة العربية السعودية

THESIS ABSTRACT

FULL NAME OF STUDENT   ABDULLAH SAID M. AL–TALGI AL–AHMARI

TITLE OF STUDY   EFFECTS OF DIVERSITY COMBINING, COD-ING AND EQUALIZATION ON DIGITAL MI-CROCELLULAR MOBILE COMMUNICATION SYSTEMS

MAJOR FIELD   ELECTRICAL ENGINEERING

DATE OF DEGREE   JUNE 1994

The effects of diversity combining, coding, and equalization on the performance of digital microcellular mobile communication systems, operating over frequency–selective fading channels, are studied using computer simulations. The presence of co–channel interference and additive white Gaussian noise is assumed. The multiple–access channel is statistically modelled by Rician distributed plus lognormally shadowed desired signal and several uncorrelated Rayleigh plus lognormally shadowed interfering signals, propagating according to dual path loss law with a turning point. The modulation schemes considered are BPSK, and DPSK. The channel is modeled by two beams with a relative delay between them. The performance is determined in terms of bit error rate (BER), and spectrum efficiency.

It is shown from the computer simulations done on the system that with dual diversity combining and BPSK modulation the irreducible bit error rate (IBER), due to co–channel interference and intersymbol interference (ISI), is reduced from 3.0×10^{-3} to 1.35×10^{-4}. Also, with linear adaptive equalization and BPSK modulation, the IBER is reduced to 8.0×10^{-4}. The use of Golay (23, 12) code with BPSK modulation enhances the performance of the system by 23.8 dB coding gain at 3.0×10^{-3} BER.

MASTER OF SCIENCE DEGREE

KING FAHD UNIVERSITY OF PETROLEUM AND MINERALS

Dhahran, Saudi Arabia

June 1994

v

Contents

List of Figures

List of Symbols

BCH codes	Bose–Chaudhuri–Hocquenghem codes.
BER	Bit error rate.
BPSK	Binary phase shift keying.
BS	Base station.
erfc $(\cdot)$	Complementary error function.
DPSK	Differential phase shift keying.
G	Normalized turning point.
IBER	Irreducible bit error rate.
ISI	Intersymbol interference.
LMS	Least mean square.
MU	Mobile unit.
R	Cell radius.
Ru	Normalized reuse distance.
SNR	Signal to noise ratio.

CHAPTER 1

INTRODUCTION

1.1 Overview

Telephone is a very important communication tool in our modern life. However, it is constrained by the presence of wires. This constraint has been removed by the development of mobile radio telephony.

Previously, the capacity of public mobile radio telephony was limited by the amount of frequency spectrum available. So any further expansion in the mobile telephony would have to be in a different frequency band. The first problem that faced the spread of mobile services is the unavailability of the required spectrum. The first solution used for this problem is the use of trunking which is the ability to combine several channels into a single group so that a mobile system can be connected to any unused channel in the group for either an incoming or an outgoing call. This concept reduces blocking probability[50], [16].

In the conventional mobile system, one or more channels from a specific frequency allocation is selected to serve a geographical region. The region is planned to be as large as possible which puts the need for high amount of

1

transmitted power in that region. Also, each region is completely independent of the other regions, see Figure 1.1; so, when a user is entering a new geographical region, he has to terminate his call initiated in the first region and re–initiate it from the new region [22]. Hence, the conventional mobile system does not have the handoff process, which is changing the frequencies serving a mobile unit call as it moves into a different frequency zone automatically and without re–dialing the call.

Because of the continuous increase in the number of subscribers in each region and the limited number of channels, a high–capacity system for mobile telephones was needed other than the conventional mobile system. In addition, the conventional system does not utilize the available spectrum efficiently because each channel can only serve one customer at a time in a whole area. These shortcomings triggered the need for a new mobile telephone system which needs minimal bandwidth and provides high usage capacity.

Recently, cellular and microcellular systems have been introduced to fulfill the increasing requirement of higher capacity mobile communication systems. The performance measures of such systems are investigated over non–selective fading environments, including co–channel interference. In
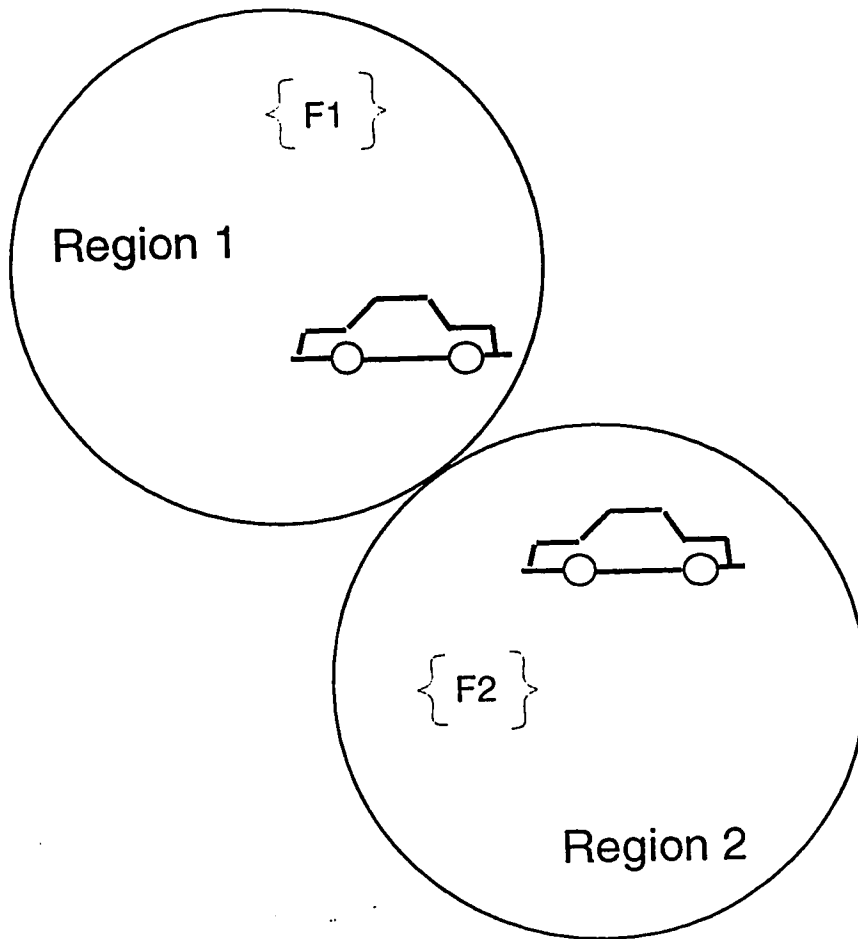
Figure 1.1 : Conventional mobile system.

addition, over–frequency–selective fading channels, the performance of cellular and microcellular systems is studied without considering the effect of co–channel interference [5], [6].

In our work, we propose diversity combining, coding and equalization to improve the performance of digital microcellular mobile communication systems operating over frequency–selective fading environments. In this work we will consider the presence of Rayleigh faded and log–normal shadowed co–channel interference, and additive noise.

1.2 History of Mobile Communication

Using radio waves to communicate between moving points was recognized early in the history of radio communication. In 1920, police vehicles used radio waves to communicate with each other. Connecting the radio link to fixed telephone network was implemented in USA as the so–called Public Correspondence Service in 1946. In 1964, automatic trunking was introduced representing a first step in the improvement of the efficiency of spectrum usage. The Advanced Mobile Phone System (AMPS) was installed in Chicago in 1978 as an operational system. Later on, in the 1980's commercial cellular services were effectively introduced in Europe and in the

U.S.A. In that year the expected number of subscribers, served by cellular systems, was 18 million around the world. In 1982, the Grope Special Mobile (GSM) system working in a 900 MHz band was launched in Europe. In addition, the GSM technology is adapted to the newly reserved frequency band 1800 MHz and renamed DCS [13].

1.3 Literature Review

To overcome the problem of fast–growing number of mobile users and the demand for new mobile systems, which use the scarce–frequency spectrum efficiently, the cellular mobile system was brought as a solution [26], [22]. Several research papers and books such as [44], [29], [42], [26], [22], [1], [15] and [33], reported different aspects of the performance analysis of this new system configuration.

Recently, microcellular mobile systems started to provide enhanced spectrum efficiency and low power consumption, especially in crowded cities with large number of users [23].

Although microcellular mobile radio is relatively a new subject, numerous researchers have studied the propagation, and channel models for this new field. Also, they tried to study the co–channel interference effects on the

performance of these systems.

The propagation characteristics of microcellular systems are reported in [19], [12], [7], [11], [38], [35], [10] and [4]. Several statistical models are used to describe the amplitude probability density of both the desired signal, and the undesired co-channel interferers. Rayleigh distribution is used to represent the two types of signals [40]. In [36] and [49], log-normal distribution is used to model the fading environment. However, in [17], [46] and [41], the superimposed Rayleigh fading and log-normal shadowing statistical model are used.

In [26], the model of Rician/Rayleigh is introduced. The desired signal is assumed to have Rician statistics implying that a dominant multipath reflection exists within cell transmission area. On the other hand, the interference signals from co-channel cells are assumed to be subject to Rayleigh fading because of the absence of a line of sight propagation. In [47], the desired and undesired signals are assumed to have different statistical characteristics. Both signals are assumed to have Nakagami characteristics. However, the signals have different parameters assuming different statistical characteristics.

In [48], Yao and Sheikh discussed the outage probability of microcellular

systems without considering the dual path loss law, while Prasad, Kegel, and Olsthoorn considered it in [30]. In addition, in [30] and [48], the desired signal is assumed to be Rician and the co-channel interferers are assumed to have Rayleigh distribution.

The bit error rates for binary phase shift keying (BPSK), binary frequency shift keying (BFSK), and quadrature phase shift keying (QPSK) radio signals in the presence of Rayleigh-faded co-channel interference with shadowing and additive white Gaussian noise (AWGN) are found in [25]. In that paper different error correction/detection BCH codes were used.

In [28], Prasad and Kegel presented a mathematical model to analyze the spectrum efficiency within microcells assuming log-normal shadowed Rician desired signal and Rayleigh distributed interfering signals with log-normal shadowing from co-channel microcells. In addition, Prasad Kegel, and Vos, in [31], developed a model for performance analysis of a microcellular digital mobile radio system with Rayleigh-faded co-channel interference, Gaussian noise, narrow-band impulsive noise, and Rician-faded desired signal.

1.4 Thesis Contribution

In the past, researchers have investigated the performance of digital microcellular mobile communication systems operating over frequency–non–selective fading channels. However, at high transmission rates the mobile communication channels become frequency–selective in nature, which necessitates the study of the performance and the way of enhancing the performance of the digital microcellular mobile communication systems over such type of channels.

In this thesis, the effects of diversity combining, coding and linear adaptive equalization on the performance of digital microcellular mobile communication systems, operating over frequency–selective fading channels are studied using computer simulations. The frequency–selective fading channels are modeled by the sum of two delayed and independent beams. The desired signal is statistically modeled by fast Rician distribution with slow lognormal distribution. The presence of several uncorrelated Rayleigh plus lognormally shadowed interfering signals and additive white Gaussian noise (AWGN) are assumed. A propagation which is according to dual–path loss law with a turning point is assumed.

The modulation schemes considered are binary phase shift keying (BPSK) and differential phase shift keying (DPSK). The bit error rate (BER) and spectrum efficiency are used to measure the performance of digital microcel-

lular mobile communication systems.

1.5 Thesis Organization

The thesis organization is as follows. Chapter two will be devoted to the cellular concept and its properties. Then, the microcellular systems will be introduced with some previous work done to evaluate the performance of such systems operating in flat fading environments. Chapter three will start with discussing multipath fading. Then, some explanation will be given about mobile radio environments, such as propagation path loss, slow fading and fast fading. At the end of that chapter, fading counter-measures will be discussed.

Chapter four will start with explaining the baseband representation used in our simulation programs. Then, our system will be described and the system block diagrams will be shown. Modulation schemes, path loss model, fading statistics and the channel model will be discussed. After that, the performance measures, which are bit error rate (BER) and spectrum efficiency, will be discussed.

In chapter 5 of this thesis, the effect of system parameters on the BER will be shown. Then the performance enhancement of using diversity, coding and/or adaptive equalization will be illustrated using computer simulations. In the last chapter, summary, main results, conclusions, and recommendations for future work will be discussed.

CHAPTER 2

CELLULAR SYSTEMS

2.1 Introduction

In conventional mobile telephone systems a service area is divided into distinct regions and each region is served by part of the frequency spectrum allocated for mobile telephony. Since the allocated frequency spectrum is limited, each region is designed to be as large as possible, which means that the transmitted power should be as high as allowed. Also, in conventional systems there is no way of transferring the service from a region to another region when the mobile unit (MU), which is having a call, is leaving the first region and entering the second region. Many operational problems have appeared with the use of these mobile systems.

First, the number of active users in a certain service area is limited to the number of allocated mobile channels so the service capability of conventional systems is limited. Second, because of the huge number of customers and limited channels, a high blocking probability is created during busy hours, which is an indication of poor service performance. Thirdly, as far as frequency spectrum utilization is concerned, the conventional system does

not utilize the spectrum efficiently since each channel can only serve one customer at a time in a whole area.

2.2 Cellular Mobile Systems

In order to accommodate the expanding nature of mobile communication systems, the concept of cellular communication systems has been introduced. The cellular concept is based on the fact that a desired service area is divided into regions called cells; and each cell has its own radio base station (BS) which gives the radio coverage for the mobile units (MU's) within that cell [44], [42], [26], [15].

With this new concept the service area of a cellular radio system is divided into an array of C cells grouped into identical clusters. Each cluster occupies the total bandwidth allocated for the mobile radio system in that service area, and the available bandwidth for the mobile system is reused in each cluster [26]. The performance of cellular mobile communication systems such as the outage probability and spectrum efficiency are discussed in [29], [27].

2.2.1 Cell Shapes

In cellular mobile systems, a cell can take any geometrical shape. However, certain shapes are more attractive because of certain reasons. For example, circular shapes are suitable because of the propagation characteristics of omnidirectional transmitting antennas, and the shape of the coverage area of such antennas is desirable. Out of the other shapes regular hexagonal ones approximate the circular shapes and give a very good coverage characteristic. Also, they are the only shapes which cover a certain service area with less cells if you compare it with equilateral triangular and square shapes; see Figure 2.1. Hence, the use of regular hexagonal shapes will require fewer antennas and less amount of power to cover a service area.

We have to realize that hexagonal–shaped communication cells are artificial and that such a shape cannot be generated in practice. However, they are used by engineers to simplify the planning and design of a cellular system because they approach circular shapes. Also, the hexagonal shapes fit the planned area with no gap and no overlap.

In cellular mobile system, the mobile unit is served by a mobile communication channel belonging to the cell in which it is roaming. However, when the mobile is leaving that cell a certain process called handoff is happening
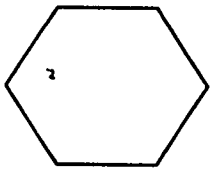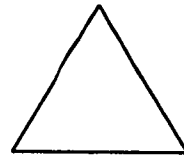
Hexagonal   Squarer   Triangular

Figure 2.1 : Cell shapes.

to transfer the service of that mobile unit to another mobile communication channel belonging to the destination cell. The conventional cell radius ranges from 0.2 km to 20.0 km and the power rating of a cell ranges from 0.6 W to 10 W. The base station antenna which is located at the cell center is 30 m to 100 m high and the antenna at the mobile unit is about 3.0 m high [25].

For a typical array of regular hexagonal cells there are some good things about their geometry. There are two shift parameters i and j which determine the distance between the centers of two adjacent clusters. When you move from a center of a certain cell i cells along any chain of hexagons, then you turn counter–clockwise 60 degrees and move j cells along the new chain in that direction, you will reach a center of a new cluster, see Figure 2.2. Also, the previous two parameters determine the number of cells in each cluster which is equal to C [26]

$$C = i^2 + ij + j^2 \qquad (2.1)$$

Also, the number of cells per cluster is a parameter of major interest since it determines the number of mobile channels in each cell.

The distance between two cells, using the same frequency band, and belonging to two adjacent clusters is called the co–channel distance (D).
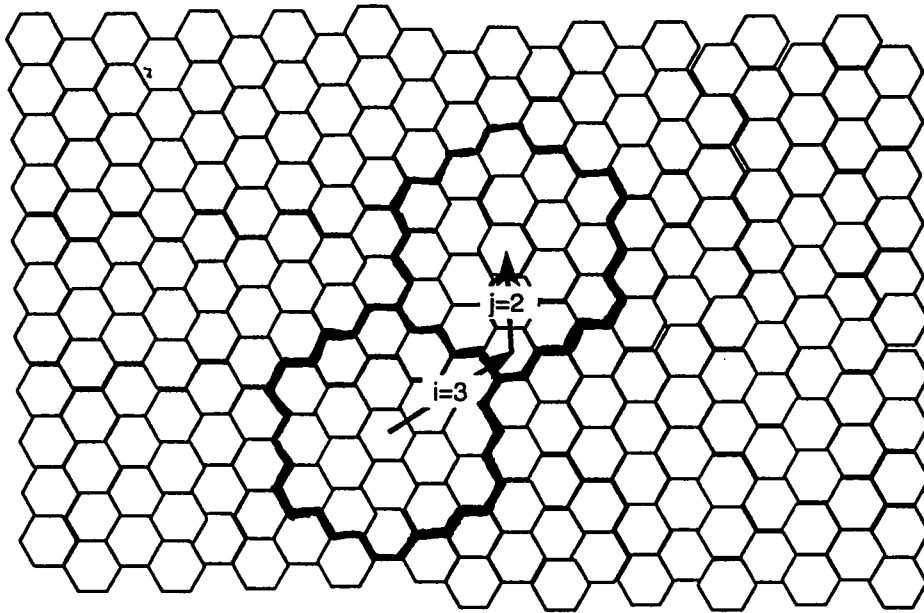
$$i = 3, \qquad j = 2$$

$$C = i^2 + j^2 + i\,j = 19$$

Figure 2.2 : Cellular system shift parameters.

The ratio of D to the radius of each cell (R) is called the co-channel reuse ratio or simply the reuse distance (Ru); see Figure 2.3. This ratio is related to the number of cells per cluster, C by the following relation [26]

$$Ru = D/R = \sqrt{3C}. \qquad (2.2)$$

For practical considerations the choice of the number of cells per cluster is governed by the co-channel interference. As the reuse distance increases the amount of co-channel interference decreases.

2.2.2 Frequency Reuse

Frequency reuse refers to the use of radio channels on the same carrier frequency to cover different areas which are separated from one another by sufficient distances to make the co-channel interference as small as possible. By the reuse of frequency, in cellular mobile telephone system, a number of simultaneous handled calls can be much greater than the allocated channel frequencies in a certain service area.

Frequency reuse is the core concept of the cellular mobile radio system. By this concept, users in different geographic locations (different cells) may simultaneously use the same frequency channel. Due to common use of the
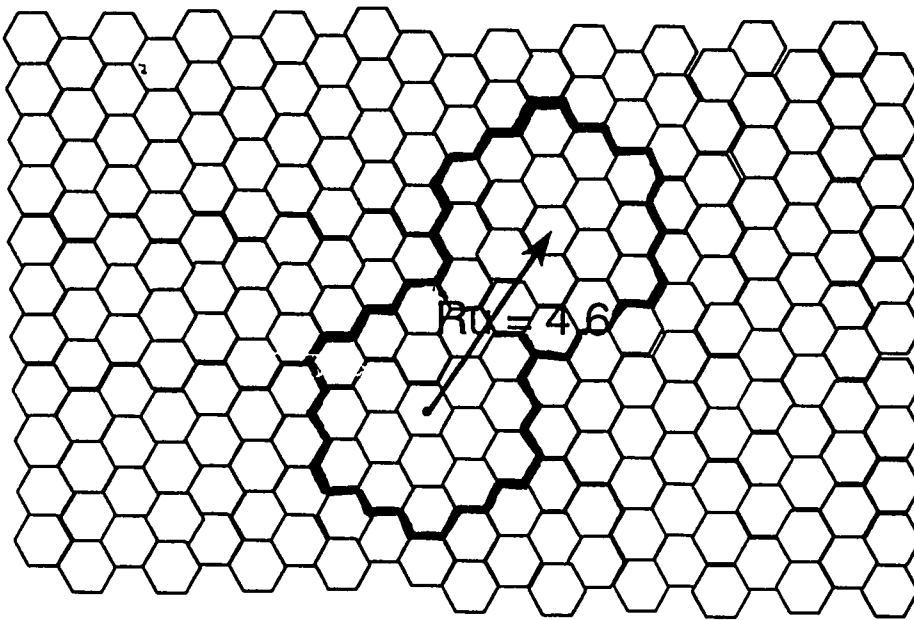
Figure 2.3 : Reuse distance.

same channel, co–channel interference will occur. Hence, co–channel inter-
ference is of major concern in the concept of frequency reuse. The minimum
distance D which allows the same frequency to be reused is dependent on
many factors such as the number of strong co–channel cells, the type of geo-
graphic region, the base station antenna height and the transmitted power.

2.2.3   Cell Splitting

In cellular mobile system, a certain area is divided into clusters, and
each cluster consists of C cells. The number of clusters in a certain region
depends on the number of users in that region because each cluster is serving
a fixed number of users. Since there is a fixed number of mobile channels in
a certain cell, the area of that cell is inversely proportional to its number of
users. When the telephone traffic demand in some cell reaches its capacity,
further increase in the demand of mobile telephone in that cell leads to
splitting that cell to smaller cells each serving the same number of users as
the large cells. Cell splitting, which is always accompanied with less height
antennas and less transmitted power, is a special process in cellular mobile
systems to treat the continuous increase in demand of this kind of service.
Usually, after cell splitting, the new cell radius is one–half the original cell

radius, see Figure 2.4. This will result into smaller cells each of which is serving almost the same number of subscribers as the old cells.

2.3 Microcellular Systems

Recently, the conventional cellular systems have shown their inability to cope with the overwhelming demand for mobile communication systems. Therefore, the concept of microcellular system was introduced. In this system, cells are subdivided into smaller cells each with its own base station but with less power and lower antenna heights. These small cells are called microcells.

Microcells are small cells which may be a small segment of a highway, a street along the side of a city block, or part of a park, where the teletraffic is high. Usually, microcells are with less area than conventional cells but with the same number of mobile radio channels.

For the performance of digital microcellular radio systems, an analytical model is developed [25]. In the model, the presence of co-channel interference and additive white Gaussian noise is assumed. The modulation schemes considered are BPSK, BFSK, and QPSK. In the paper narrowband mobile communication channels are considered. UHF ground wave path loss,

Smaller
cells

Original cell
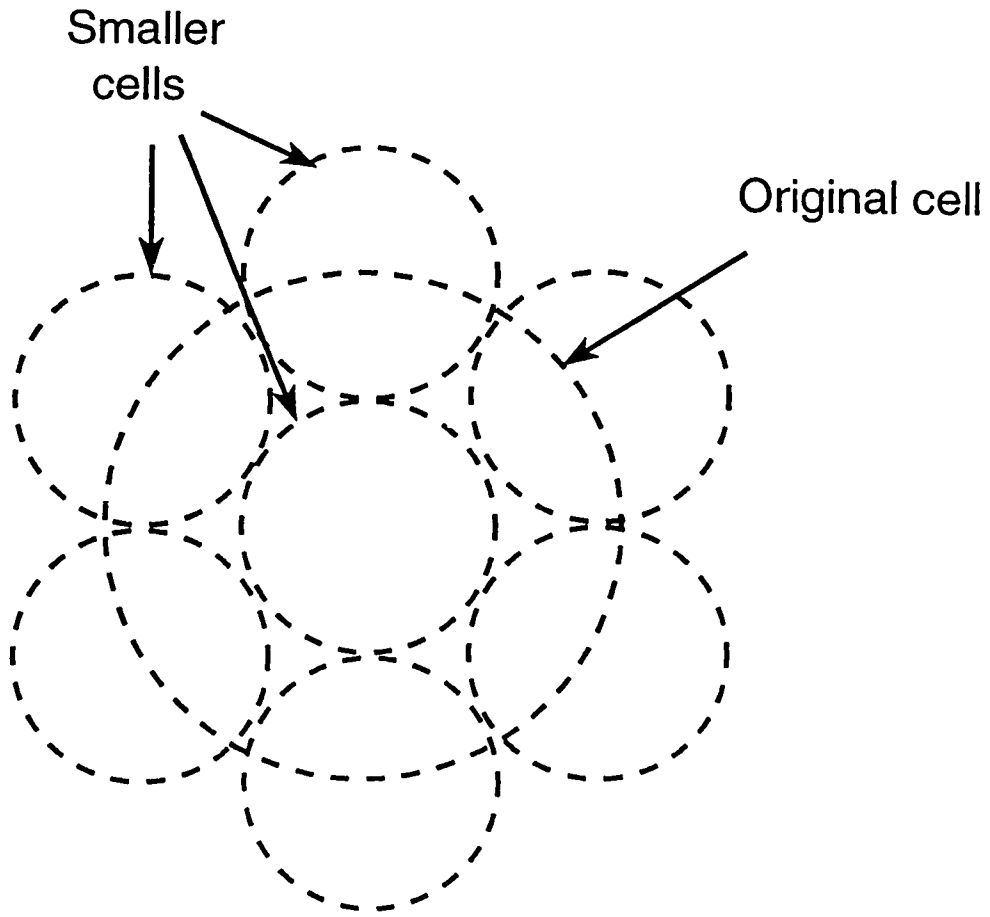
Figure 2.4 : Cell splitting.

multipath fading, and shadowing were considered as the three different and mutually independent propagation phenomena influencing the power of the received signal in cellular mobile radio.

The received signal area–mean power P_r is described by the dual path loss law with a turning point g [25]

$$P_r = cP_t \frac{r^{-a}}{\left(1 + \frac{r}{g}\right)^b} \tag{2.3}$$

where c is a constant, P_t represents the transmitted power, a represents the basic propagation loss exponent for short distances, and the exponent b represents the additional propagation loss exponent for distances greater than the turning point g.

In a mobile channel, the locally received signal level is modeled by a Rician distribution. So, the instantaneous signal power has the following pdf around the local–mean power p_{od} [25]

$$f_{pd}(p_d/p_{od}) = \frac{1}{\sigma_{r,d}^2} \exp\left(-\frac{2p_d + s^2}{2\sigma_{r,d}^2}\right) I_0\left(\frac{\sqrt{2p_0 s^2}}{\sigma_{r,d}^2}\right) \tag{2.4}$$

where s is the line–of–sight component of the desired signal, $\sigma_{r,d}^2$ is the local–mean power of the reflected component and $I(\cdot)$ is the Bessel function of the first kind and zeroth order. Also, the local–mean power is $p_{od} = \frac{1}{2}s^2 + \sigma_{r,d}^2$.

On the other hand, the interfering signals arrive from larger distances

where their line–of–sight components are assumed to be negligible. Hence, the locally received signal of an interferer is assumed to have a Rayleigh pdf, and as a result of that the instantaneous power will be exponentially distributed about the local–mean power p_{oi}

$$f_{pi}(p_i/p_{oi}) = \frac{1}{p_{oi}} \exp\left(-\frac{p_i}{p_{oi}}\right).$$

(2.5)

Moreover, the interfering signals propagate over obstructed paths, so they experience significant shadowing and p_{oi} is assumed to be lognormally distributed around the area mean power $\overline{p}_{oi}$

$$f_{p_{oi}}(p_{oi}/\overline{p}_{oi}) = \exp\left[-\frac{1}{2\sigma_i^2} \ln^2\left(\frac{p_{oi}}{\overline{p}_{oi}}\right)\right]$$

(2.6)

where σ_i represents the logarithmic standard deviation of the shadowing. However, the desired signal is assumed not to suffer from any shadowing effect.

Coherent addition of co–channel interferers is assumed. So, if we have n active co–channel interferers at a certain instant of time, each with a Rayleigh distribution with a local mean power p_{oi} the net effect of co–channel interference is a Rayleigh distribution with mean power equal to the sum of local mean interference powers. Since the local mean power p_{oi} is lognormal-lay distributed, the sum of several lognormal signals is another lognormal

signal with different logarithmic standard deviation and logarithmic mean, σ_n and m_n respectively [14], [37], [27].

For a BPSK detector, the received signal $r(t)$ is multiplied by a locally generated cosine wave and integrated over the entire bit duration.

In [28], only interfering signals from the nearest neighboring six co-channel cells are considered. Out of the six co-channel cells only n of them are active during any instant of time. The probability of n active co-channel cells is [28]

$$F_n(n) = \begin{pmatrix} 6 \\ n \end{pmatrix} a_c^n (1 - a_c)^{6-n} \qquad (2.7)$$

where $a_c = A_c/n_c$, A_c is the carried traffic and n_c is the number of channels in a cell.

The joint interference–plus–noise sample has a Gaussian distribution with zero mean and $(p_n + N_0/T_b)$ variance, where $p_n = \sum_i p_{oi}$ with $i = 1, \ldots, n$ is the local-mean power of the total n co-channel interferers, N_0 is the noise spectral density, and T_b is the bit duration. The conditional BER for a receiver locked to the desired signal in case of BPSK modulation is

$$p_e(e/p_d, p_n) = \frac{1}{2}\text{erfc}\left(\sqrt{\frac{p_d T_b}{p_n T_b + N_0}}\right) \qquad (2.8)$$

where erfc($\cdot$) represents the complementary error function.

Using the variable y defined as

$$y = \frac{1}{\sqrt{2}\sigma_n} \ln\left(\frac{p_n}{\bar{p}_n}\right) \qquad (2.9)$$

and the normalized reuse distance defined as

$$Ru = D/R = (3C)^{1/2} \qquad (2.10)$$

where D represents the nearest distance between two co–channel cells, R represents the cell radius, and C represents the number of cells per cluster, the reciprocal of the local–mean total received signal to interference–plus–noise ratio $\bar{\gamma}$ at the receiver is found to be

$$\frac{1}{\bar{\gamma}} = \frac{p_n + N_0/T_b}{(K+1)\sigma_{r,d}^2} = 10^{m_n/10} R_u^{-a} \left(\frac{g+R}{g+RuR}\right)^b \cdot$$
$$\cdot \exp(\sqrt{2}y\sigma_n) + \frac{N_0/T_b}{\sigma_{r,d}^2(1+K)} \qquad (2.11)$$

where $\sigma_{r,d}^2(1+K)/(N_0/T_b)$ is the local–mean signal–to–noise ratio, and m_n and σ_n are the logarithmic mean and logarithmic standard deviation, respectively, of the area–mean power of n interfering signals, as we defined previously. Also, K is the Rician factor

$$K = \frac{s^2}{2\sigma_{r,d}^2} \qquad (2.12)$$

With the instantaneous signal–to–interference–plus–noise ratio γ defined as

$$\gamma = \frac{p_d}{\bar{p}_n \exp(\sqrt{2}y\sigma_n) + N_0/T_b} \qquad (2.13)$$

the bit error rate $p_e(r)$ is

$$p_e(r) = \frac{1}{\sqrt{\pi}} \sum_n \binom{6}{n} a_c^n (1 - a_c)^{6-n} \int_{-\infty}^{\infty} \int_0^{\infty} \frac{1}{2} \operatorname{erfc}(\sqrt{\gamma}) \frac{(K+1)}{\bar{\gamma}} \cdot$$

$$\cdot \exp\left(-y^2 - \frac{\gamma(K+1)}{\bar{\gamma}} - K\right) I_0 \left(\sqrt{\frac{4\gamma K(K+1)}{\bar{\gamma}}}\right) d\gamma dy \quad (2.14)$$

In Figure 2.5, the area–mean BER with BPSK modulation is given as a function of the normalized reuse distance (Ru) where $K = 6$ dB, $A_c = 5$ Erlang, $n_c = 10$ channels per cell, $G = 0.67$ and σ_s is taken to be a parameter [25]. Figure 2.6 shows the relation between the local–mean BER and the local–mean SNR [25].
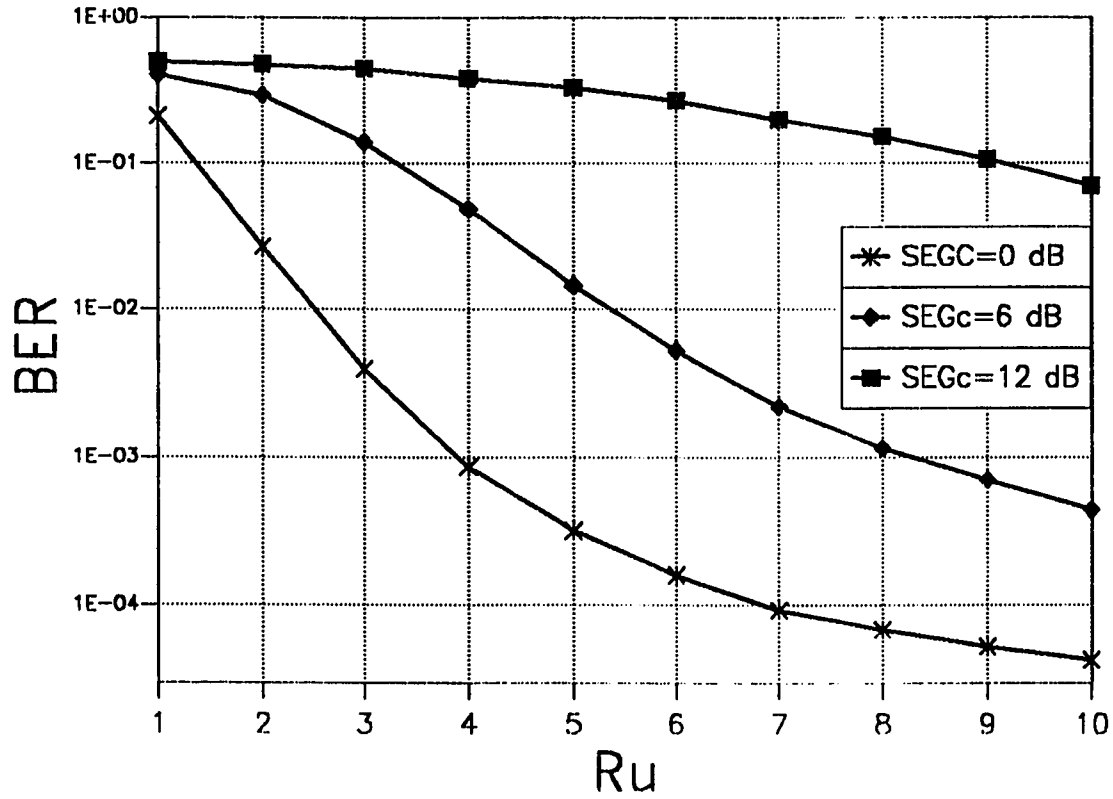
Figure 2.5 : BER versus Ru for $K = 6dB$, $A_c = 5$ **Erlang,** $n_c = 10$ **channels per cell, and a)** $\sigma_c = 0\,dB$, **b)** $\sigma_c = 6\,dB$, **c)** $\sigma_c = 12\,dB$.
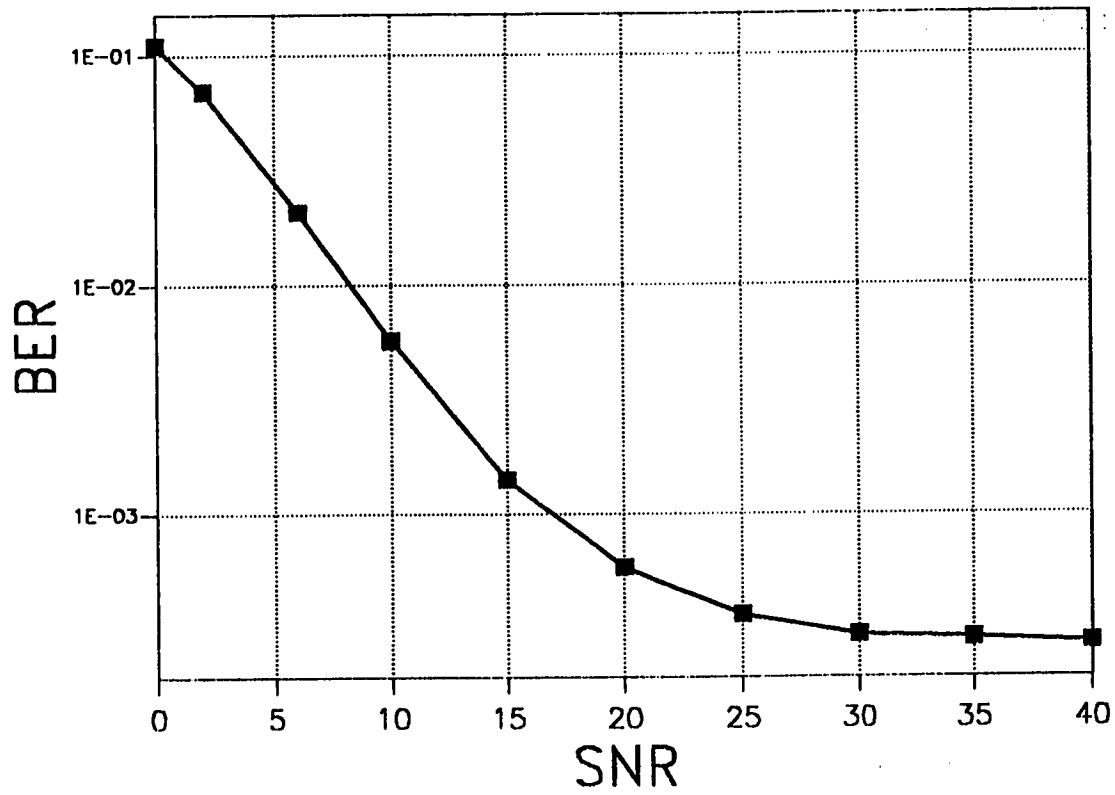
Figure 2.6 : BER versus SNR for $Ru = 5, K = 6dB$, $A_c = 5$ **Erlang,** $n_c = 10$ **channels per cell and** $\sigma_c = 0\,dB$.

CHAPTER 3

MOBILE FADING CHANNELS AND
COUNTER–MEASURES

3.1   Multipath Fading

Radio communication links are often subjected to multipath fading in which the wave can take more than one path when it is propagating from the transmitter to the receiver. Each path will change the amplitude and the phase differently. Also, each path has a different length from the others resulting in different delays for the received signal. The previous phenomenon is called signal spreading. Moreover, the nature of each path characteristic is time–variant which gives rise to undeterministic formulation of the received signal.

The multipath fading in mobile radio is caused by reflection and scattering from buildings, trees and other obstacles along the paths. Hence, radio waves arrive at a mobile receiver from different directions, with different delays. These waves combine vectorially at the receiver antenna to give a resultant signal which depends totally on the multipath characteristics at

a particular time. The combination of waves can happen either constructively or destructively. In addition, there is a relative motion, between the transmitter and the receiver due to the mobile unit motion with different speeds in different directions, which will make the resultant received signal change rapidly. Therefore, the mobile radio channel can have the following time–variant impulse function [32]

$$h(\tau, t) = \sum_n \alpha_n(t) \exp[-j2\pi f_c \tau_n(t)] \cdot \delta(\tau - t_n) \qquad (3.1)$$

where $\alpha_n(t)$ is the attenuation factor for the signal received on the n–th path, $\tau_n(t)$ is the propagation delay for the n–th path and f_c is the carrier frequency.

Due to the continuous change of the channel medium properties and the moving of the mobile unit, $\alpha_n(t)$ and $\tau_n(t)$ are random processes [32]. When there are large number of paths, the central limit theorem can be applied and the received signal, when the transmitted signal is unmodulated carrier $r(t)$ can be modeled as a complex-valued Gaussian random process in the t variable

$$r(t) = \sum \alpha_n(t) e^{-j2\pi f_c \tau_n(t)} \qquad (3.2)$$

The amplitude variation of this received signal is called signal fading.

When the impulse response $C(\tau, t)$ is modeled as a complex–valued Gaus-

sian process, the envelope $|C(\tau, t)|$ at any instant of time is either Rayleigh–distributed or Rician–distributed depending on whether the mean of the complex–valued Gaussian process is zero or non–zero. Usually, when there is no line of sight between the base station antenna and the antenna of the mobile unit, which is the case with cellular mobile, the mean of the complex–valued Gaussian process is equal to zero, because there is no direct path. Hence, the mobile channel is said to be a Rayleigh–fading channel.

On the other hand, if there is a line of sight between the transmitter and the receiver, the mobile channel is said to be a Rician–fading channel.

3.2 Mobile Radio Environment

Over relatively short distances the received mean signal is essentially constant, but the received signal level can vary rapidly. These rapid variations are known as fast fading.

If you consider a BS transmitting an unmodulated carrier which covers the whole cell in which a MU is travelling, the MU does not receive one version of the transmitted carrier. However, it receives a number of signals which are reflected and diffracted by buildings and other urban con-

structions. Actually, in most environments, each version of the transmitted signal received by the MU is subjected to a specific time delay, amplitude, phase and Doppler shift depending on its path from the BS to the MU.

As a result of that, the constant amplitude carrier transmitted signal may be substantially different from the signal the MU receives. When the signals from various paths sum constructively at the MU antenna, the received signal is enhanced. However, when the multipath signals vectorially sums to a small value, we say that the received signal is in a fade and this phenomenon is called multipath fading. As the MU travels it passes through an electromagnetic field which results in the received signal level experiencing fades approximately every half wavelength along its route. When a very deep fade occurs, the received signal is essentially zero and the receiver output is composed of the channel noise only.

The above discussion relates to the transmission of unmodulated carrier. However, with digital mobile communications the propagation phenomena are highly dependent on the ratio of the symbol duration to the delay spread of the time variant mobile radio channel. The delay spread may be considered as the length of the received pulse when an impulse is transmitted and it is the reciprocal of the coherent bandwidth of the channel. We can see

that if we transmit data at a slow rate the data can easily be resolved at the receiver because the extension of a data pulse due to the multipath is completed before the next impulse is transmitted. However, if we increase the transmitted data rate a point will be reached where each data symbol significantly spreads into adjacent causing an intersymbol interference ISI. Hence, the bit error rate may become unacceptably high.

The propagation waves in mobile systems are affected by three different factors:

1. Propagation path loss law

2. Slow fading statistics

3. Fast fading statistics

The first factor determines the area–mean power of the signal. Moreover, in a small area a mobile radio signal $r(t)$ can be characterized by two components $m(t)$ and $r_0(t)$. So, $r(t)$ can be written as [22]

$$r(t) = m(t)r_0(t) \tag{3.3}$$

The component $m(t)$ is called local mean or long–term fading. The $r_0(t)$ is known as multipath fading or short–term fading. The long–term fading

$m(t)$ can be expressed from the following equation [22]

$$m_t = \frac{1}{2T} \int_{t_0-T}^{t_0+T} r(t)dt \qquad (3.4)$$

where $2T$ is the time interval for averaging $r(t)$. T can also be determined based on the fading rate of $r(t)$, which is 40 to 80 fades per second. Moreover, the long–term fading can be explained in spatial domain as [22].

$$m(x_0) = \frac{1}{2L} \int_{x_0-L}^{x_0+L} r(x)dx \qquad (3.5)$$

where the length of $2L$ is taken to be 20 to 40 wavelengths.

The variation of the first component is due to the terrain contour between the base station and the mobile unit. This factor is known also as signal shadowing and is characterized by log–normal distribution.

As the distance between the base station (BS) and the mobile unit (MU) increases, the received signal level decreases. This decrease in signal level is due to two reasons. First, in free space the received power p_r is

$$p_r = p_t G_t G_r \left(\frac{\lambda}{4\pi d}\right)^2 \qquad (3.6)$$

where p_t is the transmitted power, G_t and G_r are the gain of the transmitter antenna and the gain of the receiver antenna, respectively, λ is the wavelength of the carrier wave and d is the distance between the transmitter and the receiver. Hence, as d increases p_r decreases with different rates.

In cities there are losses in power due to reflection, diffraction around structures and refraction within them. Hence, the path loss law depends on the environment in which the transmission happens and the range of distances between the MU and the BS. Also, the path loss depends on the height of the BS antennas.

3.3 Classification of Mobile Fading

Generally, characterizing the mobile radio channel is a very difficult task. However, this problem is dealt with in two fronts. Firstly, when the signals occupy a narrow bandwidth much less than the coherence bandwidth of the channel, the spread of time delays in the multipath environment is sufficiently small. This means that spectral components within the transmitted message ar affected in a similar way. This case is known as frequency non-selective fading.

However, when the bandwidth of the transmitted signal is comparable to the coherence bandwidth of the mobile channel, the spectral components of the transmitted signal are changed differently. This case is known as frequency-selective fading.

3.4 Fading Counter Measures

3.4.1 Diversity

To improve the reliability of communications on wireless frequency-selective fading channels, some measurers have to be employed to reduce the effects of Intersymbol Interference (ISI) produced by the multipath delay spread. Some of the counter measures that can be taken are combining equalization and diversity [32].

Since reducing the power consumption in the mobile receivers is an important goal of some applications, the equalization is not highly recommended. However, the advances in low-powered integrated circuits technology have changed the case and made it practical to use equalization to improve the performance of mobile communication systems.

Diversity reception is a useful technique for combating multipath fading in radio transmission [18], [3]. Several antennas are used to give us space diversity. The antennas are separated from each other by at least one half the wavelength of the carrier to ensure the reception of statistically independent signals.

Because the received signals are statistically independent there is a good chance that they will not fade at the same time [5].

Diversity combining is used to improve the performance of mobile communication systems without an increase in the power consumption or bandwidth allocated for transmission. However, it adds complexity to the receivers.

In high capacity mobile radio systems, the reduction of co–channel interference may be the most important advantage of diversity. The use of diversity combining to suppress the effects of co–channel interference in cellular mobile radio systems is investigated in [2], and [8].

Although diversity combining is used to combat multiplicative frequency-non–selective fading, it also improves the performance of mobile communication systems in the presence of frequency–selective faded received signals [45].

3.4.2 Error Control Coding

To provide more reliable transmission of digital information over the channel, error control coding is used to facilitate error detection and error correction at the receiver. The channel encoder accepts message bits and adds redundancy according to a prescribed rule. At the receiver side the decoder exploits the redundancy to decide which message bit actually transmitted. Thus error control coding minimizes the effect of channel noise [39].

Generally, error correction codes can be classified as block codes and convolutional codes. In the first class, which is block codes, the channel encoder accepts information in successive k-bit blocks, and adds $(n - k)$ redundant bits, which are related to the k message bits algebraically. As a result of that a code word, consisting of n bits, is generated for each k message bits. The code rate for an (n, k) block code is k/n.

Golay Codes [24]

As an example of cyclic codes we have the Golay (23, 12) code which has a block length equal to 23 digits out of which 12 digits are information symbols. This code has the capability of correcting any combination of three

or less random errors. The Golay (23, 12) code can be generated by either $g_1(x)$ or $g_2(x)$ where

$$g_1(x) = 1 + x^2 + x^4 + x^5 + x^6 + x^{10} + x^{11} \tag{3.7}$$

and

$$g_2(x) = 1 + x + x^5 + x^6 + x^7 + x^9 + x^{11} \tag{3.8}$$

Bose–Chaudhuri–Hocquenghem (BCH) Codes [24]

The BCH codes are the best constructive famialy of codes for channels in which errors affect successive symbols independently. They are part of the cyclic codes and can be described in terms of generator polynomial. The BCH parameters are block length

$$n = 2^m - 1; m = 3, 4, 5, \ldots \tag{3.9}$$

Information digits: $k \geq n - mt$ and minimum distance $d_{min} \geq 2t + 1$ where any (n, k, d_{min}) can correct any combination of t symbol errors occurring in a block of n symbols. Also, some BCH codes beside correcting any combination of t errors, it can also correct part of the $(t + 1)$ error combinations. The BCH (15, 7) code has a minimum distance equal to 5 and is capable of correcting any combination of two or fewer random errors. In addition, it can correct some combinations of three errors. This code can be generated

using the generator polynomial

$$g(x) = 1 + x^4 + x^6 + x^7 + x^8 \tag{3.10}$$

On the other hand, the BCH (15, 11) code has the capability of correcting any single random error in a block of 15 digits. It has a rate equal to 11/15 and can be generated using the generator polynomial

$$g(x) = 1 + x + x^4 \tag{3.11}$$

Block Encoder

The encoding of cyclic codes involves three operations: (1) multiplying the message polynomial $m(x)$ by x^{n-k}, (2) dividing the result by the generator polynomial $g(x)$ and obtaining the remainder polynomial of this division as $b(x)$, and (3) adding $b(x)$ to $x^{n-k}m(x)$ to form the desired code word polynomial $c(x)$. The previous three operations are implemented using the following encoding circuit which is shown in Figure 3.1. The circuit is composed of $(n - k)$ delay elements, a gate, and $n - k$ modulo–2 adders. Through k transitions the message bits are shifted into the channel, while the gate is switched on to allow the division operation in the circuit. As a result of the division, the coefficients of the remainder polynomial $b(x)$ are at the $(n - k)$ registers. Then, through $(n - k)$ transitions, while the gate is switched off, the contents of the registers are shifted into the channel [20].
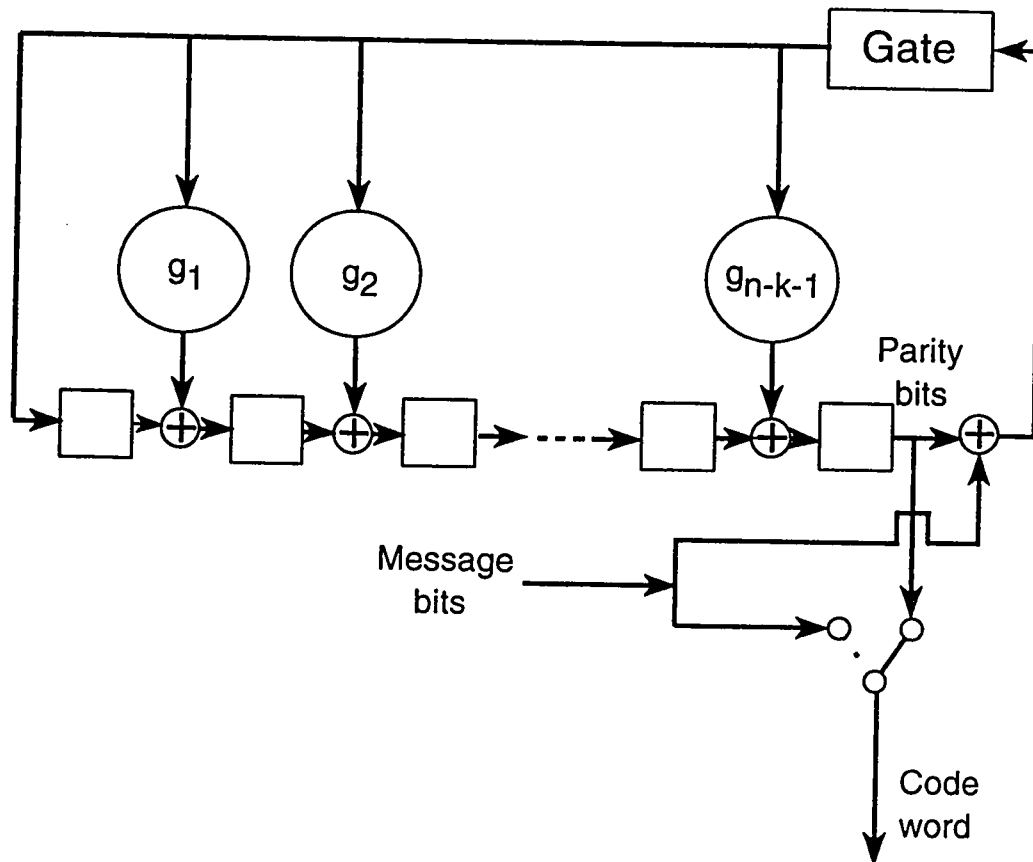
Figure 3.1 : Block encoder circuit.

Block Decoder

When the code word $c(x)$ is transmitted over a mobile communication channel some of the code words digits are changed due to multipath fading and additive noise. So, the received word polynomial is $r(x)$. The rule of decoder is to map the received word to one of the code words which is most likely the transmitted code word.

The decoder uses the received word to calculate what is called the syndrome polynomial $s(x)$. If the syndrome is equal to zero, the decoder will conclude that there is no transmission error. Otherwise, if the syndrome is non–zero, the received word contains transmission errors which require correction. The correction is done if the error pattern is known to the receiver.

For cyclic codes the calculation of the syndrome polynomial is done using the generator polynomial of the code. The syndrome polynomial is the remainder of dividing the received word polynomial on the generator polynomial

$$s(x) = r(x) - a(x)g(x) \tag{3.12}$$

The circuit shown on Figure 3.2 is used to calculate the syndrome polynomial coefficients [20].
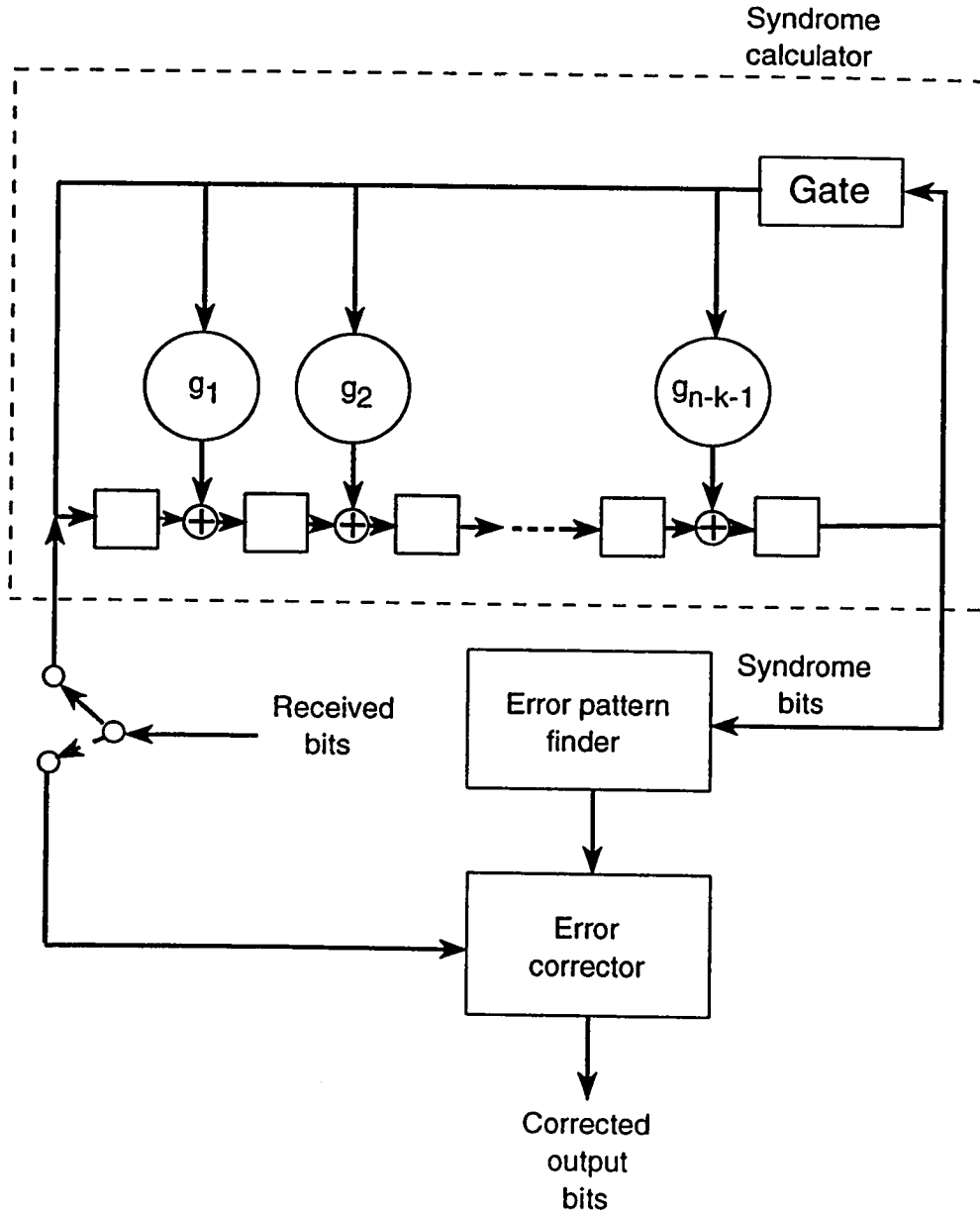
Figure 3.2 : Block decoder circuit.

The circuit is composed of $(n-k)$ delay elements (registers) and a gate. First, the gate is switched on and through n transitions, the received word is shifted into the $(n-k)$ registers. As a result of that, the syndrome coefficients are in the registers. Then the $(n-k)$ coefficients are used by another circuit in the decoder to reorganize the error pattern.

3.4.3 Interleaving

In mobile radio systems, transmission errors do not occur at random, but occur in clusters or bursts, due to fading, co-channel interference, or use of certain modulation schemes such as DPSK. Our codes, e.g. BCH and Golay codes, are designed to combat random errors and not burst errors. Hence, we combined interleaving with coding to combat burst errors as well as random ones. Since our codes are block codes it is appropriate to use block interleaving with this kind of codes [32], [20].

An $n \times n$ block interleaver is used in our receiver. The interleaver comes between the block encoder and the modulator. It receives m codewords from the encoder and stores them on an $n \times m$ array row-wise. Then reads the array column-wise and passes the column of length m bit by bit to the modulator. At the receiver the deinterleaver comes between the demodu-

lator and the decoder to do the reverse operation of the interleaver at the transmitter.

Most of the well-known codes that have been devised to increase the reliability of communication systems are effective when the errors caused by the channel are statistically independent, which is the case with the additive white Gaussian noise (AWGN). However, the class of channels characterized by multipath and fading, such as mobile radio channels, exhibits bursty errors. Signal fading due to time variant multipath propagation often causes the signal to have a large number of errors clustered together.

To deal with burst error channels, we transform the coded data in such a way that the channel errors will occur independently. This process is called interleaving. The interleaver comes after the channel encoder to record the encoded data and change their sequence and output them to the modulator. Then the deinterleaver, at the receiver, comes after the demodulator to put the data in a proper sequence and passes it to the decoder, see Figure 3.3.

The interleaver can take a form of a block structure. A block interleaver arranges the encoded data in a rectangular array of m rows and n columns. Each row is a code word of length n. This array is composed of m code words. After this arrangement the bits are read column-wise and transmitted over the mobile radio channel. At the receiver side, the deinterleaver stores the
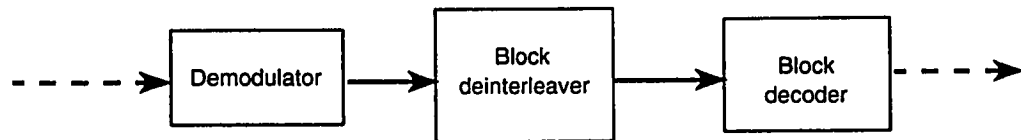
Figure 3.3 : Deinterleaver position.

data in the same array, column–wise. Then the data are read row–wise.

As a result of this interleaving, a burst of errors of length $\ell = mb$ is broken up into m bursts of length b. Therefore, an (n, k) code that can handle burst errors of length $b \leq [(n - k)/2]$ can be combined with an interleaver of degree m to create an interleaved (mn, mk) block code which can handle burst errors of length mb.

3.4.4 Equalization

Generally, when the size of the cell is decreased the delay spread decreases, enabling us to increase the transmitted symbol rate while still maintaining flat fading conditions. However, with very high symbol rate the channel becomes dispersive which results in intersymbol interference (ISI). A modest amount of ISI can be combatted using symbol interleaving and channel coding. When the ISI becomes severe it is essential to mitigate its effects by using channel equalization [45], [32]. Because ISI is a time domain effect, the design of efficient equalization techniques has to be done in the time domain. Time domain equalizers consist of delay elements with tap gains; simply, tapped–delay line filters. The simplest type of time domain equalizers is the adaptive linear equalizer which has $2K + 1$ taps. A general

form of adaptive linear equalizers is shown in Figure 3.4. The tap gains of this type equalizers are updated according to certain criteria. As you see from the figure, the input of the equalizer is the sequence $\{V_k\}$ and its output is the estimate of the information sequence $\{I_k\}$.

The estimate of the k–th symbol may be expressed as

$$\hat{I}_k = \sum_{j=-K}^{K} C_j V_{k-j} \qquad (3.13)$$

where $\{C_j\}$ are the $(2K+1)$ tap weight coefficients of the filter. The estimate $\hat{I}_k$ is quantized to the nearest information symbol to form the decision $\tilde{I}_k$. If $\tilde{I}_k$ is not identical to the transmitted information symbol I_k, an error has been made.

Considerable research has been performed on the criterion for optimizing the filter coefficients $\{C_k\}$. Since the most meaningful measure of performance for a digital communications system is the average probability of error, it is desirable to choose the tap gains to minimize this performance index. However, this performance index is a highly nonlinear function of the tap gains $\{C_k\}$ [9]. Hence, the probability of error is impractical index for optimizing the tap weight coefficients. The criterion which has found widespread use in optimizing the equalizer coefficient is to minimize the mean square error between the output of the equalizer and the transmitted
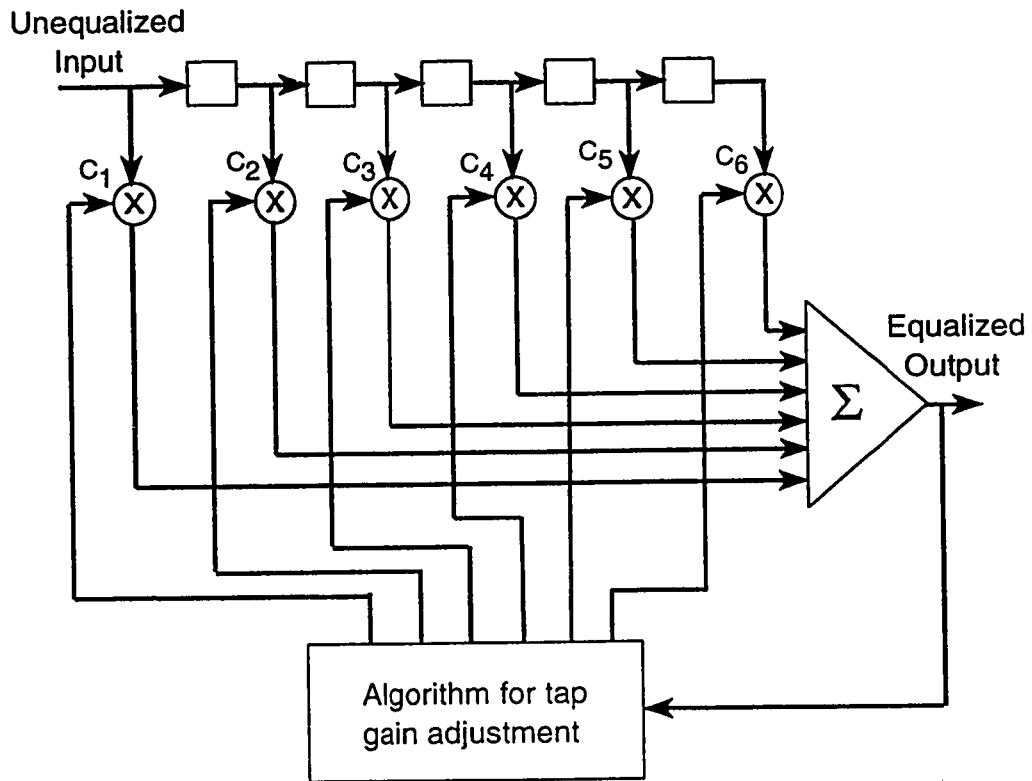
Figure 3.4 : Adaptive linear equalizer.

symbol. Since the transmitted symbols are not known at the receiver, a training sequence, known to both ends, is transmitted first to set gains at their appropriate levels prior to data transmission.

For linear equalizers the delay element value is T. One of the conditions that must be met when dealing with these equalizers is the need for accurate timing at the sampling process. Any error in the timing will cause the problem of aliasing or spectral overlap. Ideally, to remove the ISI completely, an infinite number of taps is needed. However, in multipath fading the multipath spread only over few symbols, short equalizers with few taps can be used.

The Least–Mean–Square Algorithm

Least mean squares (LMS) criterion for updating tap gains of equalizers is very commonly used in many applications. This criterion is explained as follows. Let $x(i)$, $y(i)$ and $z(i)$ denote the transmitted, received and equalized real-valued symbols, respectively. Then

$$z(i) = \sum_{k=-K}^{K} c(k)y(i-k) \qquad (3.14)$$

and the error signal is defined as

$$e(i) = x(i) - \sum_{k=-K}^{K} c(k)y(i-k) \qquad (3.15)$$

The expected value of this error signal is

$$\epsilon = E[(x(i) - \sum_{k=-K}^{K} c(k)y(i-k))^2] \qquad (3.16)$$

where $\{c(k)\}$ is a set of equalizer coefficients. The MSE criterion is based on minimizing the quantity ϵ. This can be done using the gradient method.

The update of the tap gains will be according to

$$\mathbf{C}(i+1) = \mathbf{C}(i) + \alpha E[e(i)\mathbf{Y}(i)] \qquad (3.17)$$

Now the problem is how to find $E[e(i)\mathbf{Y}(i)]$. However, an unbiased estimator is used to estimate this vector quantity. The unbiased estimator is the product $e(i)\mathbf{Y}$. The use of such an estimator leads to what is called the least mean squares (LMS) criterion which defines the following algorithm to update the tap gains of linear equalizer.

$$\mathbf{C}(i+1) = \mathbf{C}(i) + \alpha e(i)\mathbf{Y}(i) \qquad (3.18)$$

So, each coefficient is updated as follows

$$c_k(i+1) = c_k(i) + \alpha e(i)y(i-k) \qquad (3.19)$$

The convergence of properties of the LMS algorithm are governed by the step–size parameter α. The LMS algorithm is convergent in the mean square

provided that α satisfies the condition

$$0 < \alpha < \frac{2}{\displaystyle\sum_{k=-K}^{K} \lambda_k} \qquad (3.20)$$

where $\displaystyle\sum_{k=-K}^{K} \lambda_k$ is the sum of eigenvalues of the correlation matrix $\mathbf{R}_y$. Since

the sum of the eigenvalues of correlation matrix $\mathbf{R}_y$ is explicitly known to

be

$$\sum_{k=-K}^{K} \lambda_k = (2K + 1)\mathbf{R}_y(0) = \text{ total average input power} \qquad (3.21)$$

We sum up, that the LMS algorithm is convergent if step size parameter α is

chosen properly between its limit 0 and 2/(total average input power) [20].

When the LMS algorithm operates in a stationary environment, the error

performance surface has a constant shape as well as orientation. Then,

starting with zero initial conditions, the algorithm proceeds in a step-by-

step fashion closer and closer to the bottom of the error surface without

prior knowledge of the statistical parameters of the environment. However,

in mobile communication channels we have a nonstationary environment.

Hence, the bottom of the error performance surface moves constantly, while

the orientation and curvature of the surface may be changing too. In such

a situation, the LMS algorithm has the added task of continually tracking

the bottom of the error–performance surface. It turns out that the larger

we make the adaptation constant α, the faster the tracking capability of the LMS algorithm. However, a large adaptation constant α may result in an unacceptably high excess mean–squared error. Therefore, when choosing a suitable value for α, a compromise should be made between fast tracking and low excess mean–square error. The excess error is that part of the mean–squared error in excess of the minimum attainable value ϵ_{min}.

CHAPTER 4

SYSTEM DESCRIPTION AND RESULTS

4.1 Baseband Representation

All mobile communication systems are bandpass in nature. The general form of bandpass signal, $S(t)$, having a carrier f_c is

$$S(t) = A(t)\cos[2\pi f_c t + \phi(t)] \tag{4.1}$$

where either, or both, of the amplitude, $A(t)$, and phase, $\phi(t)$ are used to carry the message information. $S(t)$ can be written as

$$S(t) = S_I(t)\cos(2\pi f_c t) - S_Q(t)\sin(2\pi f_c t) \tag{4.2}$$

where

$$S_I(t) = A(t)\cos[\phi(t)] \tag{4.3}$$

and

$$S_Q(t) = A(t)\sin[\phi(t)] \tag{4.4}$$

$S_I(t)$ and $S_Q(t)$ are called the in-phase and quadrature components, respectively.

The complex envelope $\hat{S}(t)$ which can be written as

$$\hat{S}(t) = S_I(t) + jS_Q(t) \tag{4.5}$$

is a baseband signal and carries the same information as $S(t)$.

It is easy to show that $S(t)$ can be written in terms of $\hat{S}(t)$ and f_c as

$$S(t) = Re[\hat{S}(t)\exp(j2\pi f_c t)] \tag{4.6}$$

Also, a bandpass system, $h(t)$, can be represented by its complex envelope, $\hat{h}(t)$, and the carrier frequency f_c

$$h(t) = 2Re[\hat{h}(t)\exp(j2\pi f_c t)] \tag{4.7}$$

where

$$\hat{h}(t) = h_I(t) + jh_Q(t) \tag{4.8}$$

On the other hand, noise in bandpass communication systems, $n(t)$, can be written as

$$n(t) = Re[\hat{n}(t)\exp(j2\pi f_c t)] \tag{4.9}$$

where $\hat{n}(t)$ is a low-pass equivalent noise $\hat{n}(t)$ can be written as a sum of two quadrature component

$$\hat{n}(t) = n_I(t) + jn_Q(t) \tag{4.10}$$

Usually, equivalent baseband models for modulated signals, systems, noise, and received signals are used in simulations which eliminate the need of simulating the carrier frequency component.

The baseband modulated signal is

$$S(t) = \sum_n C_n g(t - nT) \tag{4.11}$$

where $g(t)$ is the transmitting filter impulse response, and C_n defines the signal constellation with two point in the case of binary modulation BPSK and DPSK. The transmitting filter impulse response which satisfies the Nyquist frequency criterion is the raised cosine filter

$$g(t) = \frac{\sin(\pi t/T)}{\pi t/T} \frac{\cos(\beta \pi t/T)}{1 - 4\beta^2 t^2/T^2} \tag{4.12}$$

with, β, the rolloff parameter and T is the sampling period. The rolloff parameter is taken to be 0.35 which gives a 35% expansion to our bandwidth.

4.2 System Description

The system used in our simulation is shown in Figure 4.1. It consists of a source generator, a channel encoder, an $n \times n$ block interleaver, a modulator, a pulse shaping filter and a channel. Then at the receiver, we have a diversity combiner, a combined equalizer and demodulator, a deinterleaver, a channel
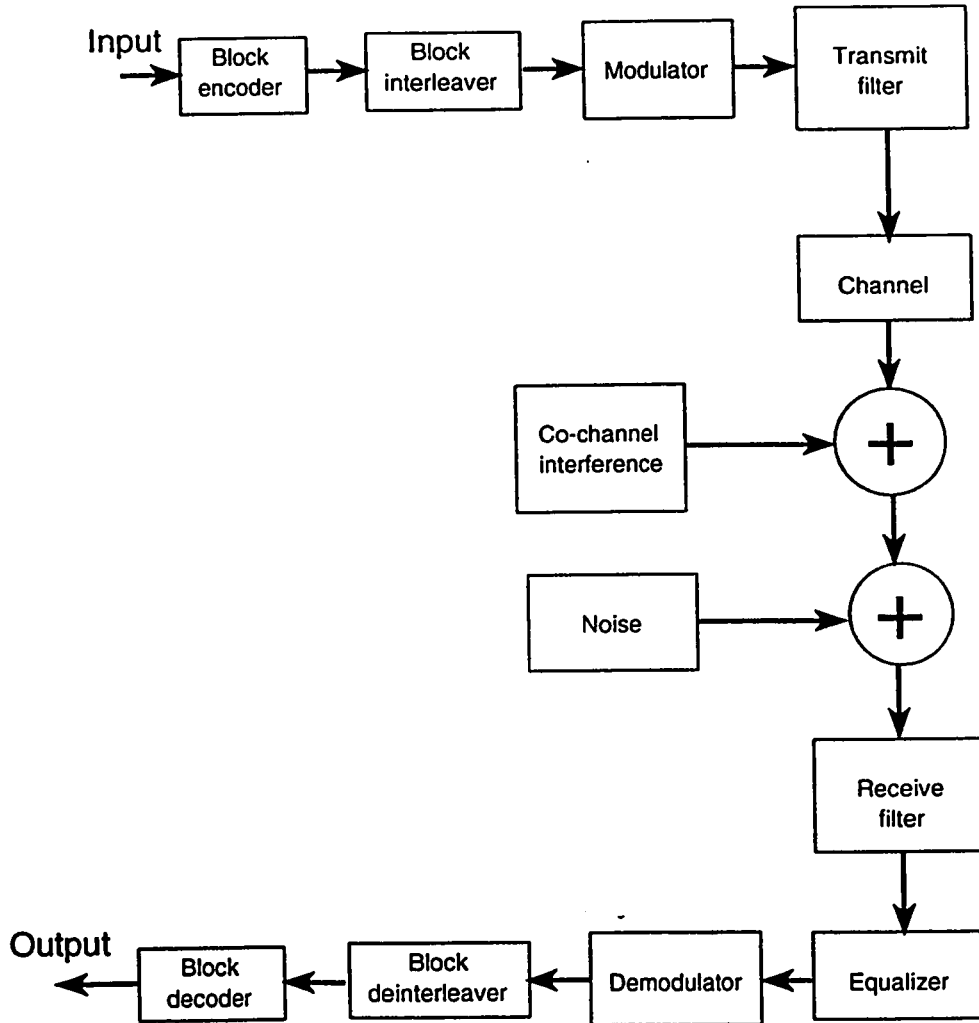
Figure 4.1 : The system block diagram.

decoder. Certain blocks such as a channel encoder and decoder, a diversity combiner and an equalizer are removed to test the performance of the system with and without them.

The source generator generates a stream of symbols which are assumed to be equally likely and statistically independent. Our source generator utilizes a uniform random generator to produce its symbols. Different channel encoders are used such as BCH (15, 11, 1), BCH (15, 7, 2) and Golay (23, 12, 3) codes. Since (n, k, t) block codes are used, it is appropriate to use an $n \times n$ block interleaver.

In the system, two different modulation schemes are used; namely, binary phase shift keying (BPSK) and differential phase–shift keying (DPSK). The pulse shaping (transmit) filter is used to limit the transmission bandwidth. This filter is a raised cosine filter with an excess bandwidth of 35% (roll–off factor β, equal to 0.35). A corresponding raised cosine filter is to be used at the receiver and it should be matched to the transmit filter. It is also used to limit noise.
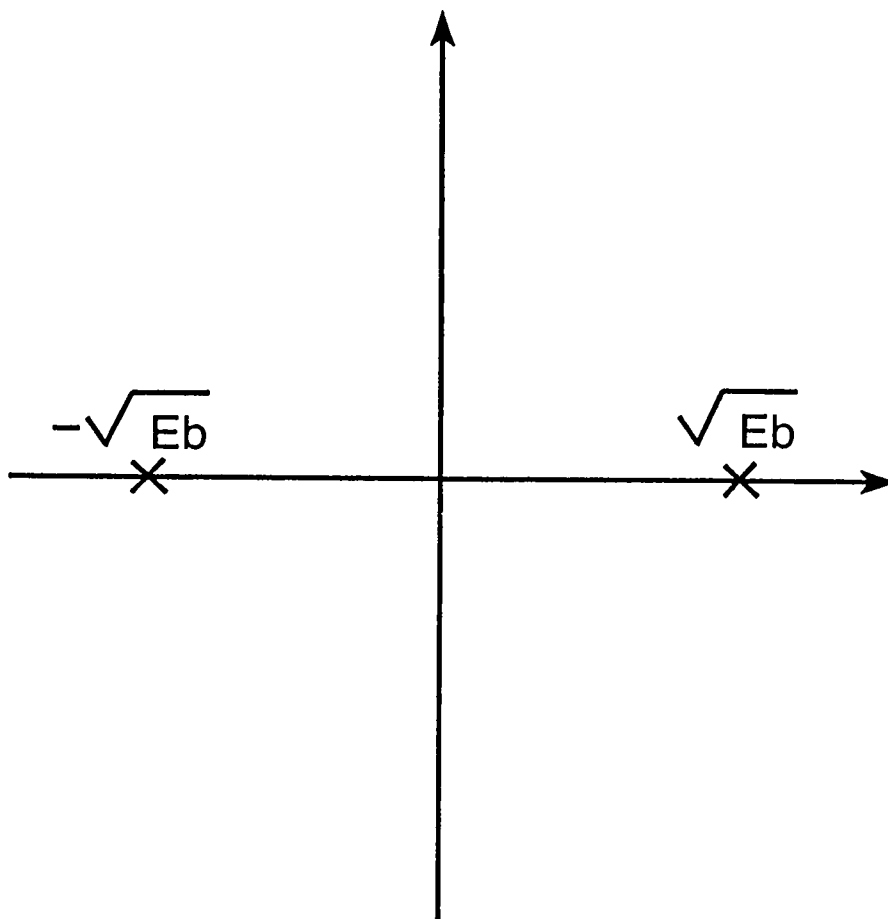
4.3 Modulation

The source generator generates a random steam of 0's and 1's and it simulates a general data source. After the source generator we have the channel encoder, which can generate a BCH or a Golay code as described in the last chapter. Then an $n \times n$ block interleaver is implemented after the channel encoder.

The output of the interleaver is fed to the modulator which can be a BPSK or a DPSK modulator. The signal is passed through the channel model which involves multipath fading and shadowing. The co–channel interference is added to the output of the channel plus some additive AWGN.

Throughout, our simulation baseband equivalent models are considered, without any loss of generality. Binary phase shift keying (BPSK) is considered as the modulation scheme. However, this kind of modulation needs coherent detection at the receiver side. Coherent detection is difficult in mobile radio environments because the time varying multipath fading complicates phase tracking. However, new methods are under investigation to facilitate near–coherent demodulation. Simply, the modulator is equivalent to signal space encoder. The modulator sends $\sqrt{E}$ when the message bit is 1 and $-\sqrt{E}$ when the message bit is 0; see Figure 4.2.
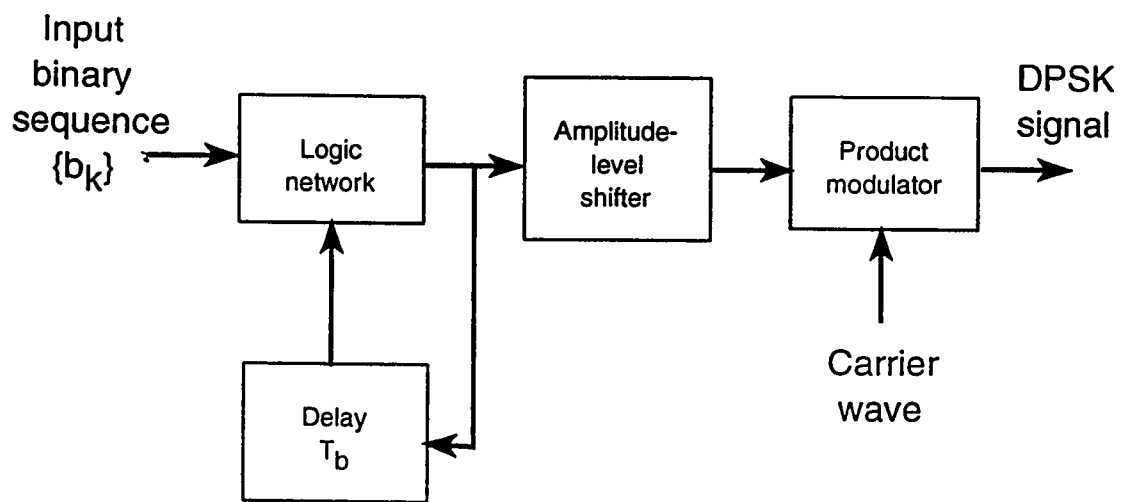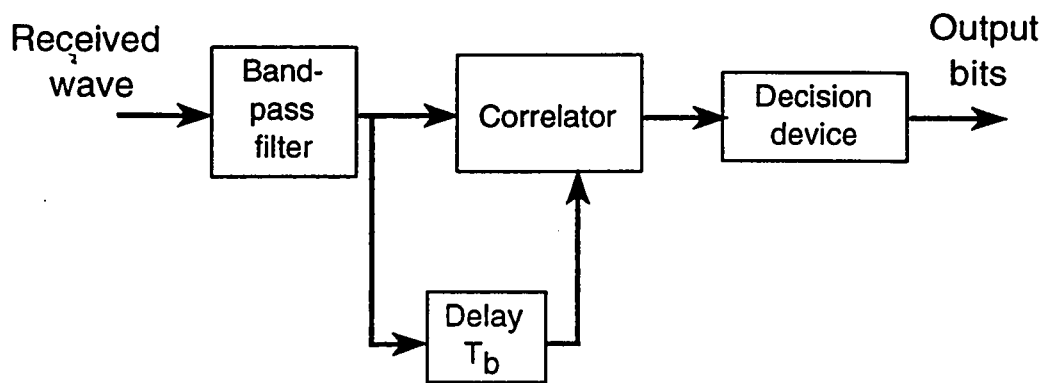
Figure 4.2 : Signal space diagram for BPSK modulation scheme.

The other type of modulation which will be used is the differential encoded phase shift keying (DPSK). The advantage of DPSK over many modulation types is that in DPSK no absolute phase reference is needed, only nearby constant carrier phase during two bit successive intervals is required. This property of DPSK makes it appropriate for a fading environment. DPSK eliminates the need for a coherent reference signal at the receiver by combining two basic operations at the transmitter: (1) differential encoding of the input binary wave, and (2) phase–shift keying [21] and [31]. Hence the name of differential phase–shift keying (DPSK) is given to this type of modulation. So, at the transmitter, to send a symbol 0 the current signal waveform phase is advanced by 180°. However, the phase of the current signal waveform is left unchanged when the symbol 1 is transmitted. The block diagram of the DPSK transmitter is shown on Figure 4.3

On the other hand, the receiver is equipped with a storage capability, so that it can measure the relative phase difference between the waveforms received during two successive bit intervals. The block diagram of the DPSK receiver is shown in Figure 4.4. Provided that the unknown phase θ contained in the received wave varies slowly, the phase difference between waveforms received in two successive bit intervals will be independent of θ.

Input
binary
sequence
$\{b_k\}$ → | Logic network | → | Amplitude-level shifter | → | Product modulator | → DPSK signal

| Delay T_b |

Carrier
wave

Figure 4.3 : Block diagram for DPSK transmitter.

Figure 4.4 : Block diagram for DPSK receiver.

4.4 Propagation Model

The power of the received signal is affected by three different and mutually independent propagation phenomena namely, UHF ground path loss, multipath fading, and shadowing.

First, the geometry and electromagnetic properties at UHF causes the received power to vary gradually. These variations determine the "area–mean" power of the signal. The area–mean power p_0 can be described by the normalized propagation law [28]

$$p_0 = c p_t \frac{r^{-a}}{\left(1 + \frac{r}{g}\right)^b} \tag{4.13}$$

where p_t is the transmitted area–mean power, c is a constant, and r is the propagation distance between transmitter. The exponent a is the propagation loss exponent for short distances, and $(a + b)$ is the propagation loss exponent for distances greater than the turning point g of the attenuation curve. Usually, the turning point in microcellular is between 100 and 200 m. This propagation law is referred to as the dual path loss law with a turning point.

In the microcellular radio environment, the desired signal level r around the local mean is given by a Rician distribution where the probability density

function (pdf) is given by [28]

$$f_r(r/p_{od}) = \frac{r}{p'_{od}} \exp\left[-\frac{r^2 + s^2}{2p'_{od}}\right] I_0\left(\frac{rs}{p'_{od}}\right) \qquad (4.14)$$

$$K = \frac{s^2}{2p'_{od}}; \quad p_{od} = (K+1)p'_{od} \qquad (4.15)$$

where $I_0(\cdot)$ is the modified Bessel function of the first kind and zeroth order, s is the peak value of the specular radio signal, p'_{od} is the average power of the scattered signal, K is the Rician factor which depends on the ratio of the signal power from the dominant signal path relative to that of the scattered signal, and p_{od} is the local mean power.

The pdf for the instantaneous signal power p_d is given by using $p_d = (1/2)r^2$

$$f_{pd}(p_d/p_{od}) = \frac{1}{p'_{od}} \exp\left(-\frac{2p_d + s^2}{2p'_{od}}\right) I_0\left(\frac{\sqrt{2p_d}s}{p'_{od}}\right) \qquad (4.16)$$

where, also, $p'_{od} = p_{od}/(K+1)$.

The slow–varying local mean p_{od} is given by a log–normal pdf.

$$f_{p_{od}}(p_{od}) = \frac{1}{\sqrt{2\pi}\sigma_d p_{od}} \exp\left\{-\left(\ln p_{od} - m_d\right)^2 / 2\sigma_d^2\right\} \qquad (4.17)$$

where σ_d^2 and $\xi_d = \exp(m_d)$ are the logarithmic variance and the area mean power of the desired signal.

However, for co–channel interference signals, the signal level around the local mean is given by a Rayleigh distribution. Hence, the instantaneous

power of a co–channel interference p_i is [28]

$$f_{p_i}(p_i/p_{oi}) = \frac{1}{p_{oi}} \exp\left(-\frac{p_i}{p_{oi}}\right) \qquad (4.18)$$

where p_{oi} is the local mean of the interfering signal.

The pdf for the p_{oi} is described by the following log–normal distribution

$$f_{p_{oi}}(p_{oi}) = \frac{1}{\sqrt{2\pi}\sigma_i p_{oi}} \exp\left\{-\left(\ln p_{oi} - m_i\right)^2 / 2\sigma_i^2\right\} \qquad (4.19)$$

Here, σ_i^2 and $\xi_i = \exp(m_i)$ are the logarithmic variance and the area mean power of the co–channel interference signal.

The area mean power of both the desired signal and the co–channel interference signals depend on the dual–path loss law

$$p_r = c p_t \frac{d^{-a}}{(1 + \frac{d}{g})^b} \qquad (4.20)$$

where c is a constant, p_r is the average received power, p_t is the average transmitter power, d is the distance between the base station and mobile unit, g is the turning point of the path–loss curve, a is the basic attenuation rate for short distances, and b is the additional attenuation rate coefficient for distances greater than g.

If we assume that the transmit power p_t is the same for desired and

interfering mobiles ξ_d and ξ_i can be related by the following equation

$$\xi_d = \xi_i \frac{R_u^a(G + Ru)^b}{(G+1)^b} \tag{4.21}$$

Here, Ru is the normalized reuse distance, which is defined as the ratio of the distance D between the centers of the nearest neighboring co-channel cells and the cell radius R and G is the normalized turning point:

$$G = g/R \tag{4.22}$$

Equation (4.21) has two limiting cases:

1. At distances significantly less than the turning point (g) the equation becomes

$$\frac{\xi_d}{\xi_i} = R_u^a. \tag{4.23}$$

2. At distances greater than the turning point g, the equation becomes

$$\frac{\xi_d}{\xi_i} = Ru^{a+b} \tag{4.24}$$

4.5 Channel Model

The performance of digital microcellular mobile communication systems depends on the model assumed for the communication channel. For narrow

bandwidth systems the communication channel is assumed to be flat (frequency non–selective) fading channel in which the bandwidth of the system is much less than the coherent bandwidth of the channel. Hence, there is no time spreading in the received signal. However, in many environments, the mobile radio channels are mainly frequency–selective multipath faded. Therefore, the need for frequency–selective multipath fading channel models is necessary. Some of these models are presented by Rummler in [34].

A realizable and mathematically tractable model for frequency–selective multipath faded channel is a quasi–stationary situation, in which the channel is assumed to be time invariant over some time period [5], [6]. Hence, we can characterize our channel by M–received Rayleigh or Rician–fading rays according to [43]. The complex envelope impulse response of such channels is

$$h(t) = \sum_{m=1}^{M} p_m(\alpha_m + j\beta_m)\delta(t - \tau_m) \qquad (4.25)$$

where each of the M beams is characterized by a triplet $(\alpha_m, \beta_m, \tau_m)$ with α_m and β_m being independent Gaussian random variables. The τ_m are the path delays and p_m is the amplitude of the m–th scatterer. The number of beams M depends on the proposed model, but M ranges between 2 and 70.

In our situation, a two-beam model is taken to represent the mobile

radio channel. Generally, there is no restriction to any specific number of beams but one can view the two beams model as a mathematical fit to the M scatter model with proper choice of parameters. The complex envelope impulse response of the channel will be [5]

$$h(t) = p_1(\alpha_1 + j\beta_2)\delta(t) + p_2(\alpha_2 + j\beta_2)\delta(t - \tau) \qquad (4.26)$$

where $\alpha_1, \alpha_2, \beta_1,$ and β_2 are independent identically distributed, Gaussian random variables and τ is the relative delay between the two beams.

The impulse response of the two beams can be rewritten as

$$h(t) = a\delta(t) + b\delta(t - \tau) \qquad (4.27)$$

where

$$a = p_1(\alpha_1 + j\beta_1) \text{ and } b = p_2(\alpha_2 + j\beta_2) \qquad (4.28)$$

Diversity reception is usually regarded as a mean of combating fading in radio transmissions. In space diversity, for example, several antennas are used, separated in space by at least one half the wavelength of the carrier to ensure the reception of statistically independent various received signals. Because the received signals are statistically independent, there is a good chance that they will not fade at the same time.

The space diversity comes in the form of L different antennas separated

by half wavelengths. Hence, their outputs signals can be regarded as uncorrelated among themselves. The impulse response of the l-th diversity path can be modeled by

$$h_\ell(t) = a_\ell \delta(t) + b_\ell \delta(t - \tau) \tag{4.29}$$

where the relative delay spread τ is assumed identical for all diversity components.

4.6 Performance Measures

Bit Error Rate

By computer simulations, the area–mean bit error rate can be evaluated using

$$P_b = \sum_{n=0}^{N} P_n(e/n) F_n(n) \tag{4.30}$$

where $F_n(n)$ is the probability of n active co–channel interferers, and $P_n(e/n)$ is the probability of error conditioned on the presence of n different co–channel interferers in the same time.

It is assumed that all co–channel interferers are statistically independent and identically distributed. Furthermore, if it is assumed that only interfering signals from the nearest neighboring six co–channel cells are considered, the blocking probability B is the same in all cells, and the channel

is uniformly loaded, $F_n(n)$ is given as [28]

$$F_n(n) = \begin{pmatrix} 6 \\ n \end{pmatrix} a_c^n (1 - a_c)^{6-n} \qquad (4.31)$$

where $a_c = A_c/n_c$, n_c is the number of channels per cell, and A_c is the carried traffic per cell defined as

$$A_c \triangleq A(1 - B) \qquad (4.32)$$

Here, A is the offered traffic per cell in Erlang, and B is the blocking probability which is determined using Erlang B formula [28]

$$B = \frac{A^{n_c}}{n_c \sum_{n=0}^{n_c} \left(\frac{A^n}{n!} \right)} \qquad (4.33)$$

Spectrum Efficiency

Since the service area of a cellular or a microcellular radio system is divided into a regular array of hexagonal cells called clusters, and each cluster occupies the total bandwidth available for the mobile system, another performance measure can be defined. This measure is spectrum efficiency E_s, which is defined as [28]

$$E_s \triangleq \frac{A_c}{n_c W C S_a} \qquad \text{Erlang}/MHz/km^2 \qquad (4.34)$$

where A_c represents the current traffic per cell, n_c represents the number of channels per cell, W represents channel bandwidth, C represents the number

of cells per cluster, and S_a represents the cell area. For hexagonal cells

$$K = i^2 + ij + j^2, \quad i,j \geq 1$$
$$= \frac{R_u^2}{3} \tag{4.35}$$

with integers i and j, and normalized reuse distance Ru. Also, S_a can be written as

$$S_a = 2\sqrt{3}R^2 \tag{4.36}$$

with cell radius R.

Hence, E_s can be rewritten as

$$E_s = \frac{\sqrt{3}A_c}{2n_c W R_u^2 R^2} \tag{4.37}$$

CHAPTER 5

SIMULATION RESULTS

5.1 Introduction

In this chapter, computer simulation programs will be used to evaluate the performance of digital microcellular mobile communication systems operating over frequency–selective fading environments. Also, the effect of fading counter–measures on such systems will be seen. The systems treated are bandpass systems that use BPSK and DPSK modulation schemes to transmit digital data. The system description, propagation model and channel model are explained in the previous chapter. Computer simulations provide the only alternative approach to hardware evaluation in cases where the system might be too complicated to analyze.

In section 5.2, the effect of the different system parameters on the performance will be shown. In section 5.3, the effect of diversity combining, error control coding, interleaving and linear adaptive equalization, as fading counter–measures, on the performance of the discussed system will be evaluated.

## 5.2 The Effect of System Parameters and Modulation Schemes

To see the effect of the system parameters on the performance of the system, Figure 5.1 shows the bit error rate (BER) versus SNR for $A_c = 5$ erlang, $n_c = 10$ channels per cell, $G = 0.67$, $\sigma_i = 6$ dB, $\sigma_d = 0$ dB, $K_1 = 7$ dB, $K_2 = 4$ dB, $\tau_1 = 0.2\,T$, and $\tau_2 = 0.4\,T$. In the figure, the normalized reuse distance is taken as a parameter. As can be seen from the figure, the BER decreases with the increase of Ru. However, increasing Ru means decreasing the spectrum efficiency E_s as we can see in Figure 5.2. The figure shows E_s versus Ru. Figure 5.3 shows the relation between BER and E_s. From the figure, we can see that a decrease in E_s will result in an increase in BER. So, in the design of microcellular systems, a compromise should be made between BER and E_s.

In Figure 5.4, we see BER versus SNR and the logarithmic standard deviation of the desired signal σ_d is a parameter. As σ_d increases, BER decreases which reflects the effect of the desired signal shadowing on the performance of the system. On the other hand, Figure 5.5 shows the relation between BER and σ_i, the logarithmic standard deviation of the local–mean power of the co–channel interference signals. The figure shows the decrease
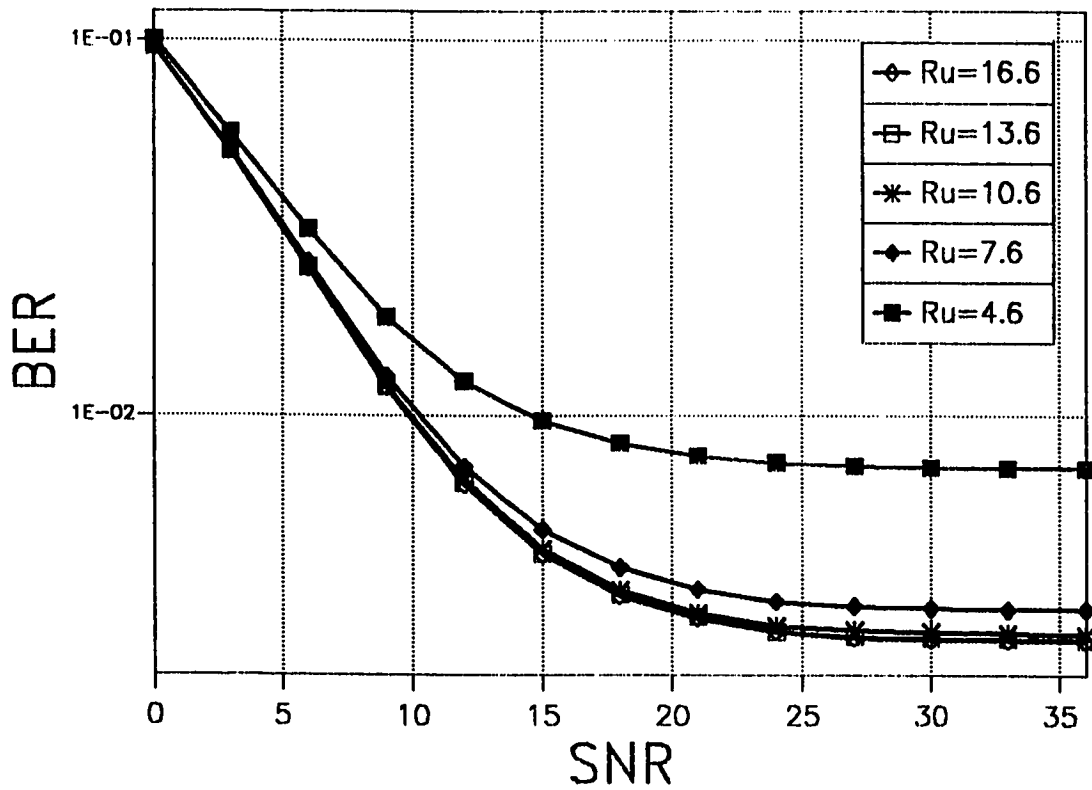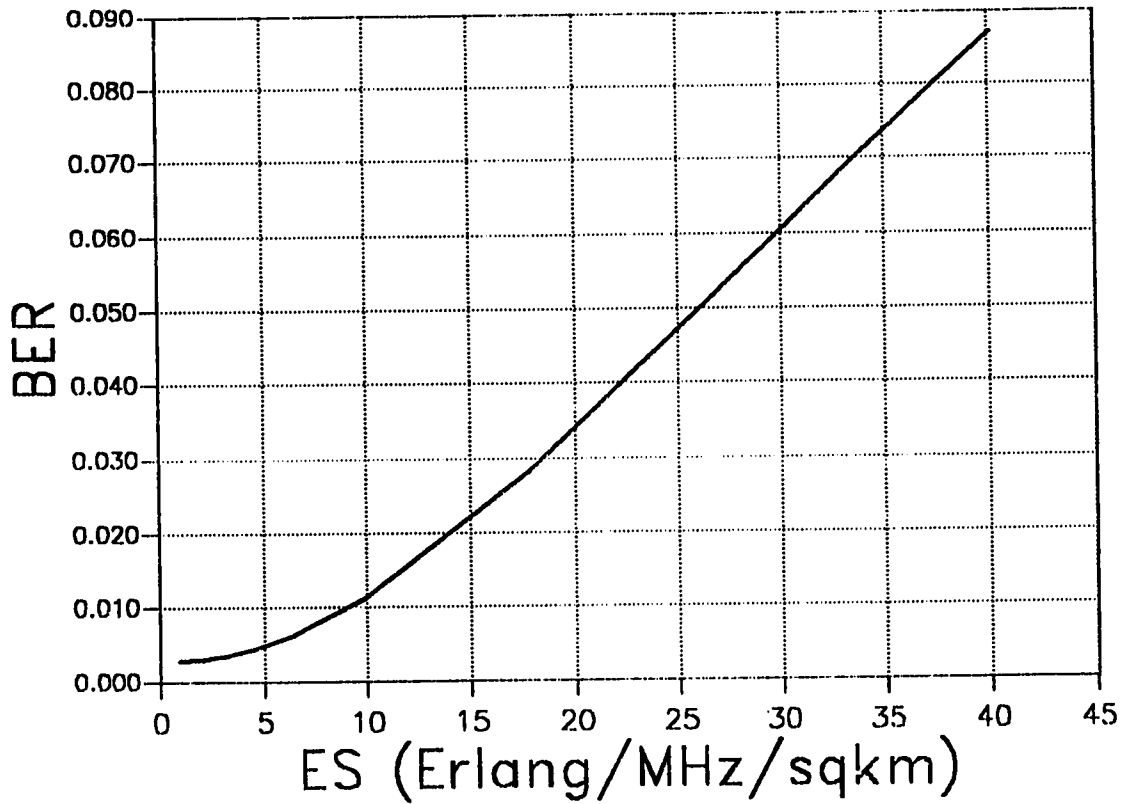
Figure 5.1 : Bit error rate (BER) versus signal to noise ratio (SNR) for different normalized reuse distances (Ru), $A_c = 5$ **Erlang,** $n_c = 10$ **channels per cell ,** $G = 0.67$, $\sigma_d = 0 dB$, $\sigma_i = 6 dB$, $K_1 = 7 dB$, $K_2 = 4 dB$, $\tau_1 = 0.2T$, **and** $\tau_2 = 0.4T$.
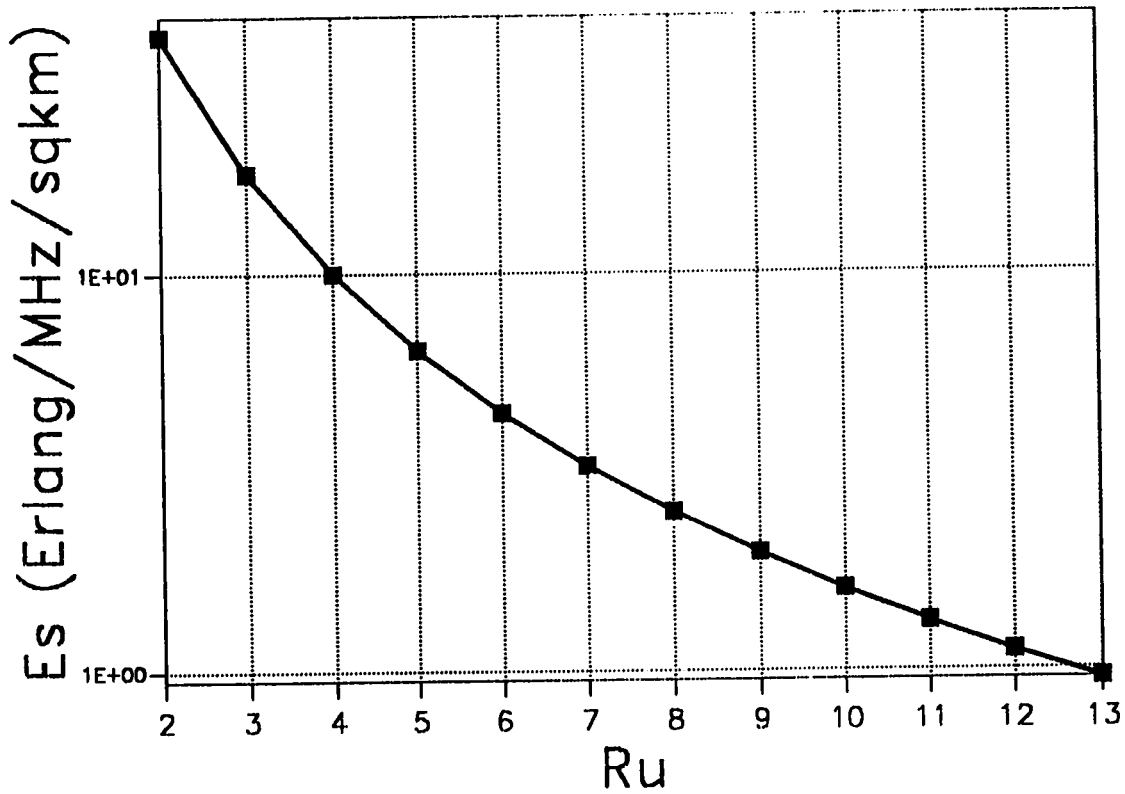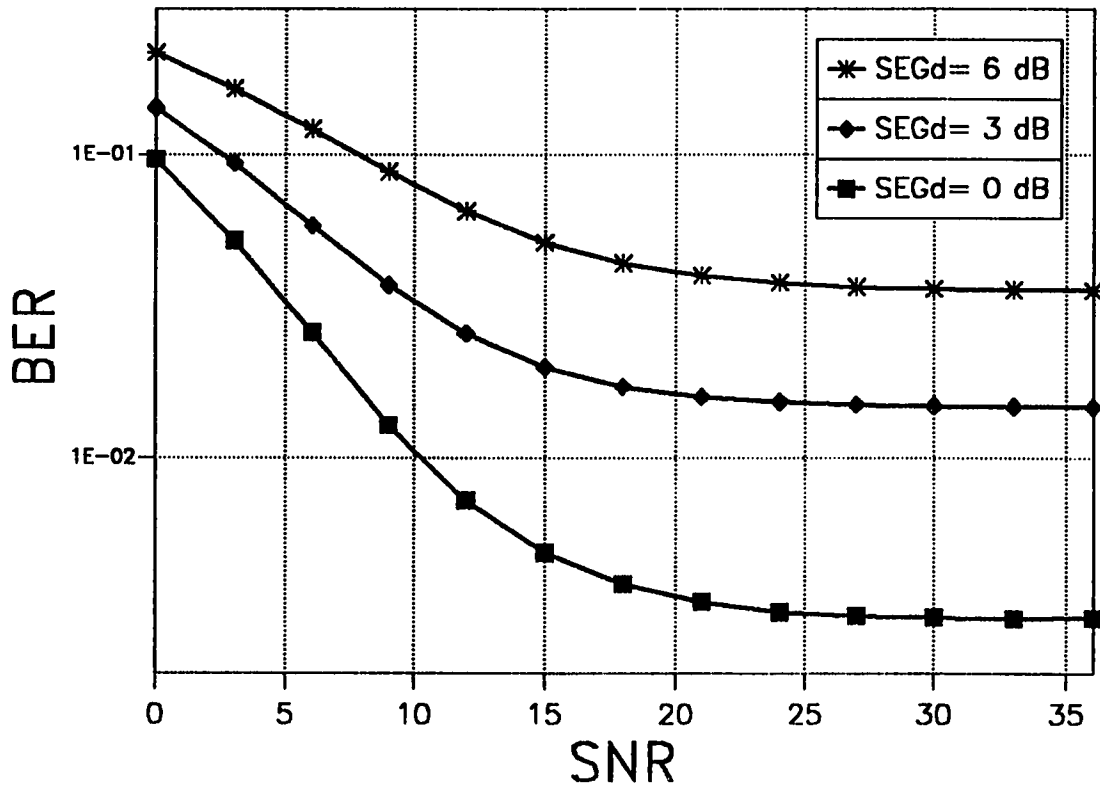
Figure 5.2 : Spectrum Efficiency (E$_s$) versus Ru for $A_c = 5$
Erlang, $n_c = 10$ **channels per cell,** $G = 0.67$, $\sigma_d = 0\,dB$,
$\sigma_i = 6\,dB$, $K_1 = 7\,dB$, $K_2 = 4\,dB$, $\tau_1 = 0.2T$, **and**
$\tau_2 = 0.4T$.

Figure 5.3 : BER versus E$_s$ while changing Ru for $A_c = 5$
Erlang, $n_c = 10$ **channels per cell,** $G = 0.67$, $\sigma_d = 0 dB$,
$\sigma_i = 6$ dB, $K_1 = 7$ dB, $K_2 = 4$ dB , $\tau_1 = 0.2T$, **and**
$\tau_2 = 0.4T$.

Figure 5.4 : BER versus SNR where the logarithmic standard deviation of the desired signal (σ_d) is a parameter for $A_c = 5$ **Erlang,** $n_c = 10$ **channels per cell,** $Ru = 7.6$, $\quad G = 0.67$, $\quad \sigma_i = 9\,dB$, $\quad K_1 = 7\,dB$, $K_2 = 4\,dB$, $\tau_1 = 0.2T$, **and** $\tau_2 = 0.4T$.
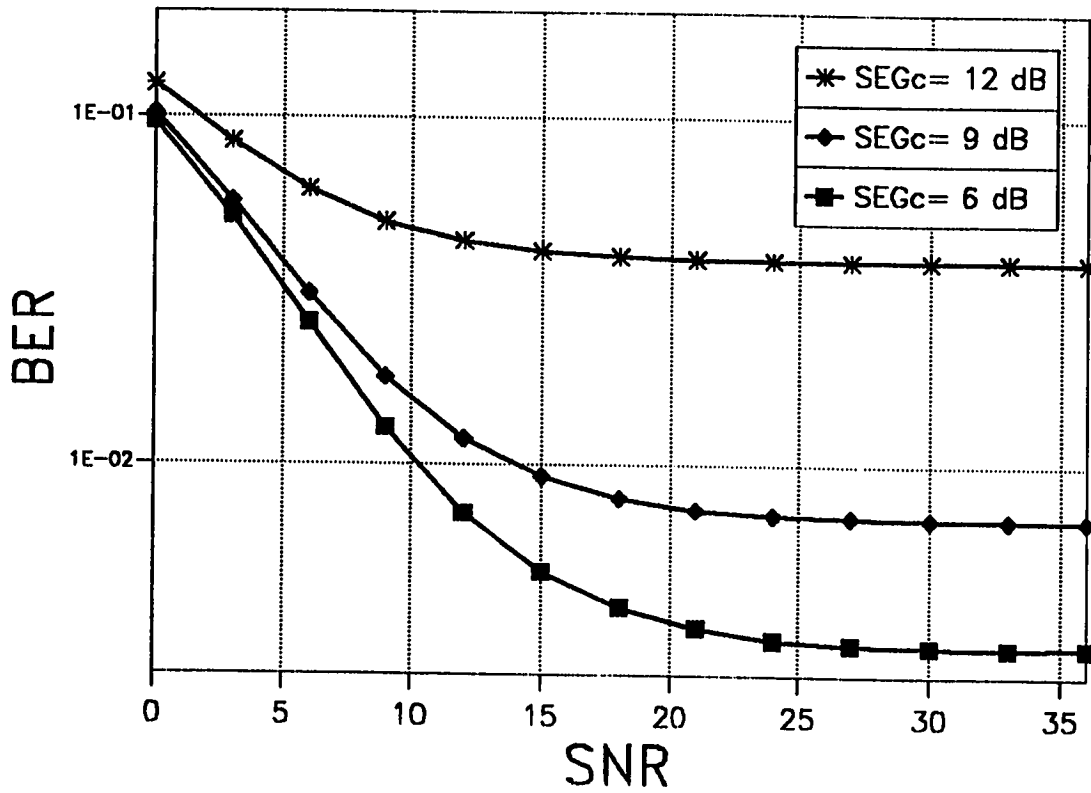
Figure 5.5 : BER versus SNR where the logarithmic standard deviation of the co-channel interferer (σ_i) **is a parameter for** $A_c = 5$ **Erlang,** $n_c = 10$ **channels per cell,** $Ru = 7.6$, $G = 0.67$, $\sigma_d = 0dB$, $K_1 = 7\,dB$, $K_2 = 4dB$, $\tau_1 = 0.2T$ **, and** $\tau_2 = 0.4T$.

in BER as σ_i increases.

Figure 5.6 depicts the effect of the relative delay between the two beams of the desired signal τ_1 on the BER. From the figure, as τ_1 decreases the BER decreases as a result of the decrease in Intersymbol Interference (ISI).

Figure 5.7 shows the relation between the BER and the relative delay between the beams of the co-channel interference channel model. It can be seen from the figure that the relative delay between the beams of the co-channel interference channel model does not affect the performance of the system.

In our channel model for the desired signal, we assumed that the envelope of each beam is Rician distributed, but with different K parameters. K_1, the Rician parameter of the first beam, is assumed greater than K_2, which is the Rician parameter of the second beam. Figure 5.8 shows the relation between K_1 and BER. Clearly, as K_1 increases the BER will decrease and vice versa. Figure 5.9 shows the relation between the Rician parameter of the second beam and the BER. Similarly, when K_2 increases the BER decreases.

In the second model used for the desired signal channel, we assumed that the two delayed beams have the same power, so the ratio of the power of the
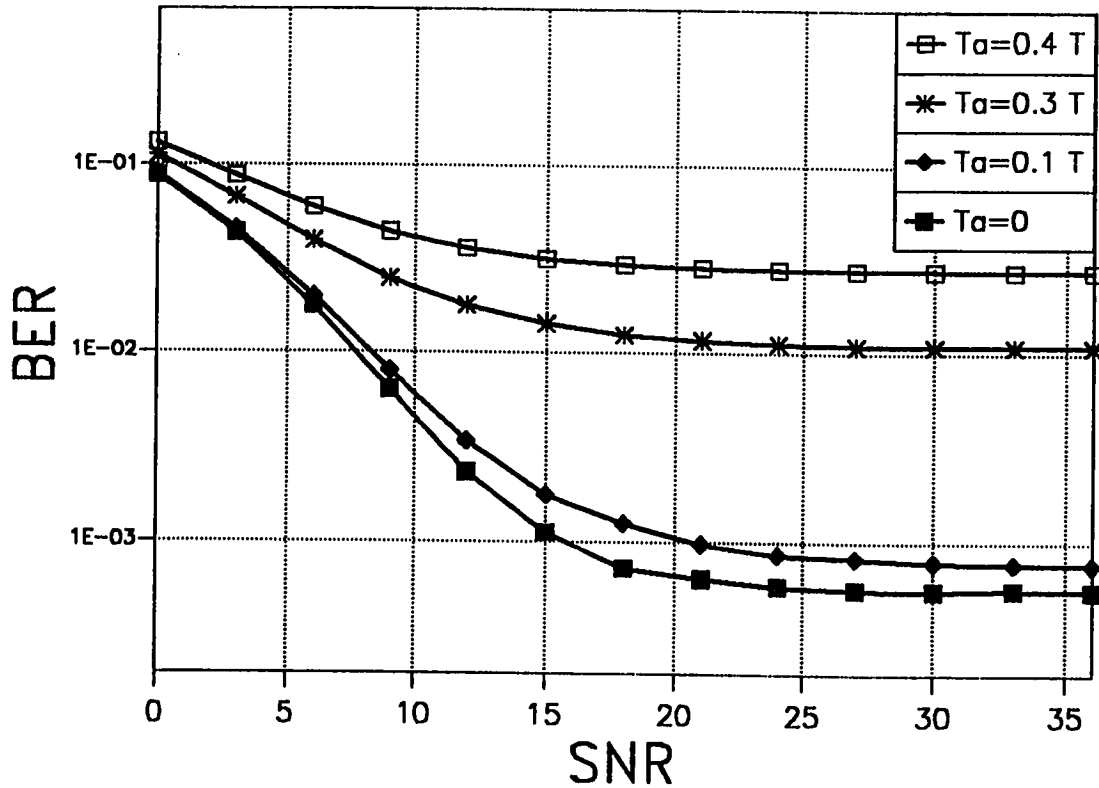
Figure 5.6 : BER versus SNR for different relative delays between the beams of the desired signal for $A_c = 5$ **Erlang,** $n_c = 10$ **channels per cell,** $Ru = 7.6$, $G = 0.67$, $\sigma_d = 0$ dB, $\sigma_i = 6dB$, $K_1 = 7$ dB, $K_2 = 4dB$, **and** $\tau_2 = 0.8T$.
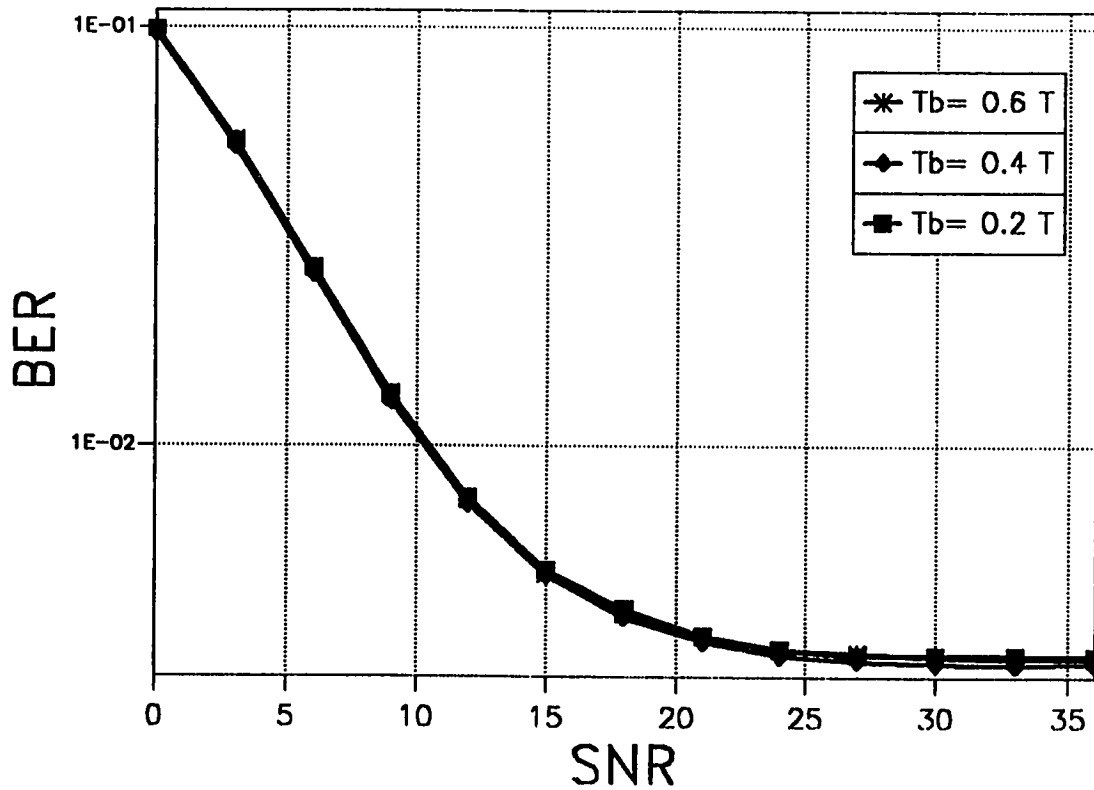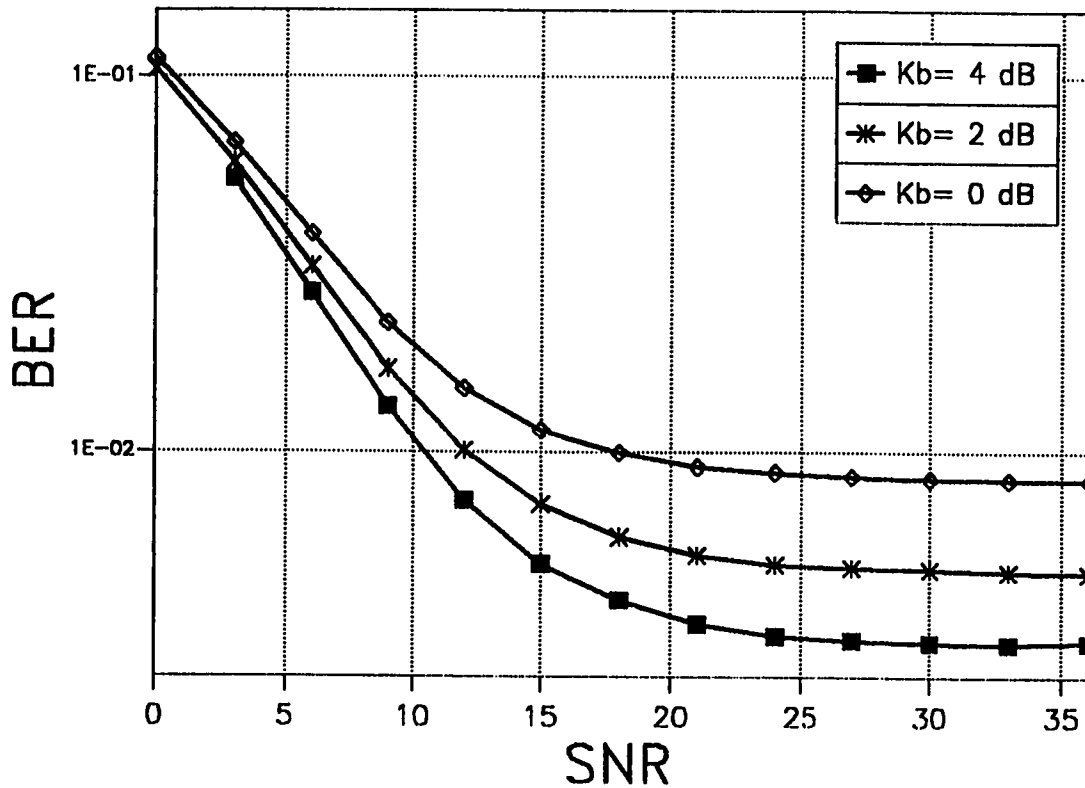
Figure 5.7 : BER versus SNR for different relative delays between the beams of the co-channel interference for $A_c = 5$ **Erlang,** $n_c = 10$ **channels per cell,** $Ru = 7.6$, $G = 0.67$, $\sigma_d = 0 dB$, $\sigma_i = 6 dB$, $K_1 = 7 dB$, $K_2 = 4 dB$, **and** $\tau_1 = 0.2T$.
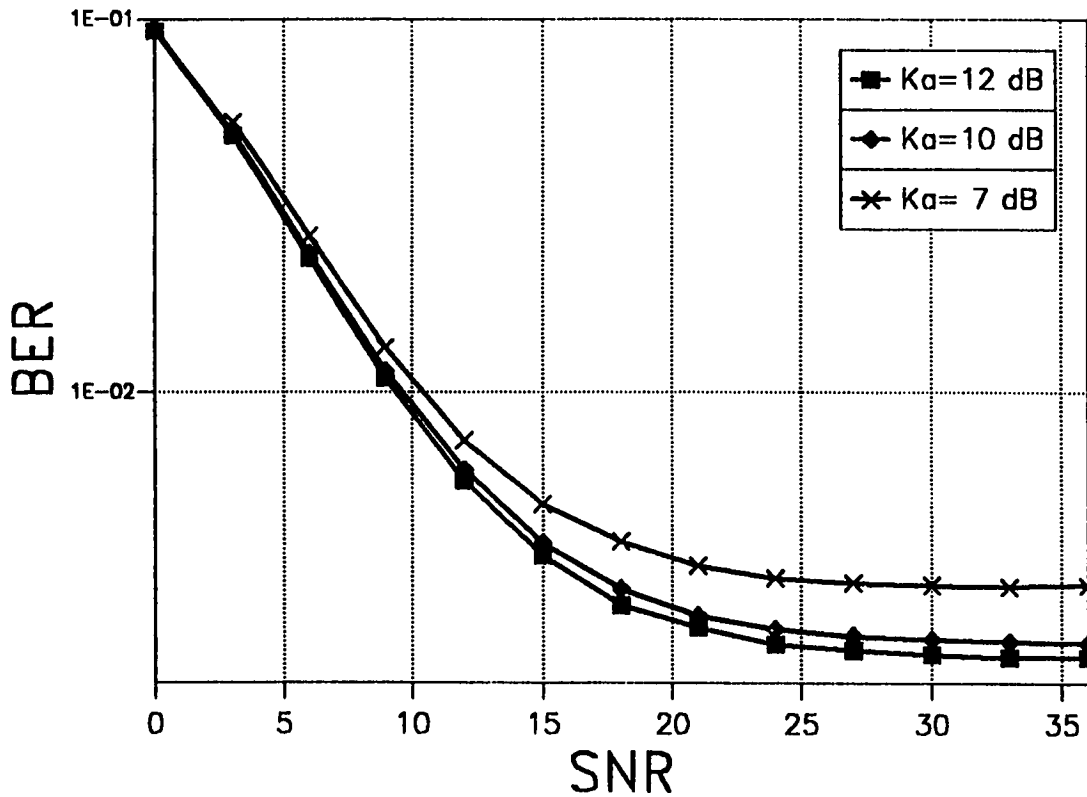
Figure 5.8 : BER versus SNR for different Rician parameters of the first beam of the desired signal for $A_c = 5$ **Erlang,** $n_c = 10$ **channels per cell,** $Ru = 7.6$, $G = 0.67$, $\sigma_d = 0 dB$, $\sigma_i = 6 dB$, $K_2 = 4 dB$, $\tau_1 = 0.2T$, **and** $\tau_2 = 0.4T$.
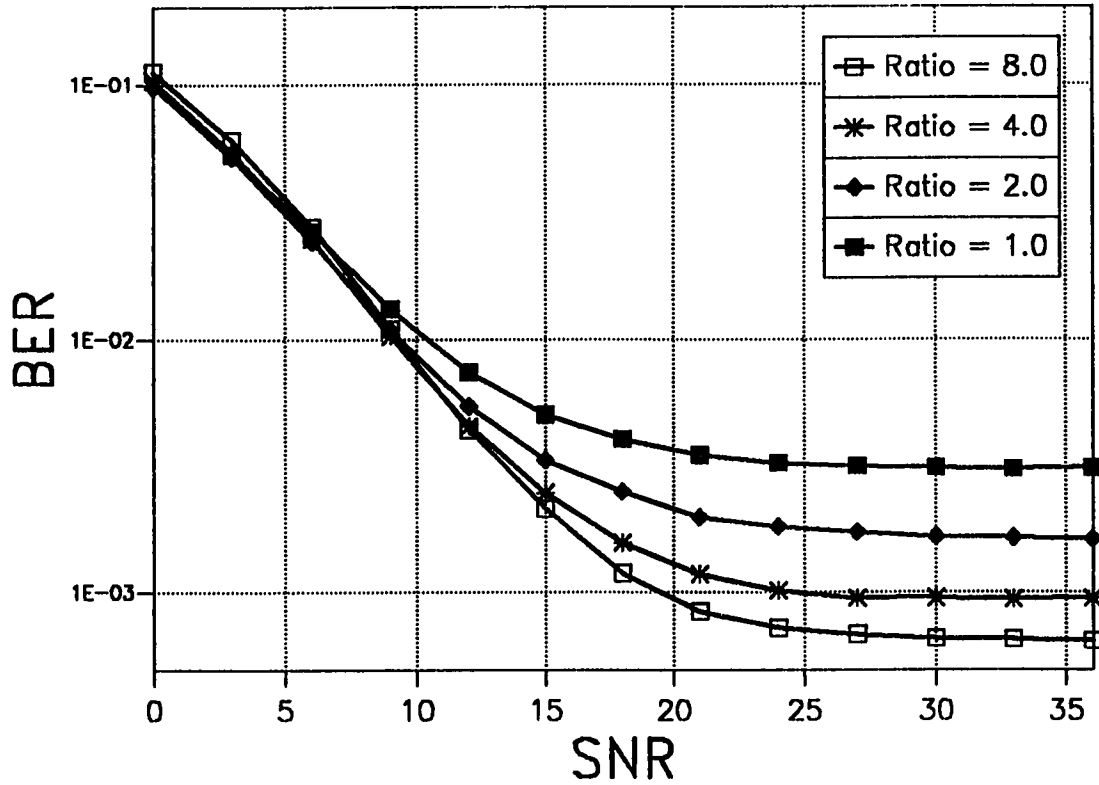
Figure 5.9 : BER versus SNR for different Rician parameters of the second beam of the desired signal for $A_c = 5$ **Erlang,** $n_c = 10$ **channels per cell,** $Ru = 7.6$, $G = 0.67$, $\sigma_d = 0dB$, $\sigma_i = 6dB$, $K_1 = 7dB$, $\tau_1 = 0.2T$, **and** $\tau_2 = 0.4T$.

first beam to the power of the second is equal to one. To see the effect of this ratio on the system performance different 1st beam to 2nd beam power ratios are used in the model and the results are shown in Figure 5.10. From the figure, as the ratio increases the BER decreases. This figure indicates the effect of frequency–selective fading channels on the digital microcellular systems performance.

Since we used two modulation schemes BPSK and DPSK, Figure 5.11 shows the relation between the two modulation schemes and the BER. Clearly, the performance of BPSK is better than the performance of DPSK. However, BPSK modulation scheme needs coherent detection at the receiver side, while DPSK does not.

Next, we fix the normalized reuse distance Ru and see the effect of increasing the cell radius R on the BER and on the spectrum efficiency E_s. As R increases the normalized turning point G will decrease because $G = g/R$ and g is found near 200 m in the literature. Figure 5.12 depicts the relation between the BER and R; as R increases, the BER decreases. However, an increase in R will result in a decrease in E_s as we can see in Figure 5.13. The decrease in G means that the cell radius has been increased approaching the conventional cellular system cell sizes. Hence, using microcellular systems

**Figure 5.10 : BER versus SNR for different 1st to 2nd beam power ratios for** $A_c = 5$ **Erlang,** $n_c = 10$ **channels per cell,** $Ru = 7.6$, $G = 0.67$, $\sigma_d = 0dB$, $\sigma_i = 6dB$, $K_1 = 7dB$, $K_2 = 4dB$, $\tau_1 = 0.2T$, **and** $\tau_2 = 0.4T$.
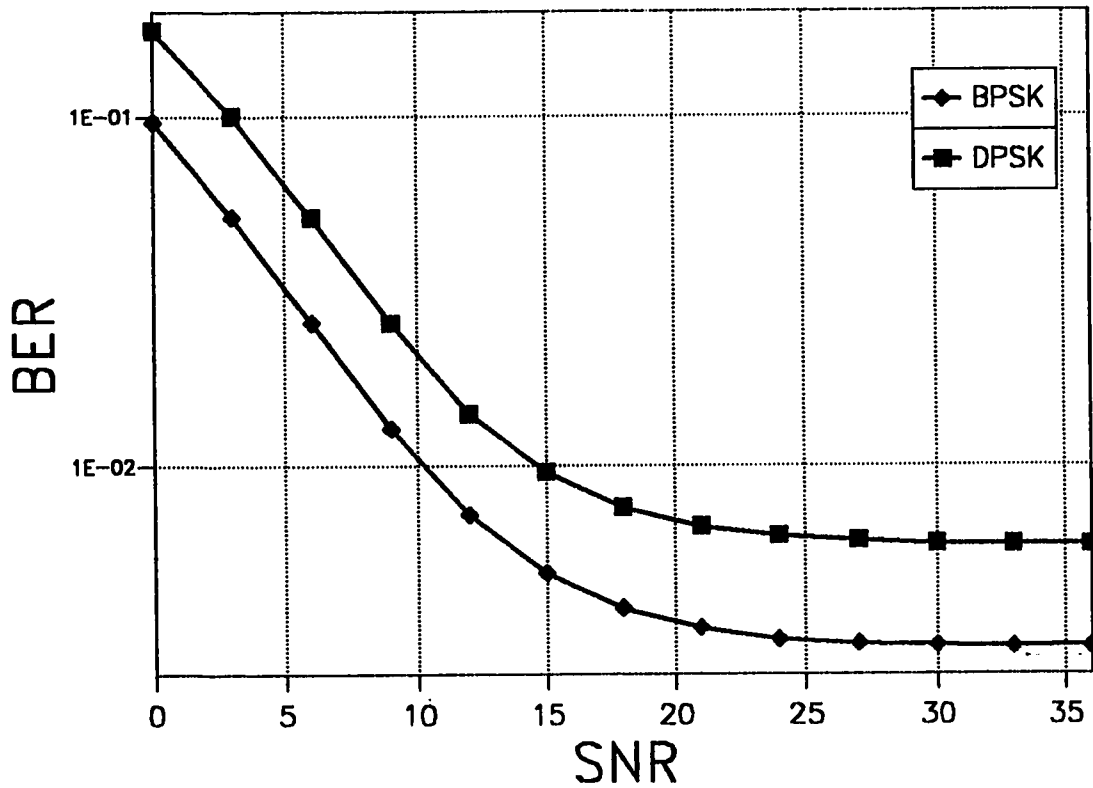
Figure 5.11 : BER versus SNR for BPSK and DPSK modulation schemes for $A_c = 5$ **Erlang,** $n_c = 10$ **channels per cell,** $Ru = 7.6$, $G = 0.67$, $\sigma_d = 0\,dB$, $\sigma_i = 6\,dB$, $K_1 = 7\,dB$, $K_2 = 4\,dB$, $\tau_1 = 0.2T$, **and** $\tau_2 = 0.4T$.
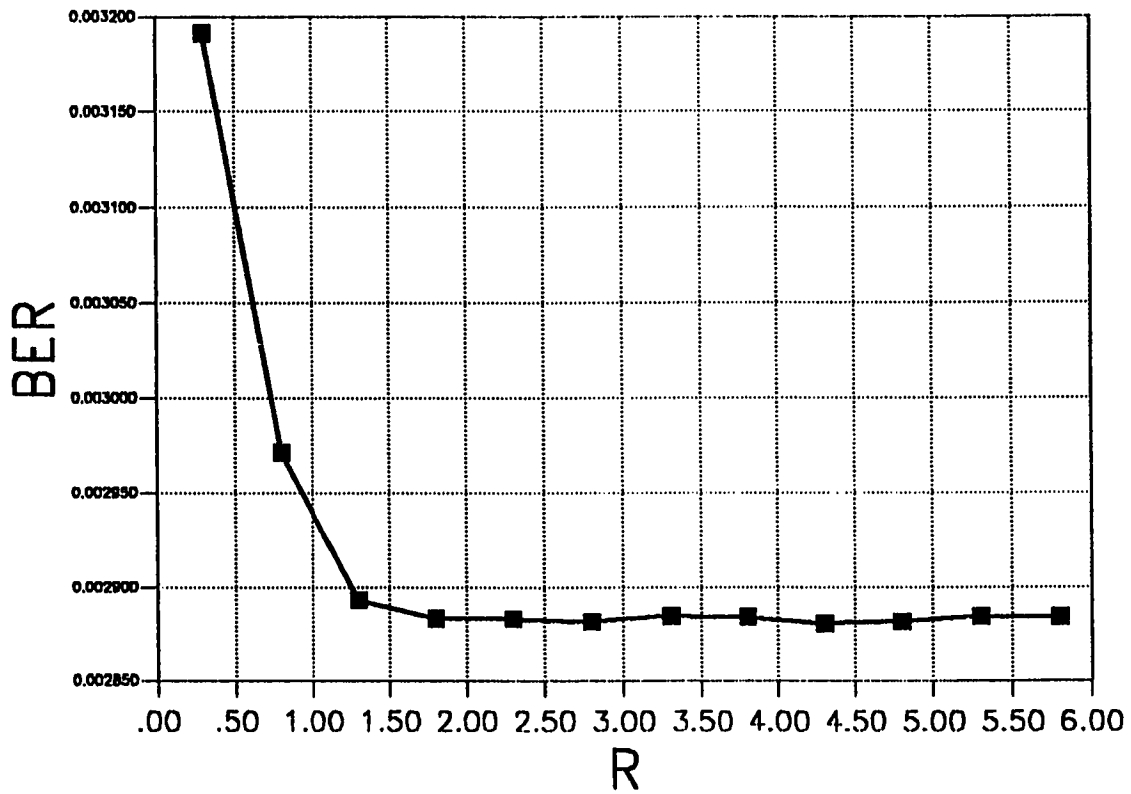
Figure 5.12 : BER versus the cell radius (R) for $A_c = 5$
Erlang, $n_c = 10$ **channels per cell,** $Ru = 7.6$, $G = 0.67$,
$\sigma_d = 0\,dB$, $\sigma_i = 6\,dB$, $K_1 = 7\,dB$, $K_2 = 4\,dB$,
$\tau_1 = 0.2T$, **and** $\tau_2 = 0.4T$.
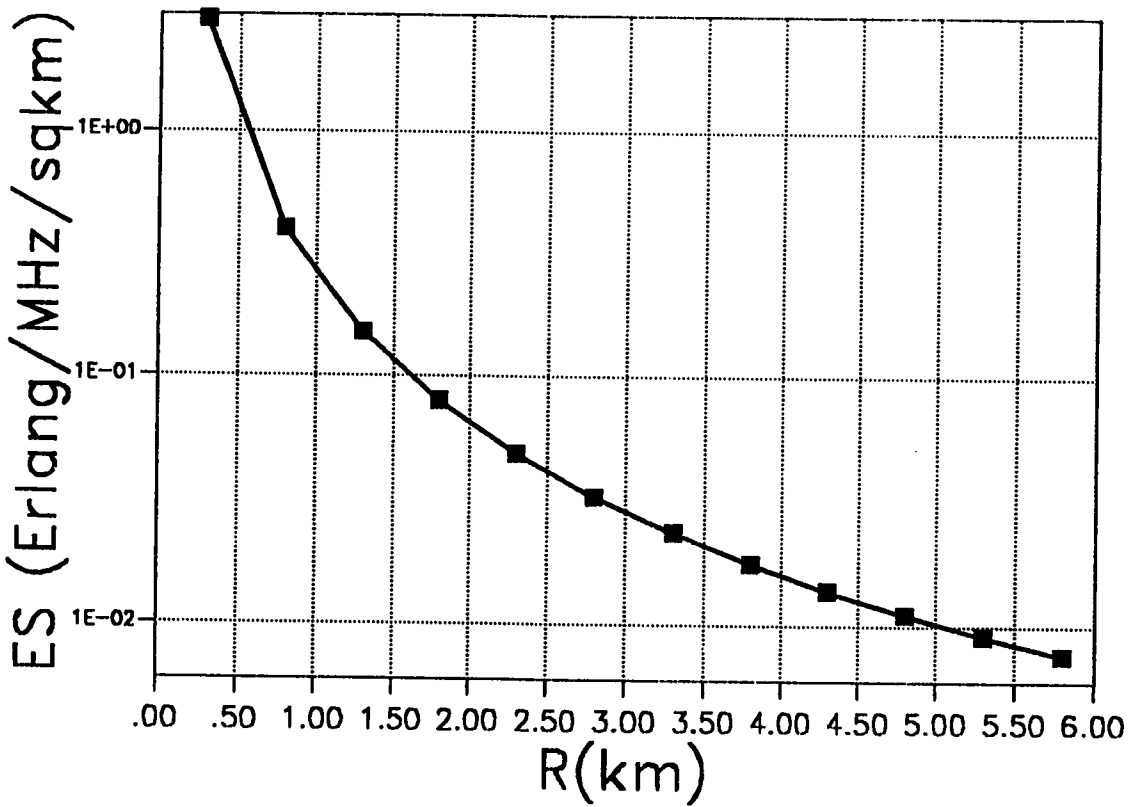
Figure 5.13 : E_s versus R for $A_c = 5$ **Erlang,** $n_c = 10$ **channels per cell,** $Ru = 7.6$, $G = 0.67$, $\sigma_d = 0\,dB$, $\sigma_i = 6\,dB$, $K_1 = 7\,dB$, $K_2 = 4\,dB$, $\tau_1 = 0.2T$, **and** $\tau_2 = 0.4T$.

enhances the spectrum efficiency as we can see from Figure 5.14 which shows the relation between the BER and E_s while changing the cell radius (R).

The function of the raised cosine used at the transmitter is to decrease the ISI spread over the adjacent symbols. The rolloff factor β plays an important role in lowering the effect of ISI. β can take a value between zero and one. As β increases the effect of the ISI decreases as we see from Figure 5.15.

As we can notice from the previous figures, which depict the relation between BER and SNR, acceptable BER, like 10^{-3} or 10^{-4}, can be reached with very high SNR. As we noticed, the degradation in digital microcellular systems' performance is caused by a combination of fading, noise and co-channel interference.

5.3 The Effect of Fading Counter–Measures

To enhance the performance of digital microcellular mobile communication systems different fading counter-measures are used. The fading counter-measures used are diversity combining, error control coding, interleaving and linear adaptive equalization.
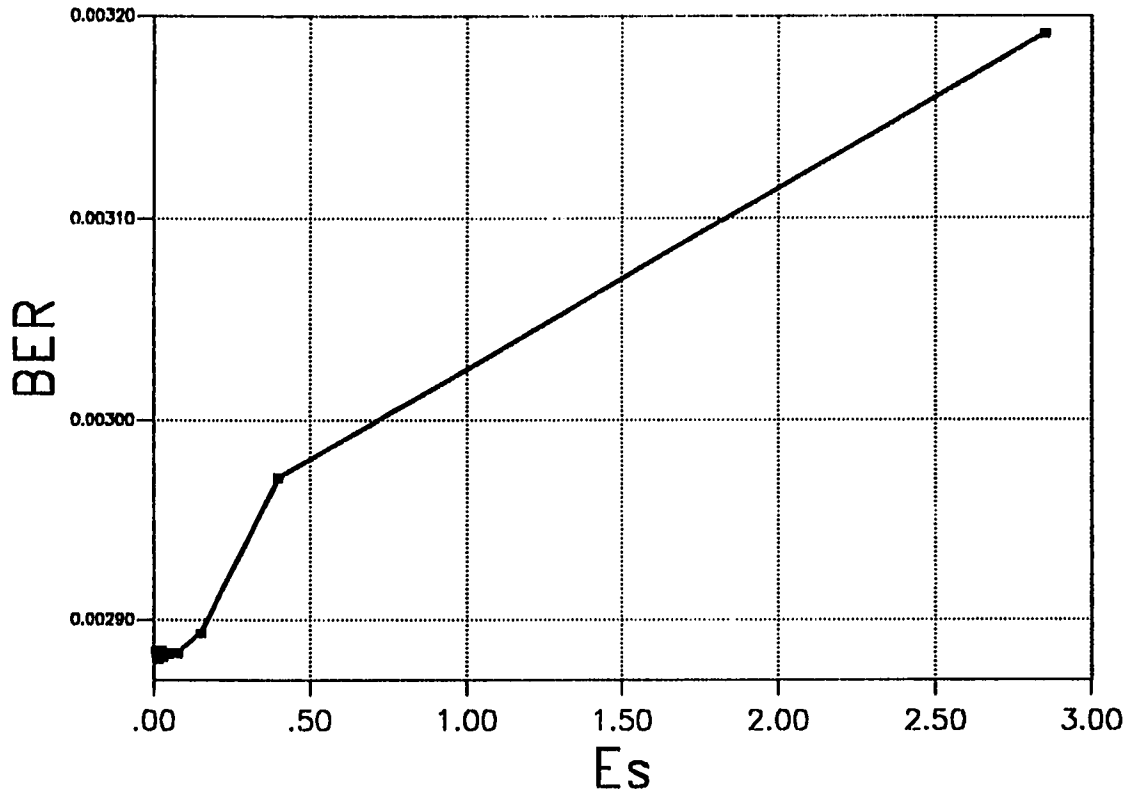
Figure 5.14 : BER versus E$_s$ while changing R for $A_c = 5$
Erlang, $n_c = 10$ **channels per cell,** $Ru = 7.6$, $G = 0.67$,
$\sigma_d = 0\,dB$, $\sigma_i = 6\,dB$, $K_1 = 7\,dB$, $K_2 = 4\,dB$,
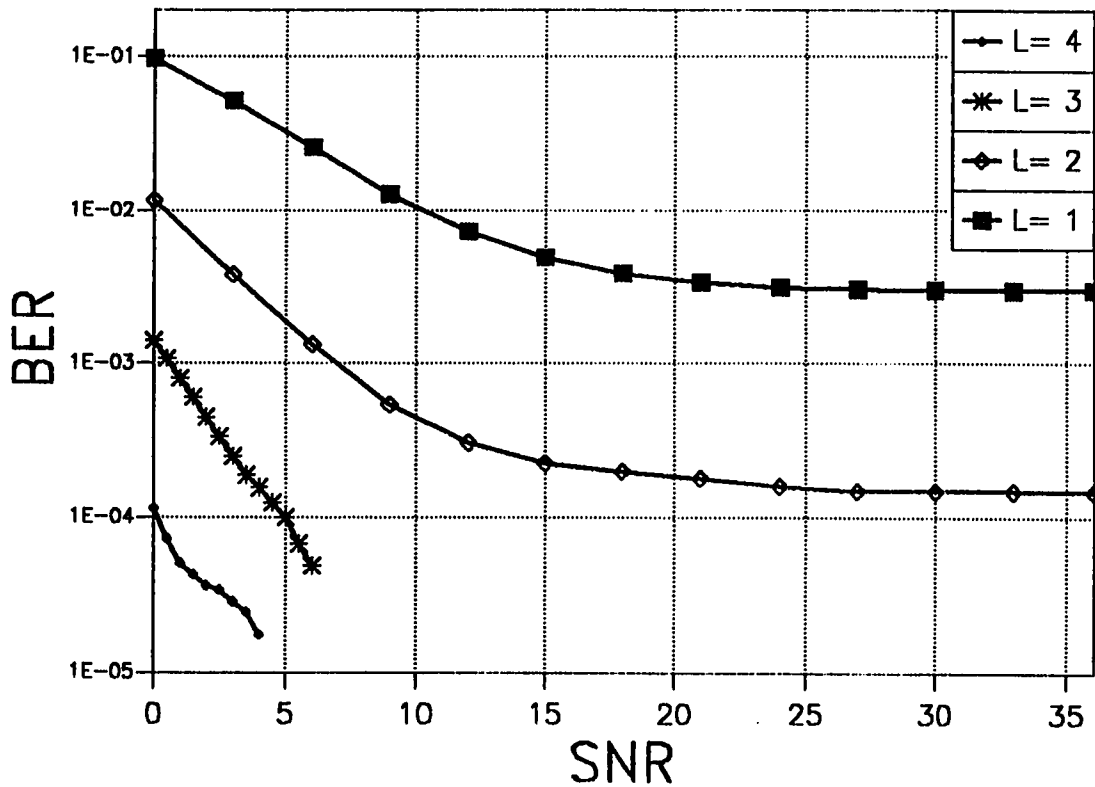$\tau_1 = 0.2T$, **and** $\tau_2 = 0.4T$.
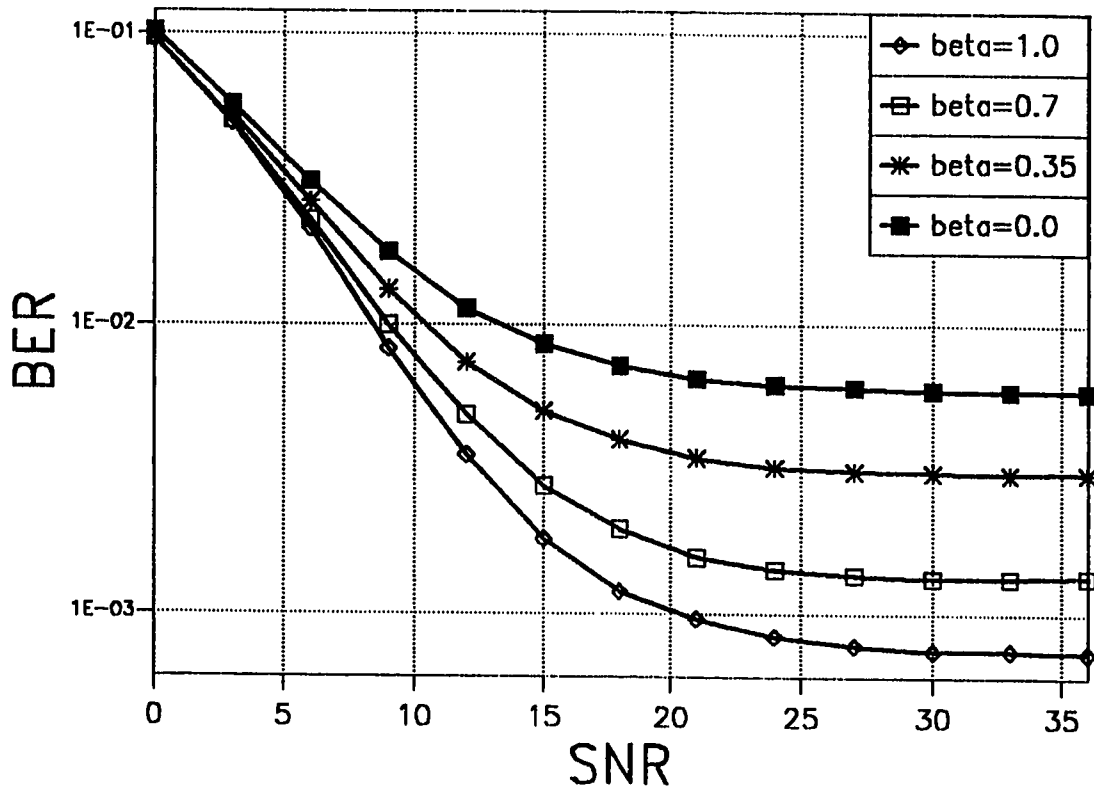
Figure 5.15 : BER versus SNR , where the raised cosine filters rolloff factor (β) is taken as a parameter for $A_c = 5$ Erlang, $n_c = 10$ channels per cell, $Ru = 7.6$, $G = 0.67$, $\sigma_d = 0 dB$, $\sigma_i = 6 dB$, $K_1 = 7$ dB, $K_2 = 4 dB$, $\tau_1 = 0.2T$, and $\tau_2 = 0.4T$.

The effect of using L diversity branches on the performance of the system with BPSK modulation, $A_c = 5$ Erlang, $n_c = 10$ channels per cell, $G = 0.67$, $\sigma_i = 6$ dB, $\sigma_d = 0$ dB, $K_1 = 7$ dB, $K_2 = 4$ dB, $\tau_1 = 0.2\ T$, $\tau_2 = 0.4\ T$, $\beta = 0.35$ and $Ru = 7.6$ is shown as the BER versus SNR in Figure 5.16. From the figure, the irreducible bit error rate (IBER), due to co-channel interference and intersymbol interference (ISI), has been decreased from 3.0×10^{-3} to 1.35×10^{-4} with dual diversity combining $L = 2$ and the gain at BER $= 3.0 \times 10^{-3}$ is around 24.25 dB. With $L = 3$ the BER $= 5 \times 10^{-5}$ at SNR $= 6$ dB, and with $L = 4$ the BER is 1.73×10^{-5} at SNR equal to 4 dB.

Figure 5.17 shows the effect of dual diversity combining ($L = 2$) with DPSK modulations. The IBER has fallen from 6×10^{-3} to 4.0×10^{-4} and the gain at 6.0×10^{-3} BER is 25.0 dB.

Figure 5.18 shows the BER as a function of SNR with BPSK when three different block codes are used. The three codes are BCH(15, 11, 3), BCH(15, 7, 5) and Golay (23, 12, 7) codes, with different code rates and with different error correction capability. From the figure, we can see that the use of the BCH (15, 11, 3) and the BCH(15, 7, 5) codes did not enhance the performance of the system and this is because of the large amount of

Figure 5.16 : The effect of using L diversity branches on the BER with BPSK modulation for $A_c = 5$ Erlang, $n_c = 10$ channels per cell, $Ru = 7.6$, $G = 0.67$, $\sigma_d = 0 dB$, $\sigma_i = 6 dB$, $K_1 = 7 dB$, $K_2 = 4 dB$, $\tau_1 = 0.2T$, and $\tau_2 = 0.4T$.
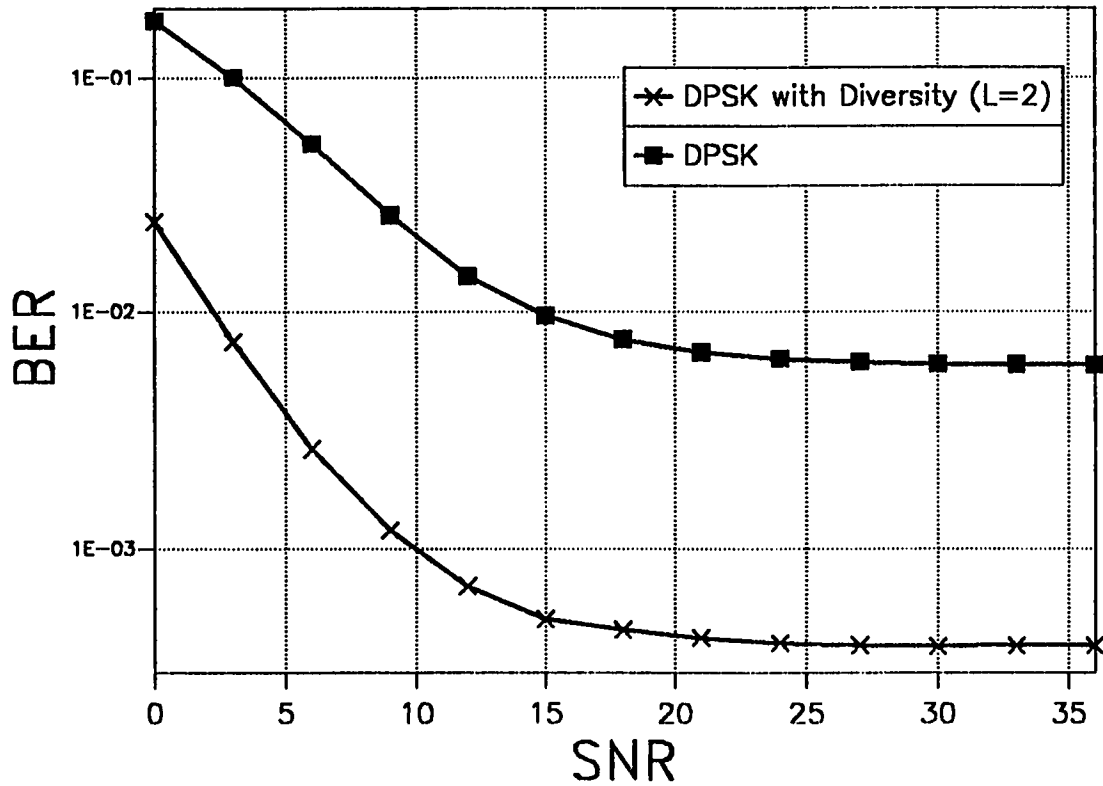
Figure 5.17 : The effect of using dual diversity on the BER with DPSK modulation for $A_c = 5$ **Erlang,** $n_c = 10$ **channels per cell,** $Ru = 7.6$, $G = 0.67$, $\sigma_d = 0\,dB$, $\sigma_i = 6\,dB$, $K_1 = 7\,dB$, $K_2 = 4\,dB$, $\tau_1 = 0.2T$, **and** $\tau_2 = 0.4T$.
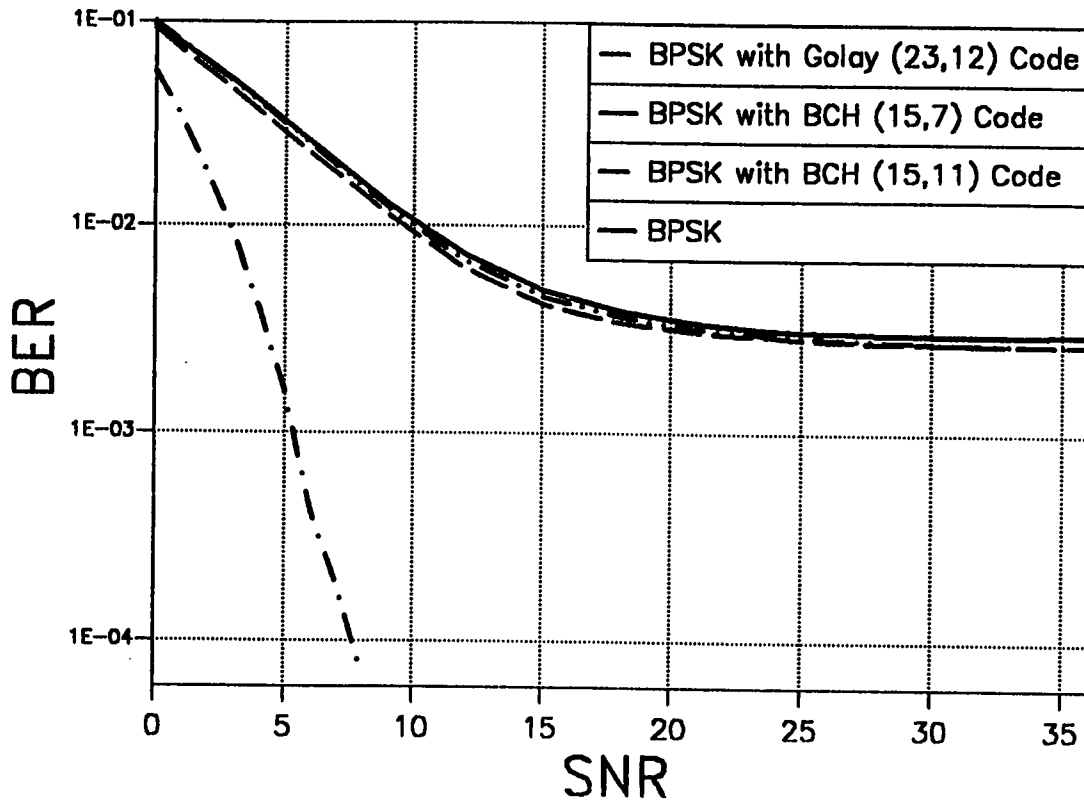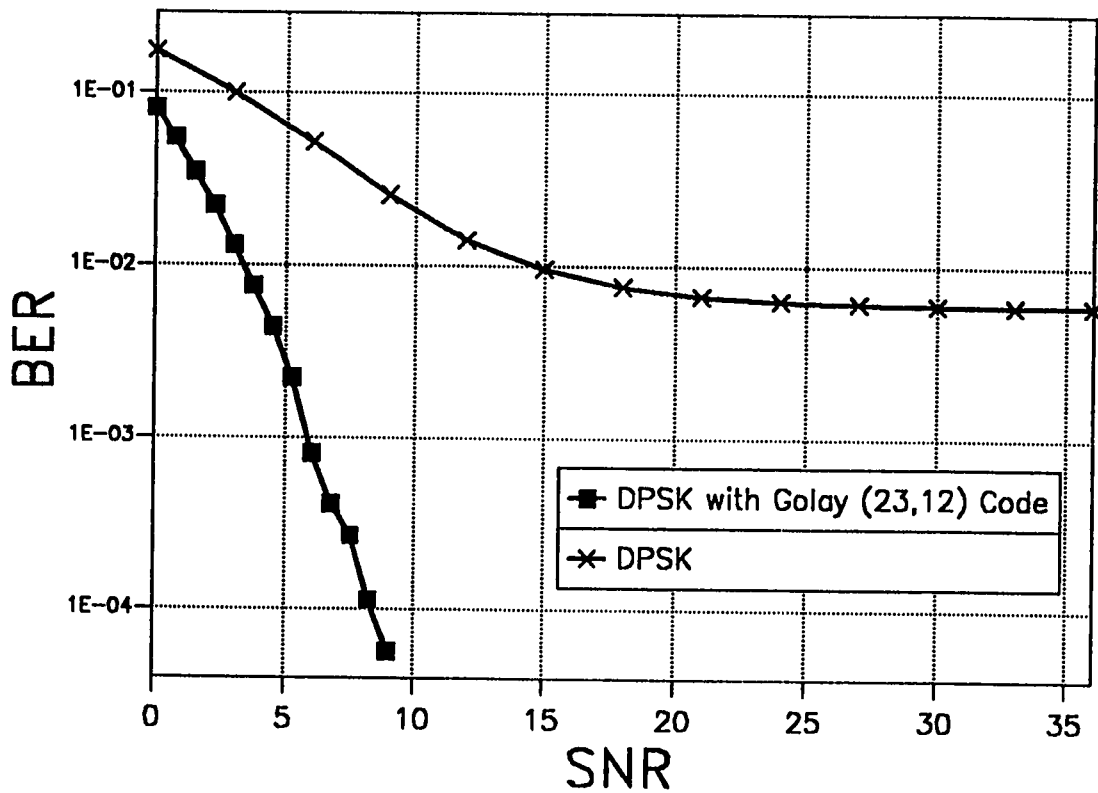
Figure 5.18 : The effect of coding on the BER with BPSK modulation for $A_c = 5$ **Erlang,** $n_c = 10$ **channels per cell,** $Ru = 7.6$, $G = 0.67$, $\sigma_d = 0\,dB$, $\sigma_i = 6\,dB$, $K_1 = 7\,dB$, $K_2 = 4\,dB$, $\tau_1 = 0.2T$, **and** $\tau_2 = 0.4T$.

co–channel interference and the effect of ISI. However, the system performance has been enhanced with the use of Golay code. With the use of Golay code, the coding gain is 23.8 dB at 3.0×10^{-3} BER.

In the proposed system, the size of the interleaver and deinterleaver is $(n \times n)$, where n is the code word length. Hence, with the BCH codes a (15×15) block interleaver is used in the transmitter and a (15×15) block deinterleaver is used in the receiver of the proposed system. However, a (23×23) block interleaver and deinterleaver are used with the Golay code. Because of the smaller size of interleavers and the smaller error correction capabilities, the two BCH codes did not enhance the performance of the system as the Golay code did.

With DPSK modulation scheme and the use of Golay code, the BER as a function of SNR is shown in Figure 5.19. The coding gain is 23.5 dB at 6.0×10^{-3} BER. Figure 5.20 shows the BER as a function of the normalized reuse distance, with BPSK modulation and SNR equal to 25 dB, when the Golay code is used. It is clear that the BER has been improved from 2.72×10^{-3} at $Ru = 10$ to 4.8×10^{-5} at $Ru = 4$.

Because our channel is frequency–selective, intersymbol interference (ISI) becomes an important cause of system degradation. To mitigate the ISI we

Figure 5.19 : The effect of using Golay (23,12) code on the BER with DPSK modulation for $A_c = 5$ Erlang, and $n_c = 10$ channels per cell, $Ru = 7.6$, $G = 0.67$, $\sigma_d = 0 dB$, $\sigma_i = 6 dB$, $K_1 = 7 dB$, $K_2 = 4 dB$, $\tau_1 = 0.2T$, and $\tau_2 = 0.4T$.
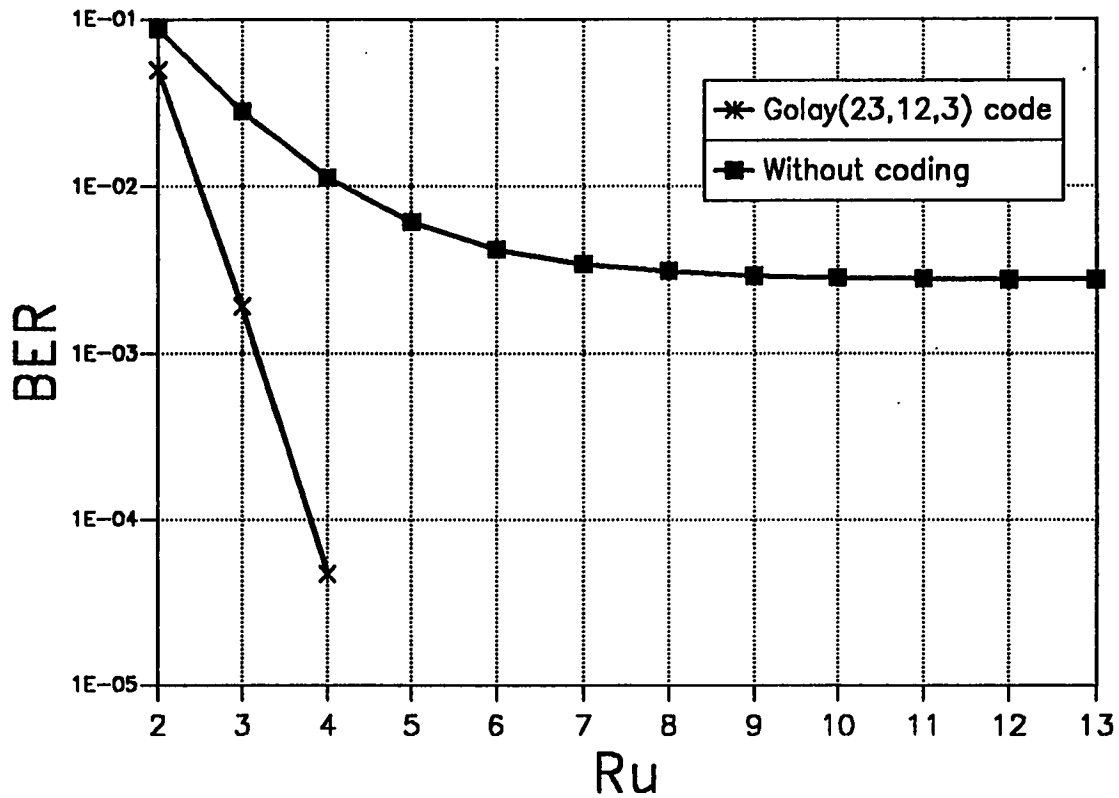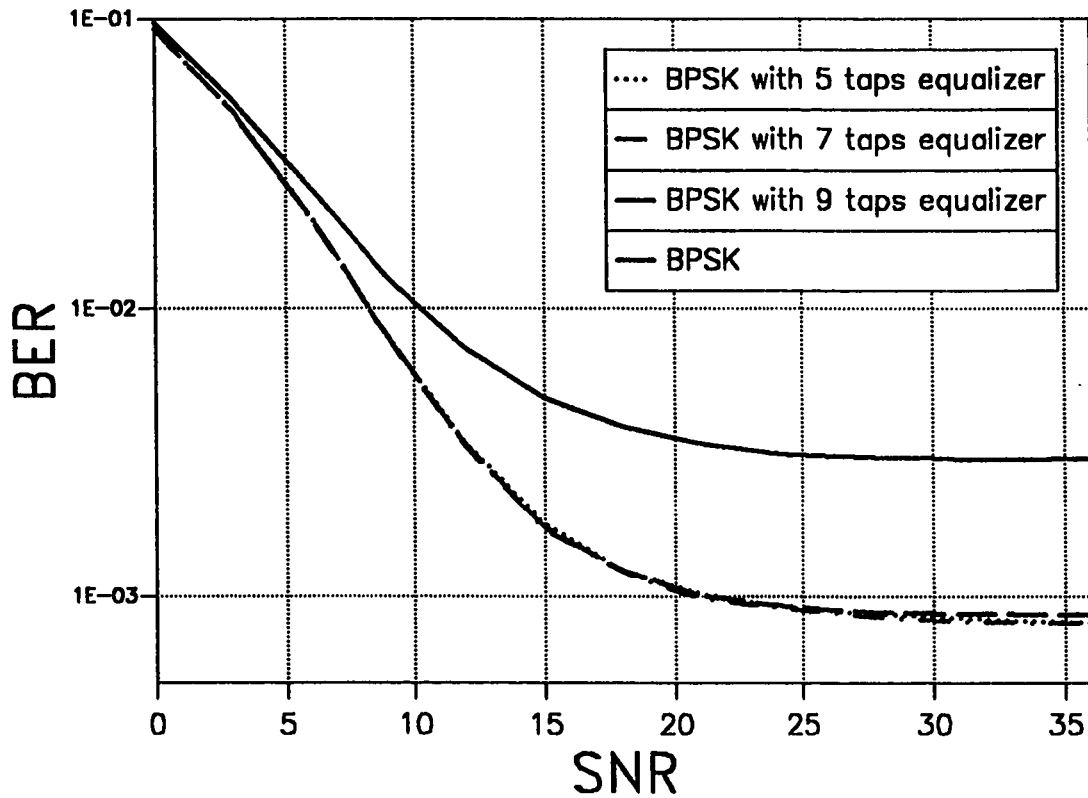
Figure 5.20 : BER versus Ru with Golay code and BPSK modulation for $A_c = 5$ **Erlang,** $n_c = 10$ **channels per cell,** $Ru = 7.6$, $G = 0.67$, $\sigma_d = 0\,dB$, $\sigma_i = 6\,dB$, $K_1 = 7\,dB$, $K_2 = 4\,dB$, $\tau_1 = 0.2T$, **and** $\tau_2 = 0.4T$.
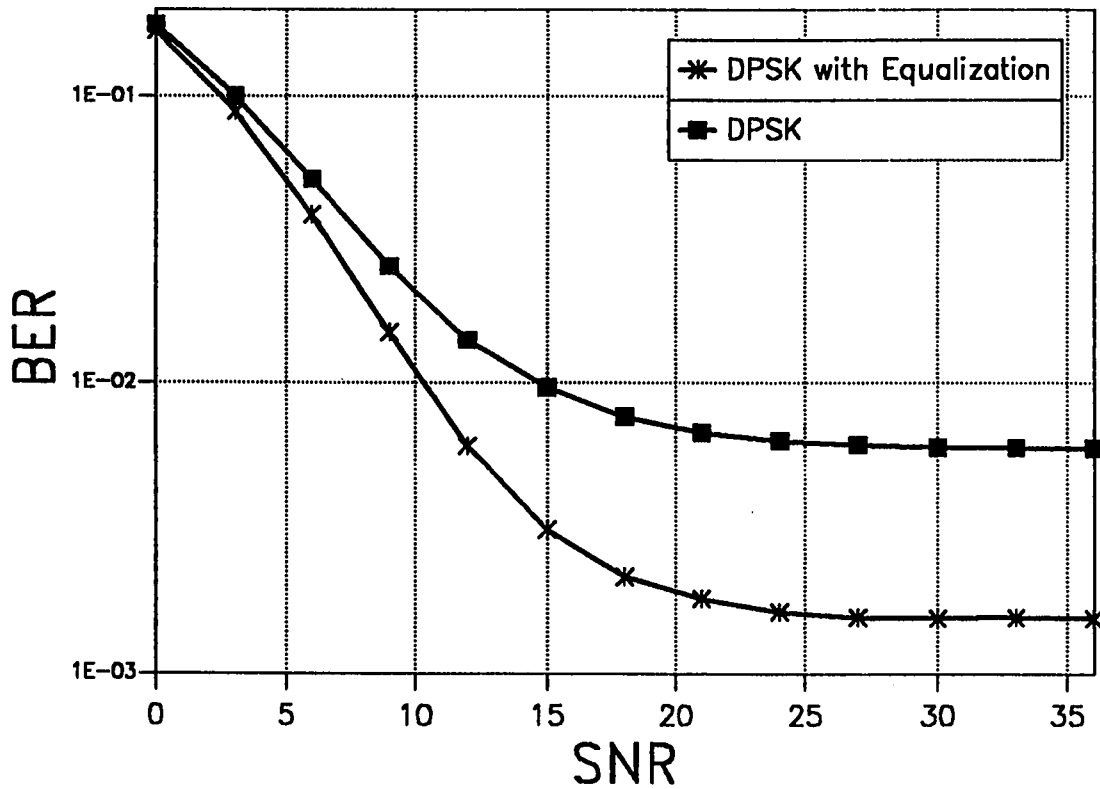
used a linear adaptive equalizer with 5, 7 and 9 taps. The adaptation of the equalizer taps is done using the LMS method. In our simulation, the first 10,000 symbols in a stream of 200,000 symbols are used to train the equalizer, then after the training symbols, the equalizer taps will be adapted using the demodulated and the equalized outputs.

Figure 5.21 shows the system performance with the equalizer number of taps as a parameter. We can see that increasing the number of taps will improve the performance slightly because, already, the spread of ISI over the adjacent symbols is larger than the spread-over non–adjacent ones. From the figure, with the use of linear adaptive equalizers the IBER has been reduced from 3.0×10^{-3} to 8×10^{-4} and the gain at 3.0×10^{-3} BER is 18.4 dB. Moreover, with DPSK modulation scheme the IBER has reduced from 6.0×10^{-3} to 1.57×10^{-3} as we can see from Figure 5.22.

Figure 5.23 shows the effect of using linear adaptive equalizer and dual diversity combining at the system receiver. In the figure, the BER is a function of SNR with BPSK modulation and the normalized reuse distance (Ru) is 7.6. It is clear that there is a large enhancement in system performance. The IBER has fallen to 6.65×10^{-5} from 3.0×10^{-3} and the gain at 3.0×10^{-3} is 25.9 dB.

Figure 5.21 : The effect of linear adaptive equalizer with different number of taps on the BER with BPSK modulation for $A_c = 5$ **Erlang,** $n_c = 10$ **channels per cell,** $Ru = 7.6$, $G = 0.67$, $\sigma_d = 0\,dB$, $\sigma_i = 6\,dB$, $K_1 = 7\,dB$, $K_2 = 4\,dB$, $\tau_1 = 0.2T$, **and** $\tau_2 = 0.4T$.

Figure 5.22 : The effect of linear adaptive equalizer on the BER with DPSK modulation for $A_c = 5$ **Erlang,** $n_c = 10$ **channels per cell,** $Ru = 7.6$, $G = 0.67$, $\sigma_d = 0dB$, $\sigma_i = 6dB$, $K_1 = 7dB$, $K_2 = 4dB$, $\tau_1 = 0.2T$, **and** $\tau_2 = 0.4T$.
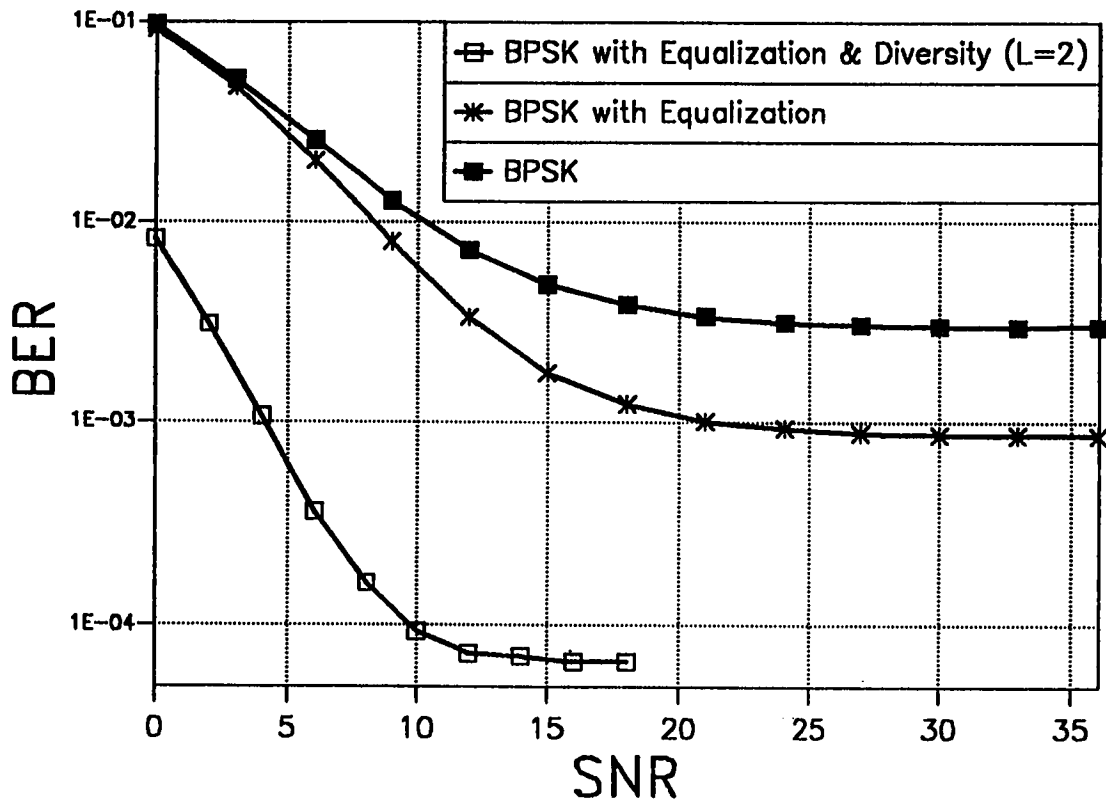
Figure 5.23 : The effect of using linear adaptive equalizer and dual diversity on the BER with BPSK modulation for $A_c = 5$ **Erlang,** $n_c = 10$ **channels per cell,** $Ru = 7.6$, $G = 0.67$, $\sigma_d = 0dB$, $\sigma_i = 6dB$, $K_1 = 7dB$, $K_2 = 4dB$, $\tau_1 = 0.2T$, **and** $\tau_2 = 0.4T$.

If a comparison is made between the system performance when a combination of dual diversity and equalization is used at the receiver and the use of equalization only at the receiver, we see that the IBER has been reduced from 8.75×10^{-4} to 6.57×10^{-5} and the gain at BER 8.75×10^{-4} is 23.2 dB.

Figure 5.24 shows the BER as a function of SNR with DPSK modulation scheme and Ru equal to 7.6 when a combination of dual diversity and linear adaptive equalization is used as a frequency–selective fading counter-measure. From the figure, the IBER has been reduced from 1.57×10^{-3}, when equalization only is used, to 1.13×10^{-4} and the gain at 1.57×10^{-3} is 21.3 dB.

Figure 5.25 shows the effect of combining equalization and coding on the BER as a function of SNR with BPSK modulation and Ru equal to 7.6. From the same figure, a comparison can be made with the use of equalization only. From this comparison, the gain at 8.7×10^{-4} BER is 23.1 dB. For the case of DPSK modulation, as can be shown in Figure 5.26, the gain at 1.58×10^{-3} BER is 21.4 dB when comparing the effect of using a combination of coding and equalization and using equalization only.

From Figure 5.27 a comparison can be made between the counter–measures with BPSK modulation and Ru equal to 7.6. It can be seen that diversity
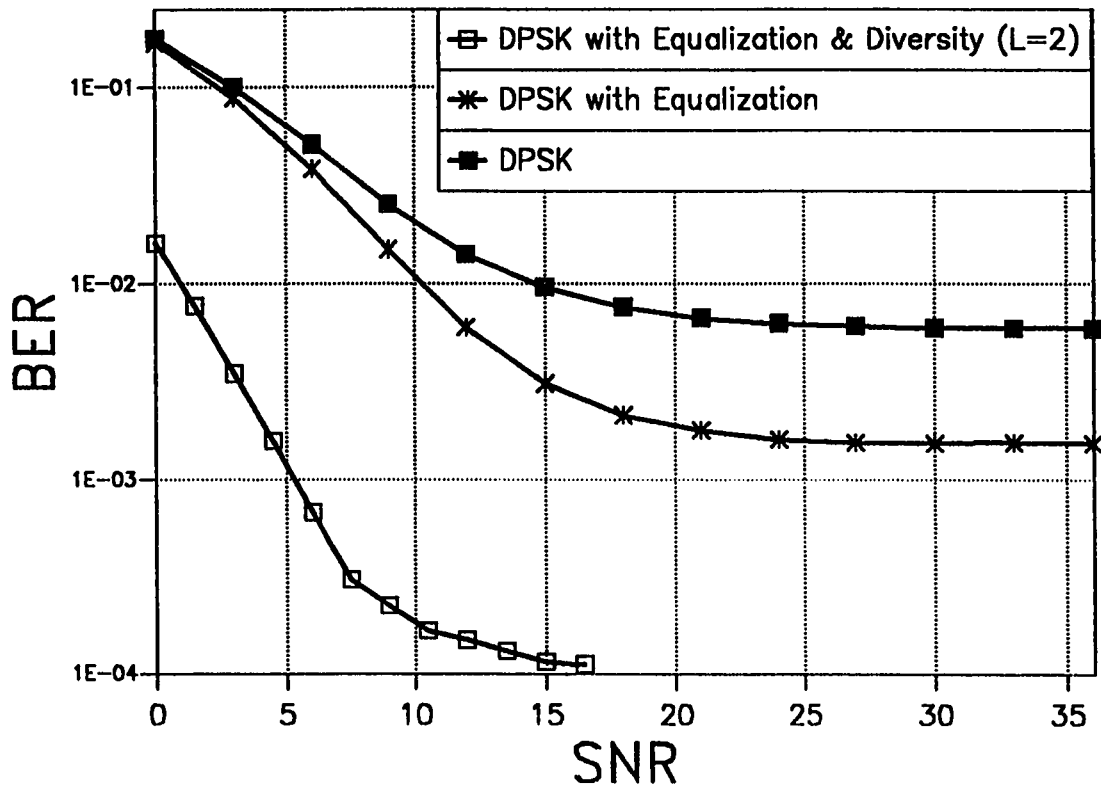
Figure 5.24 : The effect of using linear adaptive equalizer and dual diversity on the BER with DPSK modulation for $A_c = 5$ Erlang, $n_c = 10$ channels per cell, $Ru = 7.6$, $G = 0.67$, $\sigma_d = 0 dB$, $\sigma_i = 6 dB$, $K_1 = 7 dB$, $K_2 = 4 dB$, $\tau_1 = 0.2T$, and $\tau_2 = 0.4T$.
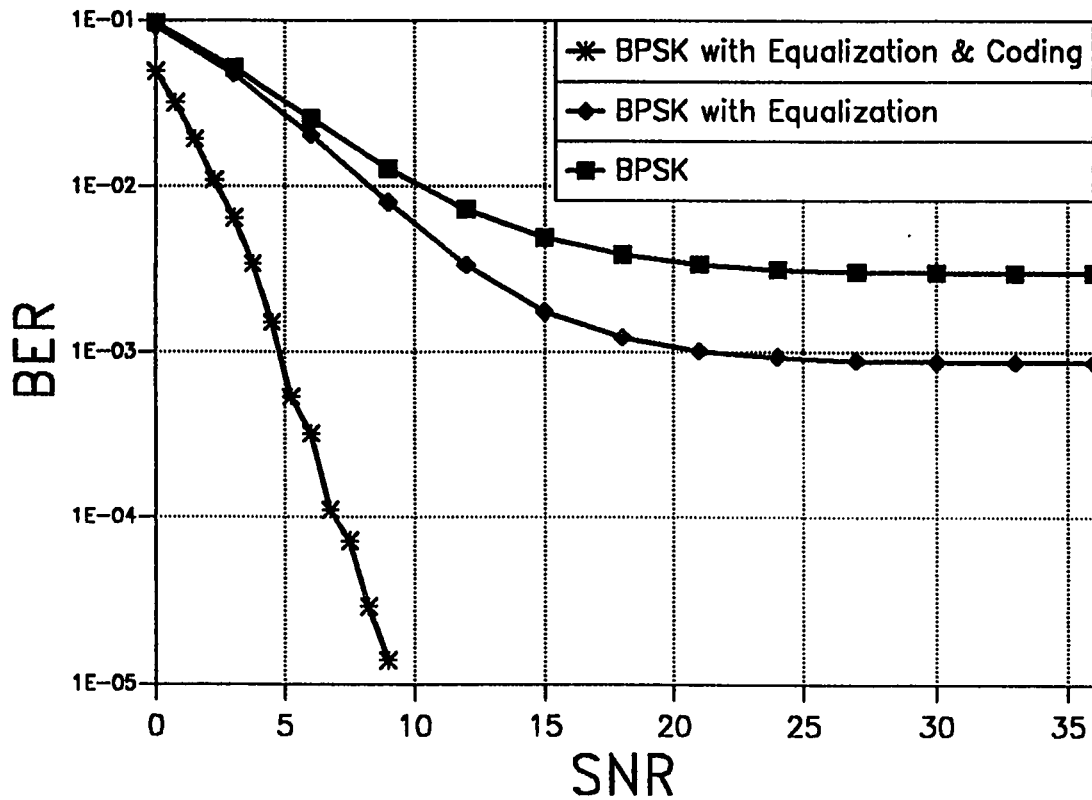
Figure 5.25 : The effect of using linear adaptive equalizer and Golay code on the BER with BPSK modulation for $A_c = 5$ Erlang, $n_c = 10$ channels per cell, $Ru = 7.6$, $G = 0.67$, $\sigma_d = 0dB$, $\sigma_i = 6dB$, $K_1 = 7dB$, $K_2 = 4dB$, $\tau_1 = 0.2T$, and $\tau_2 = 0.4T$.
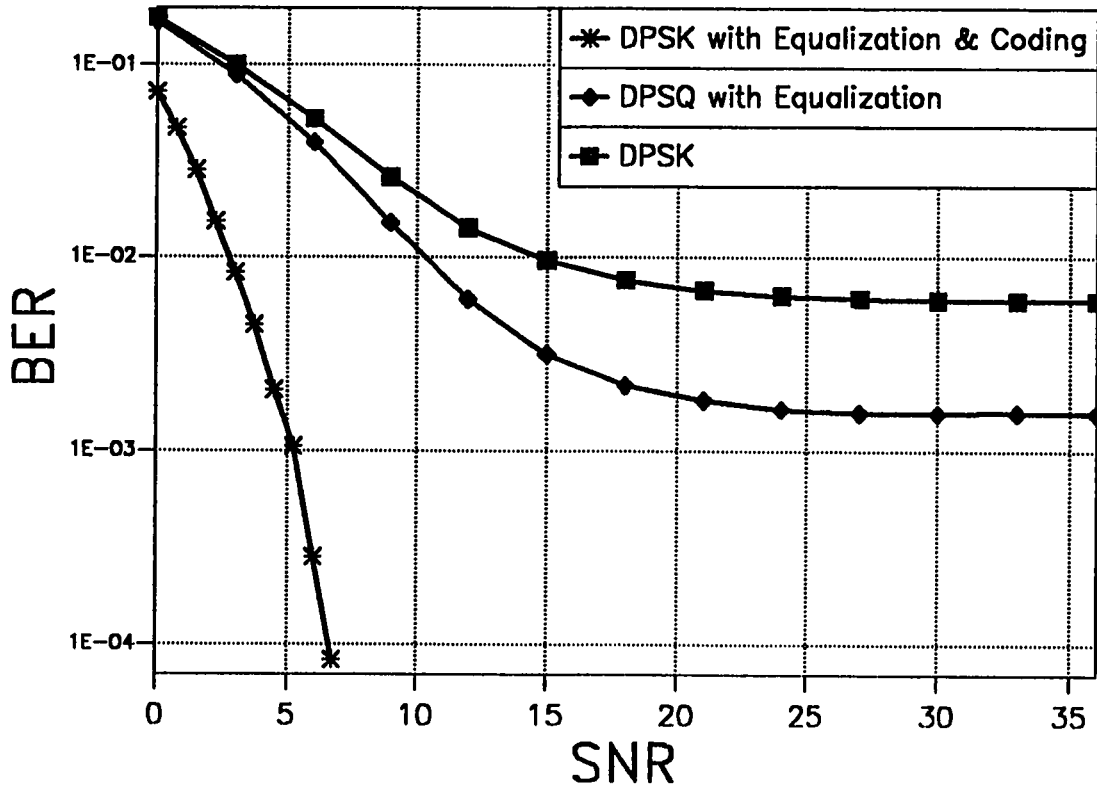
Figure 5.26 : The effect of using linear adaptive equalizer and Golay code on the BER with DPSK modulation for $A_c = 5$ **Erlang,** $n_c = 10$ **channels per cell,** $Ru = 7.6$, $G = 0.67$, $\sigma_d = 0 dB$, $\sigma_i = 6 dB$, $K_1 = 7 dB$, $K_2 = 4 dB$, $\tau_1 = 0.2T$, **and** $\tau_2 = 0.4T$.
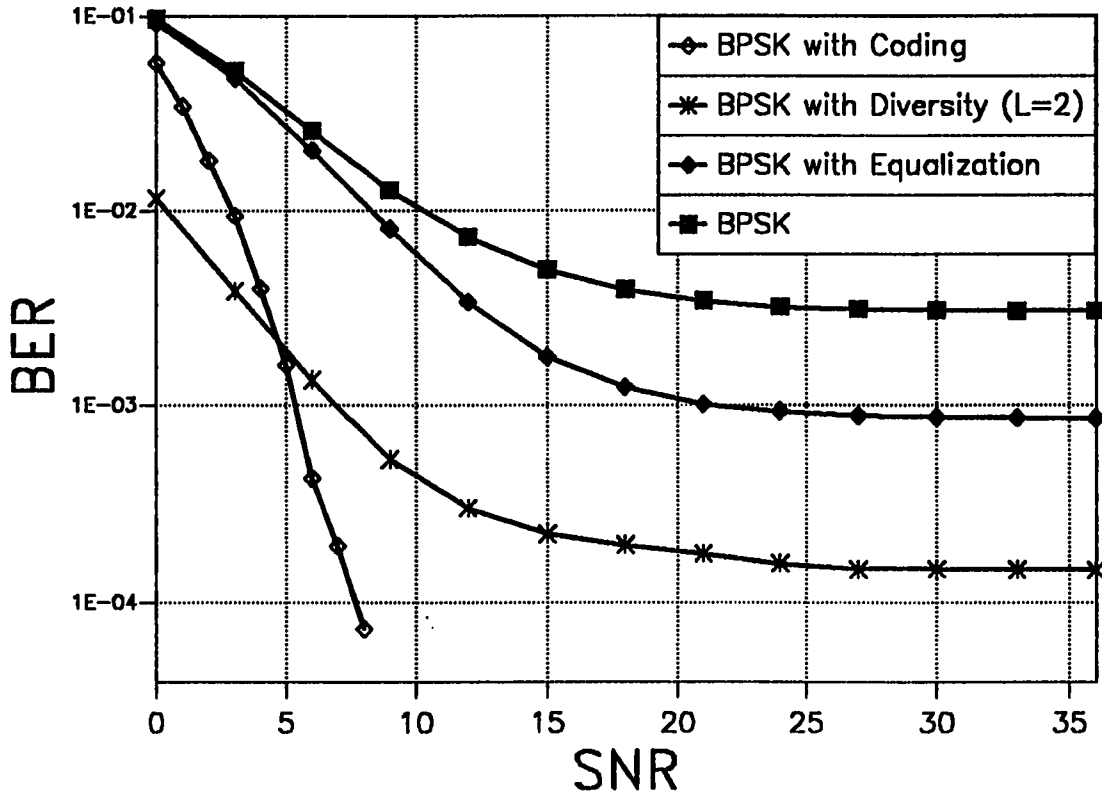
Figure 5.27 : A comparison between the effect of different counter-measures with BPSK modulation for $A_c = 5$ **Erlang,** $n_c = 10$ **channels per cell,** $Ru = 7.6$, $G = 0.67$, $\sigma_d = 0 dB$, $\sigma_i = 6 dB$, $K_1 = 7 dB$, $K_2 = 4 dB$, $\tau_1 = 0.2T$, **and** $\tau_2 = 0.4T$.

combining is the best fading counter–measure at low SNR (less than 4.7 dB). However, the enhancement in the system performance with the use of error control coding is the best at SNR greater than 4.7 dB. Similarly, error control coding is the best at high SNR with the case of DPSK modulation scheme as can be shown from Figure 5.28.

Figure 5.28 : A comparison between the effect of different counter-measures with DPSK modulation for $A_c = 5$ Erlang, $n_c = 10$ channels per cell, $Ru = 7.6$, $G = 0.67$, $\sigma_d = 0dB$, $\sigma_i = 6dB$, $K_1 = 7dB$, $K_2 = 4dB$, $\tau_1 = 0.2T$, and $\tau_2 = 0.4T$.
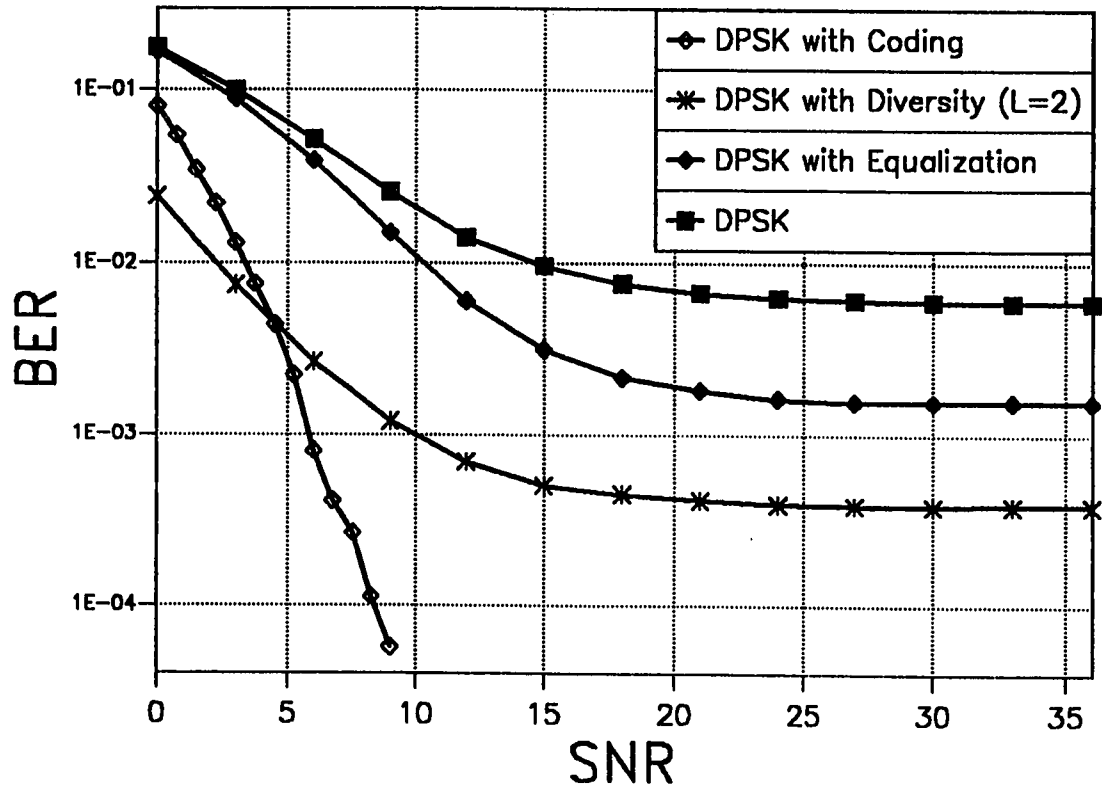
CHAPTER 6

SUMMARY, CONCLUSIONS AND
RECOMMENDATIONS FOR FUTURE WORK

6.1 Summary

In chapter one of this thesis, we had an overview of mobile communications, then the history of mobile communications was included. The remainder of the chapter was devoted to literature review, thesis contribution and thesis organization. In chapter two, cellular mobile communication systems and properties, such as cell shapes, frequency reuse and cell splitting, were introduced. Then, microcellular mobile communication systems and some previous work to evaluate their performance were presented. In chapter three, multipath fading and mobile radio environments were discussed. Moreover, classification of mobile fading channels and mobile fading counter-measures, such as diversity, error control coding, interleaving and equalization, were discussed. In chapter four, the baseband representation, which has been used in this work, was explained. Then the proposed system for digital microcellular mobile communication systems, operating over

frequency–selective fading environments, was described. In addition, the modulation schemes, used in the system, the propagation model and the channel model were discussed. Finally, the performance measures, the bit error rate (BER), and the spectrum efficiency (E_s) were explained.

The last chapter was devoted to the simulation results. The first part showed the effect of the different system parameters on the performance of the system. The different system parameters are the logarithmic standard deviations of the desired signal and the co–channel interference signals, the Rician factors of the first and the second delayed beams of the desired signal, the relative delays between the two beams of both the desired and the co–channel interference signals, the power ratio of the first to the second beams of the desired signal, and the roll–off factor of the raised–cosine filters used in the transmitter and the receiver of the system. Moreover, the effect of the cell radius and the normalized reuse distance on the BER and the spectrum efficiency were simulated. On the other part of the chapter, the effect of modulation schemes BPSK and DPSK on the BER was investigated. Also, different fading counter–measures were simulated. The counter–measures are diversity combining, error control coding, interleaving and linear adaptive equalization.

6.2   Conclusions

From the previous work it is clear that:

- The use of diversity combining enhances the performance of digital microcellular mobile communication systems by reducing the irreducible bit error rate (IBER) due to co-channel interference and intersymbol interference (ISI).

- With dual diversity combining the IBER has been reduced from 3.0×10^{-3} to 1.35×10^{-4} and the gain is found to be 24.25 dB in the case of BPSK modulation scheme.

- In the case of DPSK modulation scheme, the IBER has been reduced from 6.0×10^{-3} to 4.0×10^{-4} with the use of dual diversity.

- The price that should be paid for this enhancement is the complexity of the receiver which increases as the number of diversity branches increases.

- When increasing the SNR, the BER decreases faster with the use of Golay (23, 12) than with the use of dual diversity combining.

- With the use of Golay code the complexity of the transmitter and the receiver increases. Also, the bandwidth is increased by 91.7%.

- With BPSK modulation scheme and the use of Golay (23, 12) code, the coding gain is 23.8 dB at BER equal to 3.0×10^{-3}.

- With DPSK modulation scheme and the use of Golay (23, 12) code the coding gain is found to be 23.5 dB at the 3.0×10^{-3} BER.

- The use of linear adaptive equalizers helps in reducing the IBER of the system because the equalizer reduces the effect of ISI.

- With BPSK modulation the IBER has been reduced from 3.0×10^{-3} to 8.0×10^{-4}, and the gain is found to be 18.4 dB at 3.0×10^{-3} when using linear adaptive equalizers.

- With DPSK modulation the IBER has been reduced from 6.0×10^{-3} to 1.57×10^{-3} and the gain is found to be 15.9 dB when using linear adaptive equalization.

- A combination of dual diversity combining and linear adaptive equalization enhances the performance of the system more than the enhancement with using one of the two counter-measures alone.

- With BPSK modulation a combination of dual diversity and equalization reduces the IBER to 6.13×10^{-5} compared to 1.35×10^{-4} with dual diversity alone and 8.0×10^{-4} with equalization alone.

- With DPSK modulation scheme a combination of dual diversity and equalization reduces the IBER to 1.16×10^{-4} compared to 3.82×10^{-4} with dual diversity alone and 8.86×10^{-4} with equalization alone.

- A combination of error control coding and equalization enhances the system performance more than either one of the two counter-measures.

- With BPSK modulation, by the combination of error control coding and equalization, the gain is found to be 24.3 dB compared with 22.66 dB when coding is used alone.

- The combination of error control coding and equalization with DPSK enhances the performance by a gain of 24.3 dB at 6.0×10^{-3} BER. However, the use of coding only enhances the system performance by a 23.7 dB gain.

6.3   Recommendations for Future Work

Future work can include the following:

- The investigation of the system over multiple beams (greater than two) channel model.

- The investigation of the whole system operating over measured channel models.

- Studying the effect of other diversity techniques such as the selectivity technique.

- The effect of using more efficient bandwidth modulation schemes such as QPSK and GMSK.

- Studying the effect of other equalization techniques such as the decision feedback equalizers.

- Studying the effect of using different error control codes such as Reed–Solomon codes on the performance of the system.can be studied.

References

[1] A.A. Abu–Dayya and N.C. Beaulieu, "Outage probabilities of cellular mobile radio systems with multiple Nakagami interferers", IEEE Trans. Veh. Technol., Vol. 40, pp. 757–768, Nov. 1991.

[2] Adnan A. Abu–Dayya and Norman C. Beaulieu, "Outage probabilities of diversity cellular systems with cochannel interference in Nakagami fading", IEEE Trans. on Vehicular Technology, Vol. 41, Nol 4, pp. 343–355, Nov. 1992.

[3] F. Adachi and K. Ohno, "Block error probability for noncoherent FSK with diversity reception in mobile radio", Electron. Lett., Vol. 24, pp. 1523–1525, 1988.

[4] Noach Amitay, Larry J. Greenstein, and G.J. Owoens, "Measurement-based estimates of bit–error–rate performance in urban LOS microcells at 900 MHz", IEEE Trans. Veh. Tech., vol. 41, no. 4, pp. 414–423, Nov. 1992.

[5] Philip Balaban and Jack Salaz, "Optimum diversity combining and equalization in digital data transmission with application to cellular mobile radio – Part I: theoretical considerations", IEEE Transactions on Communications, Vol. 40, No. 5, pp. 885–894, May 1992.

[6] Philip Balaban and Jack Salaz, "Optimum diversity combining and equalization in digital data transmission with application to cellular mobile radio – Part II: Numerical Results", IEEE Transactions on Communications, Vol. 40, No. 5, pp. 895–907, May 1992.

[7] R.J.C. Baltitude and G.K. Bedel, "Propagation characteristics on microcellular urban mobile radio channels at 910 MHz", IEEE J. Selected Areas in Common., January 1989, SAC-7, pp. 31–39.

[8] N.C. Beaulie and A.A. Abu–Dayya, "Analysis of equal gain diversity on Nakagami fading channels", IEEE Trans. Commun., Vol. 39, pp. 225–234, Feb. 1991.

[9] K. Biyari and N. Shehadeh, "Minimization of the Prob. of error in a multipath fading channel", 2nd Saudi Engineering Conference, Nov. 1985, pp. 678-698.

[10] S.T.S. Chia, R. Steele, E. Green and A. Baran "Propagation and bit error ratio measurements for a microcellular system", Journal of the Institution of Electronic and Radio Engineers, Vol. 57, No. 6 (Supplement), pp. S 255-266, Nov./Dec. 1987.

[11] D.C. Cox, "Delay Doppler characteristics of multipath propagation at 910 MHz in a suburban mobile radio environment", IEEE Trans. Antennas Propagat. vol. AP-20, Sept. 1972.

[12] R. Davis, A. Simpson and J.P. Mcgreehan, "Propagation measurements at 1.7 GHz for microcellular urban communications", Electron. Lett., 1990, 26, pp. 1053-1055.

[13] C. Dechaux and R. Scheller, "What are GSM and DCS?", Electrical Communication, 2nd Quarter 1993, pp. 118-127.

[14] L.F. Fenton, "The sum of log-normal probability distribution in scatter transmission systems", IRE Trans. Commun. Syst., Vol. CS-8, pp. 57-67, Mar. 1960.

[15] M. Flack and M. Gronous, Cellular Communications for Data Transmission. NCC Blackwell, Manchester, Oxford, 1990.

[16] J.E. Flood, C.J. Hughes and J.D. Parsons, Personal and Mobile Radio Systems. Peter Peregrinus Ltd., London, 1991.

[17] R.C. French, "The effect of fading and shadowing on channel reuse in mobile radio", IEEE Trans. Veh. Technol., Vol. VT-28, pp. 171-181, 1979.

[18] B. Glance and L.J. Greenstein, "Frequency-selective fading effects in digital mobile radio with diversity combining", IEEE Trans. Commun., vol. COM-31, Sept. 1983.

[19] P. Harley, "Short distance attenuation measurements at 900 MHz and 1.8 GHz using low antenna heights for microcells", IEEE J. Selected Areas in Common, January 1989, SAC-7, pp. 5-10.

[20] Simon Haykin, Digital Communications, John Wiley and Sons, Inc., 1988.

[21] A. Kegel, H.J. Wesselman, and R. Prasad, "Bit error probability for fading DPSK signals in microcellular land mobile radio systems', Electron. Lett., Vol. 27, No. 18, pp. 1647-1648, 1991.

[22] W.C.Y. Lee, Mobile Cellular Telecommunications, New York: McGraw-Hill, 1989.

[23] W.C. Y. Lee, "Smaller cells for greater performance", IEEE Communication Magazine, November 1991, pp. 19-23.

[24] S. Lin and D.J. Costello, Jr., Error Control Coding: Fundamentals and Applications, Prentice-Hall, 1983.

[25] Jean-Paul M.G. Linnartz, Aart J.'T Jong and Ramjee Prasad, "Effect of coding in digital microcellular personal communication systems with co-channel interference, fading, shadowing, and noise", IEEE Journal on Selected Areas in Communication, Vol. 11, No. 6, pp. 901-910, August 1993.

[26] V.H. MacDonald, "Advanced mobile phone service: The cellular concept", The Bell System Technological Journal, Vol. 58, No. 1, pp. 15-41, January 1979.

[27] R. Prasad and J.C. Arnabak, "Comments on analysis for spectrum efficiency in single cell trunked and cellular mobile radio", IEEE Trans. Veh. Technol., Vol. 37, pp. 220-222, Nov. 1988.

[28] R. Prasad and A. Kegel, "Effects of Rician and Log-Normal shadowed signals on spectrum efficiency in microcellular radio", IEEE Trans. on Veh. Technol., Vol. 42, No. 3, pp. 274-281, August 1993.

[29] Ramjee Prasad and Adrian Kegel, "Improved assessment of interference limits in cellular radio performance", IEEE Trans. Veh. Technol., Vol. 40, pp. 412–419, May 1991.

[30] R. Prasad, A. Kegel and J. Olsthoorn, "Spectrum efficiency analysis for microcellular mobile radio systems", Electron. Lett., 1991, pp. 423–425.

[31] Ramjee Prasad, Adrian Kegel and Aart Vos, "Performance of microcellular mobile radio in a cochannel interference, natural, and man–made noise environment", IEEE Trans. on Veh. Technol., Vol. 42, No. 1, pp. 33-40.

[32] J.G. Proakis, Digital Communications, McGraw–Hill International Book Company, Second Edition, 1989.

[33] T.S. Rappaport, S.Y. Seidel, and R. Singh, "900 MHz multipath propagation measurements for U.S. digital cellular radiotelephone", IEEE Trans. Veh. Technol., Vol. 39, pp. 132–139, May 1990.

[34] William D. Rummler, "More on the multipath fading channel model", Vol. COM–29, No. 3, March 1981.

[35] A.J. Rustako, Jr., Noach Amitay, G.J. Owens, and R.S. Roman, "Radio propagation at microwave frequencies for line–of–sight microcellular mobile and personal communications", IEEE Trans. Veh. Tech., vol. 40, no. 1, pp. 203–210, Feb. 1991.

[36] H.M. Sacheh, "A realistic approach to defining the probability of meeting acceptable receiver performance criteria", IEEE Trans. Electromagn. Compat., Vol. EMC–13, pp. 3-6, 1991.

[37] S.C. Schwartz and Y.S. Yeh, "On the distribution function and moments of power sums with log–normal components", Bell Syst. Tech. J., Vol. 6, pp. 1441–1462, Sept. 1982.

[38] Scott Y. Seidel, Theodore S. Rappaport, Sanjiv Jain, Michael L. Lord, and Rajendra Singh, "Pathloss, Scattering, and multipath delay statistics in four European cities for digital cellular and microcellular ra-

diotelephone", IEEE Transactions on Vehicular Technology, Vol. 40, no. 4, pp. 721–730.

[39] R. Sharma, W.D. Grovr, and Witold A. Krzymein, "Forward–error–control (FEC)–assisted adaptive equalization for digital cellular mobile radio", IEEE Trans. Veh. Technol., Vol. 42, No. 1, pp. 94–102, Feb. 1993.

[40] K.W. Sowerby and A.G. Williamson, "Outage probability calculations for a mobile radio system having multiple Rayleigh interferers", Electron. Letters, Vol. 23, pp. 600–601, 1987.

[41] K.W. Sowerby and A.G. Williamson, "Outage probability calculations for mobile radio systems with multiple interferers", Electron. Letters, Vol. 24, pp. 1073–1075, 1988.

[42] Raymond Steel, Mobile Radio Communications, Pentech Press, 1992.

[43] G.L. Turin, "Introduction to spread–spectrum antimultipath techniques and their application to urban digital radio", Proc. IEEE, Vol. 68, Mar. 1980.

[44] John Walker, Mobile Information Systems, Artech House, 1990.

[45] W.T. Webb, R. Steele, "Equalizer techniques for QAM transmissions over dispersive mobile radio channels", IEEE Proceedings–I, vol. 138, no. 6, pp. 566–576, Dec. 1991.

[46] A.G. Williamson and J.D. Parsons, "Outage probability in a mobile radio system subject to fading and shadowing", Electron. Lett., Vol. 21, pp. 622–623, 1985.

[47] Yu–Dong Yao and U.H. Sheikh, "Investigations into cochannel interference in microcellular mobile radio systems", IEEE Trans., Veh. Technol., Vol. 41, No. 2, pp. 114–123, May 1992.

[48] Y.–D. Yao and A.U.H. Sheikh, "Outage probability analysis for microcell mobile radio systems with cochannel interferers in Rician/Rayleigh

fading environment", Electron. Letters, Vol. 26, No. 13, pp. 864–866, June 1990.

[49] Y.S. Yeh and S.C. Shwartz, "Outage probability in mobile telephony due to multiple log–normal interferers", IEEE Trans. Commun., Vol. COM–32, pp. 380–387, Apr. 1984.

[50] W.R. Young, "Advanced mobile phone service: Introduction, background, and objectives", The Bell System Technological Journal, Vol. 58, No.1 , pp. 1–14, January 1979.